Control and Optimisation of Grid-Connected Microgrids for Tie-Line Smoothing

Mojaharul Islam

M.Sc. in Electrical Engineering

School of Engineering and Built Environment

Griffith Sciences

Griffith University

Submitted in fulfilment of the requirements of the degree of

Doctor of Philosophy

January 2021

I would like to dedicate this thesis to my loving parents ...

Abstract

Renewable energy resources (RESs) are significantly integrated in distribution networks to promote green technologies in future power systems. The idea of microgrids (MGs) is developed for the efficient use of RESs through an appropriate control, monitoring and management system. Control and management of MGs are challenging tasks along with numerous economic and environmental benefits. The challenges of MGs operation include tie-line power fluctuations that have an adverse effect on the stability and quality of distribution networks. Tie-line power control in a residential MG is difficult due to dependency on RESs as a primary generation unit in MGs. Motivated by these, this thesis investigates the tie-line power control issues in grid-connected residential MGs and applies several controls and optimisation methods to achieve a smooth tie-line power satisfying system boundary conditions. First, a dynamic energy management system (EMS) is designed to reduce the tie-line fluctuation in a grid-connected MG through an indirect grid power control strategy. A fuzzy logic-based EMS is proposed to control the battery power due to the variations in generations and loads. The net power demand and battery state of charge (SoC) of an MG are considered inputs of the fuzzy controller to determine the battery power by keeping the battery SoC within limits. An offline optimisation method is used to optimise the membership functions and rules to shape the performance parameters. Thereafter, a golden section search-based non-linear programming method is applied to design a battery power management system to minimise the tie-line fluctuation in an MG counting the system constraints and disturbances. Two other rule-based methods are also demonstrated for comparative analysis of the proposed methods in terms of predefined performance parameters. Afterward, a dynamic grid power control method is presented to control the interlink inverters in grid-connected MGs. A grid power controller is designed based on a complete model of the MG systems to achieve a constant tie-line power on typical days of the year. The designed controller can effectively smooth tie-line fluctuation in a grid-connected residential MG. The charging/ discharging of the battery is controlled by a DC-DC converter which is also responsible to provide a stable DC bus to the input of an interlink inverter. The reference tie-line power is determined by a MG controller based on statistical power generations, load demand and battery

SoC. Moreover, an eigenvalue-based stability analysis is performed to show the sensitivity of system parameters on system stability. Furthermore, the tie-line power control in a networked MG (NMG) is investigated to obtain a smooth tie-line power in an NMG connected to a common bus. A model predictive control-based distributed power flow controller is proposed to control the interlink inverters of the NMG in a distributed manner. Charging/ discharging of battery is controlled by a decentralised model predictive power controller to provide a stable DC voltage for MGs. Communication between MGs is performed for sharing the status of the tie-line power along with the scheduled tie-line reference. The information from the network is used to determine the instantaneous reference grid power of individual MGs for achieving a smooth tie-line power for the network. Inverter switching actions are performed to minimise the difference between predictions and references. In addition, a comparative study with a decentralised operation of MGs is conducted to show the benefits of networked operation.

All the proposed methods are tested through rigorous case studies to validate the performance despite the variations in input and output system disturbances. Comparative analysis among different methods is also conducted to demonstrate the performance variations through adopting different methods. For the simulation experiment set up, MATLAB SIMULINK Simscape Electrical is used to develop a designed system model of MGs and experimental models of the proposed methods. Experiments are performed using real weather and residential load information in Queensland, Australia. The results demonstrate that the proposed methods have achieved the design objectives to solve the tie-line fluctuation problem of grid-connected residential MGs.

Declaration

Statement of Originality

This work has not previously been submitted for a degree or diploma in any university. To the best of my knowledge and belief, the thesis contains no material previously published or written by another person except where due reference is made in the thesis itself.

Mojaharul Islam

January 2021

Acknowledgements

First and foremost, I would like to express my deep gratitude to my principle supervisor A/Prof. Fuwen Yang, for his supervision, continuous support, encouragement and guidance throughout this research work. As a PhD student, I have been so fortunate to have a supervisor with such an enthusiasm and dedication. It has been an honor to have worked with him in these years, and this work could not have formed without his help. Many thanks go to my associate supervisor Professor Junwei Lu for his direction and support. I am also grateful to external supervisor A/ Prof. Mohammad Amin, Dr. Chandima Ekanayeke for their consistent support, suggestions and guidance during my PhD. I greatly acknowledge the support from Professor Jahangir Hossain.

Thanks to all the professors of the School of Engineering and Built Environment, Griffith University, Gold Coast. I appreciate their contributions of time and intriguing ideas to make my study experience productive and stimulating. I humbly thank my fellow PhD candidates for the nice and friendly working environment I have had during this period. Special thanks to dear fellow Saher, Usman and Quanwei for their help during this period.

I would like to thank my friends for their support and help. I never find words to express my most profound gratitude to my family. I am so grateful to my parents for their contributions and support throughout in my life. I would like express my love to my son Mahrush for refreshing me during stressful time. Last, but certainly not least, heartfelt thanks go to my wife, Toma for her love, encouragement and understanding.

This research was made possible through the financial support provided by Griffith University International Postgraduate Research Scholarship and Griffith University Postgraduate Research Scholarship.

THE PAPERS INCLUDED ARE CO-AUTHORED PAPERS

Acknowledgement of Published and Unpublished Papers included in this Thesis

Section 9.1 of the Griffith University Code for the Responsible Conduct of Research ("Criteria for Authorship"), in accordance with Section 5 of the Australian Code for the Responsible Conduct of Research, states:

To be named as an author, a researcher must have made a substantial scholarly contribution to the creative or scholarly work that constitutes the research output, and be able to take public responsibility for at least that part of the work they contributed. Attribution of authorship depends to some extent on the discipline and publisher policies, but in all cases, authorship must be based on substantial contributions in a combination of one or more of:

- conception and design of the research project
- analysis and interpretation of research data
- drafting or making significant parts of the creative or scholarly work or critically revising it so as to contribute significantly to the final output.

Section 9.3 of the Griffith University Code ("Responsibilities of Researchers"), in accordance with Section 5 of the Australian Code, states:

Researchers are expected to:

- Offer authorship to all people, including research trainees, who meet the criteria for authorship listed above, but only those people.
- accept or decline offers of authorship promptly in writing.
- Include in the list of authors only those who have accepted authorship
- Appoint one author to be the executive author to record authorship and manage correspondence about the work with the publisher and other interested parties.
- Acknowledge all those who have contributed to the research, facilities or materials but who do not qualify as authors, such as research assistants, technical staff, and advisors on cultural or community knowledge. Obtain written consent to name individuals.

Included in this thesis are papers in Chapters 2, 3, 4 , 5 and 6 which are co-authored with other researchers. My contribution to each co-authored paper is outlined at the front of the relevant chapter. The bibliographic details and status for these papers including all authors, are:

Part of chapter 2: **M. Islam,** F Yang, M Amin “Control and optimisation of networked microgrids - a review” accepted for publication in IET Renewable Power Generation.

Chapter 3: **M. Islam,** F Yang, C Ekanayeke, M Amin "Grid power fluctuation reduction by fuzzy control based energy management system in residential microgrids. (2018)" International Transactions on Electrical Energy Systems: e2758.

Chapter 4: **M. Islam,** F Yang, J Hossain, C Ekanayeke, UB. Tayab. Battery management system to minimize the grid power fluctuation in residential microgrids. 28th Australasian Universities Power Engineering Conference, 2018.

Chapter 5: **M. Islam,** F Yang, M Amin “Dynamic control of grid-connected microgrids for tie-line smoothing.(2020)” International Transaction on Electrical Energy Systems:e12557.

Chapter 6: **M. Islam,** F Yang, J Lu “Dynamic Power Flow Control in Networked Microgrids for Tie-line Smoothing” under preparation to submit on IEEE Transaction on Power Systems.

Appropriate acknowledgements of those who contributed to the research but did not qualify as authors are included in each paper.

Signed:_____ Date:*23.01.2021*

PhD Candidate: Mojaharul Islam (Principle Author)

Countersigned:_____ Date:*23.01.2021*

Principle Supervisor: A. Prof. Fuwen Yang (Corresponding Author)

Countersigned:_____ Date:*23.01.2021*

Associate Supervisor: Prof. Junwei Lu

Table of contents

List of figures

List of tables

Symbols

Roman Symbols

C_{bat}	Remaining charge of a battery
ω	System disturbances
A, B, C, D, E, F	System coefficients
C_{cap}	Total capacity of a battery
C_{dc}	DC link capacitance
C_f	Filter capacitance
d_1	Duty cycle of boost converter
d_2	Duty cycle of buck boost converter
d_{dq}	Duty cycle of interlink inverter
i_1/i_{res}	PV current
i_2	battery current
i_{fdq}	dq component of filter current
i_{gdq}	dq component of grid current
$K_{p,PLL}$	Proportional gain of PLL
L_1	Inductance of boost converter
L_2/L_b	Inductance of buck-boost converter

L_f Filter inductance

L_g Grid inductance

m, n Droop coefficient

P_g Active grid power

P_{load} Load power

P_{net} MG demand power

P_{pv} PV power

Q_g Reactive grid power

R_1 Resistance of boost converter

R_2 Resistance of buck-boost converter

R_f Filter resistance

R_g/Rt Grid/line resistance

SoC State of charge of battery

SoC_{max} Maximum value of SoC

SoC_{min} Minimum value of SoC

T_s Sampling time

u System inputs

v_{bat} Terminal voltage of battery

V_{dc} DC link voltage

v_{gdq} dq component of grid voltage

v_{idq} dq component of inverter output voltage

v_{odq} dq component of filter capacitance voltage

v_{pv} Terminal voltage of PV

x State variables

y System outputs

Greek Symbols

ω Rated frequency

ω_{cPLL} Cut-off frequency of PLL filter

Superscripts

$*$ Reference value

Subscripts

i ith MG

Acronyms / Abbreviations

ADMM Alternating direction method of multipliers

CRMS Cumulative root mean square

DER Distributed energy resources

DG Distributed generation

DNO Distributed network operator

DoD Depth of discharge

EMS Energy management system

ESS Energy storage system

FLC Fuzzy logic controller

GA Genetic algorithm

ICA Imperialist competitive algorithm

AI Artificial intelligence

ICT Communication technology

LV Low Voltage

MAS Multi-agent system

MF Membership function

MGCC Microgrid controller

MG Microgrid

MILP Mixed-integer linear programming

MMG Multi-microgrid

MPC Model predictive control

MPC Model predictive power control

MPPT Maximum power point tracking

MV Medium Voltage

NMG Networked microgrid

NSGA Non-dominated sorting genetic algorithm

PCC Point of common coupling

PLL Phase locked loop

PSO Particle swarm optimization

RES Renewable energy resource

SoC State of charge

Chapter 1

Introduction

1.1 Motivation

Smart grid technologies have become the leading element of next-generation electrical power networks to increase the reliability and efficiency of power systems and provide a secure and cost-effective energy generation, distribution and consumption for customers. Microgrids (MGs) are one of the leading features of smart grid technologies that integrate distributed energy resources and energy storage systems to create a small grid that feeds different loads on a low-/medium-voltage network and operate either grid-connected or island mode [1, 2]. The concept of MGs is mainly developed to utilise energy from renewable energy resources (RESs) that are distributively connected to transmission and distribution networks. The output power of RESs is usually dynamic in nature due to dynamic weather conditions throughout the day. Thus, the control and optimisation of an MG present a challenge due to dynamic variations in RESs and load demand in MGs. In addition, the dynamic nature of RESs and load demand creates a fluctuating tie-line power in grid-connected operation of MGs. The fluctuation of tie-line power has an impact on stability, quality and reliability of customer service. Moreover, integrating a number of MGs in a distribution line will increase the tie-line fluctuation significantly. Networked MG (NMG) is an extended concept of MGs that involves forming a network using multiple neighbouring MGs. The main idea of the network is to share surplus/shortage power with neighbouring MGs for local/global cost-effective operation, reducing the impact of RESs on distributed network and reliability of customer service. However, the adaptation of NMGs in distribution networks brings new challenges because of multilevel control and optimisation needed to achieve a robust control and energy management system (EMS) for the network. Furthermore, MGs in a network may have different objectives and

privacy strategies, which may lead to large variations in tie-line power. The result will further reduce the quality and stability of distribution networks. Recent studies focused on addressing the tie-line fluctuation problem in grid-connected MG considering the dramatic behaviours of RESs and load, and by preserving the system constraints. Meanwhile, additional research is necessary to solve the tie-line fluctuation problem in a grid-connected residential MG. Moreover, tie-line fluctuation in NMGs needs to be addressed. Thus, this thesis investigates the tie-line fluctuation problem of grid-connected MGs to find achievable solutions for the problem.

1.2 Scope of the Thesis

This thesis aims to study the tie-line fluctuation problem of grid-connected MGs and provide feasible solutions to achieve a smooth tie-line power for grid-connected MGs using different control and optimisation methods. A comprehensive literature review on control and optimisation of MGs is conducted to find the related research gaps. Then, the thesis systemically presents several control and optimisation methods to achieve the research objectives. Firstly, several rule-based control methods, including fuzzy logic control, are applied to a dynamic EMS to reduce tie-line fluctuation in an MG. In addition, a golden section search-based non-linear programming optimisation method is used to minimise the tie-line fluctuation in the MG. Afterwards, a grid power controller is designed using the dynamic model of the MG that effectively smooths the tie-line power fluctuations in a grid-connected MG. In addition, a distributed model predictive control scheme is proposed for controlling the interlink inverters of MGs to obtain a smooth scheduled tie-line power in an NMG connected to the same distribution feeder. The main research objectives of this thesis are summarised as follows:

1. Designing a dynamic EMS to control the battery storage power flow to achieve a minimise tie-line fluctuations;
2. Developing a dynamic model of an MG and designing a grid power control method to control the dynamic power flow of the interlink inverter for achieving a smooth tie-line power;
3. Designing a distributed tie-line power controller to achieve a smooth tie-line power in an NMG.

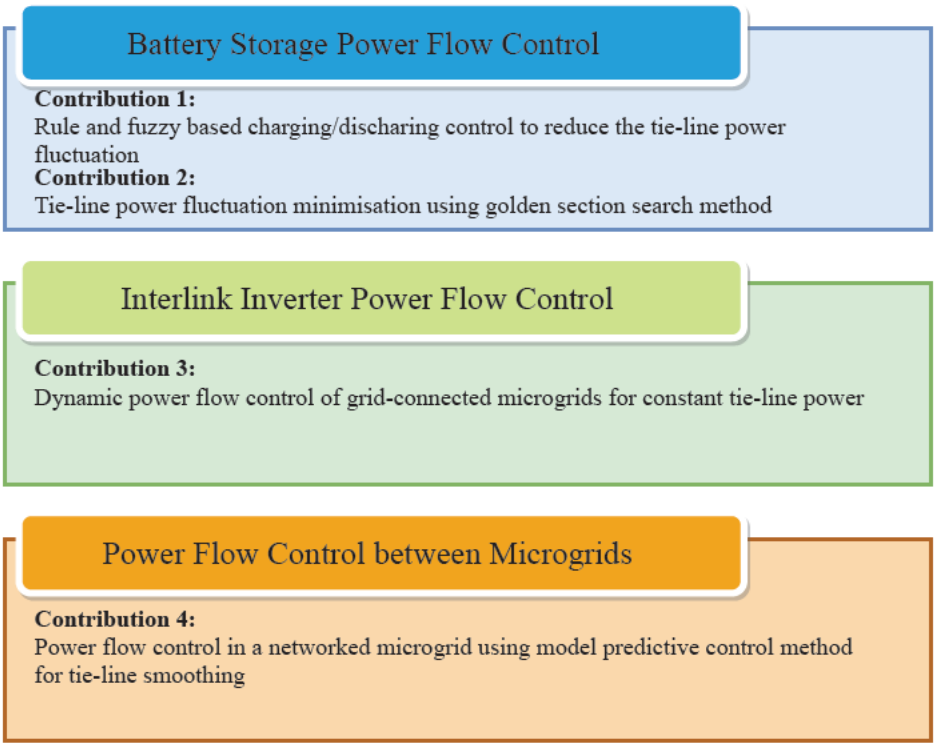

Fig. 1.1 A summary of research contributions

1.3 Main Research Contributions

This thesis offers four research contributions to solve the tie-line fluctuation problem in MGs. Fig. 1.1 summarises the main research contributions.

• Smoothing tie-line fluctuation plays a crucial role in dynamic operation of MGs. The first contribution of this thesis is the control of MG battery power by using a dynamic EMS to reduce tie-line fluctuation in grid-connected MGs. With regard to this objective, in Chapter 3, a fuzzy logic-based power flow control method is designed to determine the battery power based on the net power demand and battery state of charge (SoC) in the MG. The rule of the fuzzy logic is optimised using an off-line optimisation procedure for the predefined performance parameters. The results show that the proposed fuzzy logic control provides a reduced tie-line fluctuation in a grid-connected MG by maintaining the battery SoC in predefined limits in comparison with the other two rule-based methods.

• The second contribution, as presented in Chapter 4, is a non-linear programming method-based power flow control strategy proposed to maximise the use of battery and minimise the tie-line fluctuation in an MG using a dynamic EMS. A golden section search-based battery power management system is

designed by maintaining the battery SoC within limits. The method minimises the tie-line fluctuation in a grid-connected MG despite the variations in RESs and load demand. Moreover, a comparison with two other rule-based control methods is presented in a simulation experiment to validate the performance of the proposed control and optimisation methods.

• The third contribution, as presented in Chapter 5, is a grid-power controller designed for interlink inverters of MGs to achieve a constant tie-line power in a grid-connected residential MG on typical days of the year. The reference tie-line power of an MG is determined by the MG controller based on load dynamics, average PV generation and battery capacity. In addition, a state-space model is derived from the dynamic model of the MG for eigenvalue-based stability analysis. Several case studies have been formulated to demonstrate the performance of the proposed grid power control method by using real irradiance and typical residential customer load data in Queensland, Australia. Moreover, a comparison with a dynamic EMS-based method is performed to validate the performance of the proposed control method.

• The fourth contribution, as delineated in Chapter 6, is a distributed model predictive power controller proposed for interlink inverters of MGs to achieve a smooth tie-line power in an NMG. A dynamic model of MGs is used to predict the future value of grid power of individual MGs. In addition, tie-line power references of MGs are scheduled based on the forecasted generation and load in a network. Information sharing between MGs is conducted in a distributed manner to revise the instantaneous tie-line power references of MGs in each time step to obtain a smooth scheduled tie-line power for the network. Several case studies are illustrated in the simulation experiment to demonstrate the performance of the proposed distributed controller. Moreover, a comparison with the decentralised operation of MGs is presented to validate the performance of the distributed controllers in the NMG.

1.4 Thesis Outline

The remaining chapters of the thesis are organised as follows

Chapter 2 illustrates a comprehensive literature review on control and management of MGs.

Chapter 3 proposes a fuzzy logic-based dynamic power flow control method to reduce the tie-line fluctuation in an MG.

Chapter 4 presents a battery power management system to minimise tie-line fluctuation in an MG using a non-linear programming method.

Chapter 5 presents the development of an MG dynamic model and design of a grid power controller to obtain a constant tie-line power in a grid-connected MG.

Chapter 6 reports a distributed model predictive power control method to control the tie-line power in an NMG.

Chapter 7 summarises the research results and indicates future potential research directions in the relevant topic.

1.5 List of Publications

1. Islam M, Yang F, Ekanayek C, Amin M. Grid power fluctuation reduction by fuzzy control based energy management system in residential microgrids. Int Trans Electr Energ Syst. 2019;29:e2758.
DOI: https://doi.org/10.1002/etep.2758

2. Islam M, Yang F, Amin M. Dynamic control of grid-connected micro grids for tie-line smoothing. Int Trans Electr Energ Syst. 2020;30:e12557
DOI: https://doi.org/10.1002/2050-7038.12557

3. M. Islam, F Yang, M Amin. Control and optimisation of networked microgrids - A review. IET Renewable Power Gener.2021;15:1133-1148
https://doi.org/10.1049/rpg2.12111

4. M. Islam, F Yang, J Lu "Dynamic Power Flow Control in Networked Microgrids for Tie-line Smoothing" preparing to submit on IEEE Transaction on Power Systems.

5. M. Islam, F Yang, J Hossain, C. Ekanayeke, UB. Tayab. Battery management system to minimize the grid power fluctuation in residential microgrids. 28th Australasian Universities Power Engineering Conference, 2018.
DOI: 10.1109/AUPEC.2018.8758005.

Chapter 2

Literature Review

Chapter Contribution Declaration

This chapter addresses a comprehensive review on control and management of MGs. An introduction about MGs and NMGs in distributed power systems is presented. After that, a review on power flow control of MGs is illustrated. Moreover, a comprehensive review on control and optimisation of power flow in NMGs is demonstrated. Finally, advantages and challenges of networked operation of MGs are provided for future research integrity.

This chapter includes a co-authored paper. The bibliographic details of the co-authored paper, including all authors, are:

M. Islam, F Yang, M Amin. Control and optimisation of networked microgrids - A review. IET Renewable Power Gener.2021;15:1133-1148

https://doi.org/10.1049/rpg2.12111

My contribution to this paper involved: conceptualization, structure development, organising materials, the original draft writing, revising and proofreading.

Signed: _____ Date: *23.01.2021*

PhD Candidate: Mojaharul Islam (Principle Author)

Countersigned: _____ Date: *23.01.2021*

Principle Supervisor: A. Prof. Fuwen Yang (Corresponding Author)

Countersigned: _____ Date: *23.01.2021*

Associate Supervisor: Prof. Junwei Lu

Countersigned: _____ Date: *23.01.2021*

External Supervisor: A/Prof. Mohammad Amin

2.1 Microgrids and Networked Microgrids

2.1.1 Introduction to Microgrids

Renewable energy resources (RESs) are widely integrated in transmission and distribution power networks to reduce the carbon emission throughout the world. These RESs are one of the key driving element in smart grid power networks. The adaptation of these RESs in the distribution network has a reflection in terms of economic benefits from the customer level to the core system level for future smart grid networks. Besides that, control and protection of such power networks are challenging issues to maintain the stability and quality of the whole power system. Moreover, management of these power networks become more complex due to uncertain nature of RESs. The concept of microgrid is introduced to efficiently control, monitoring and management of the future smart grid power networks. An MG can be

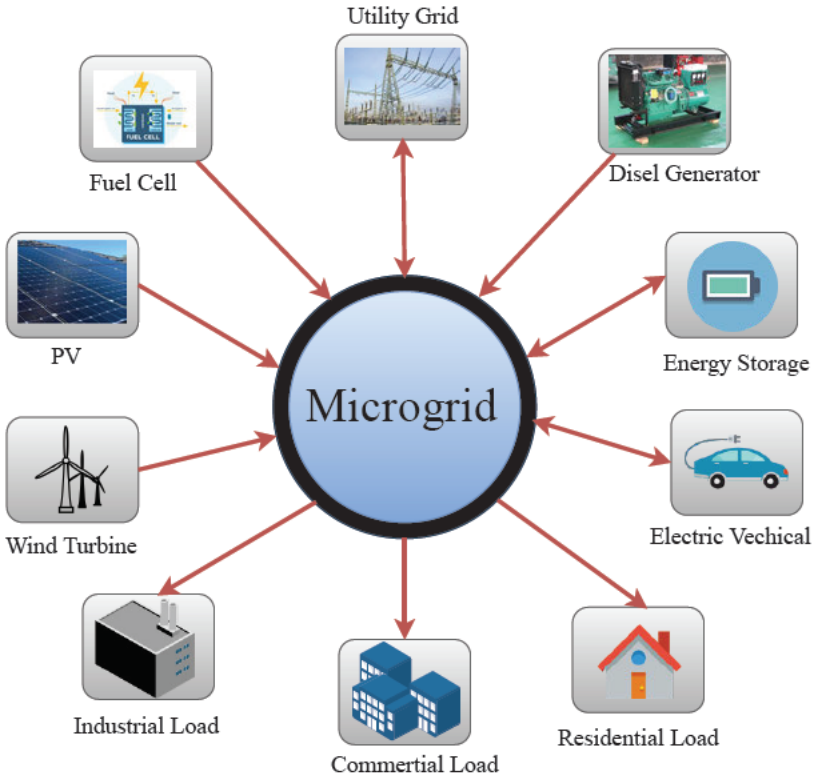

Fig. 2.1 Concept of an MG operating in the distribution networks

defined as a low/medium voltage network consists of different types of dis-patchable energy resources (diesel generator, hydroelectric, combined heat and power, micro-turbines) and non-dis-patchable energy sources (PV, wind turbine, fuel cell), energy storage systems (battery, flywheel, super-capacitor, thermal storage) and loads (control/uncontrollable loads, AC/DC loads) [1, 2]. In another word, an MG is a

small grid within a smart grid network which embedded various distributed energy resources (DERs) units, energy storage systems and load. Fig. 2.1 shows the concept of an MG operating in a distribution network. An MG has its own control and management unit to maintain the stability and optimal operation of the system. Due to independent operation capability, an MG can operate in grid-connected or island mode. In grid-connected mode, an MG is considered as an identical system in a distribution network works as a generating source during over generation period from DERs and as a load demand during power deficiency. On the other side, the autonomous island mode provides the flexibility and reliability to customers by providing continuous power supply to the time critical load inside an MG during fault situations. Thus, different control and management objectives are involved related with the operating mode of an MG. Bacuase of this, the design and development of electronic devices need careful consideration during planning stage of an MG. Several research has been done in last decay on monitoring, control and management of MG resources depend on the structural form. Jackson et al. [3] demonstrates a review of existing MG test networks around the world. Luida et al. [4] investigates the feasibility, control and management strategies of AC and DC MGs consists of RESs, ESS and load. The next section will provide a comprehensive review on control and management of single MGs.

2.1.2 Introduction to Networked Microgrids

In the last decade, distributed energy resources (DERs) have been integrated into transmission and distribution power networks to reduce the amount of carbon emissions worldwide and to meet the increasing demands of power systems [5, 6]. A microgrid (MG) is one of the leading features of a smart grid power network for integrating DERs within a distribution network [3]. An MG can be defined as a low-voltage (LV)/medium-voltage (MV) power network that integrates DERs and energy storage systems (ESSs) to create a grid that feeds different loads in the network and can operate in either grid-connected or island mode [7]. A networked MG (NMG) is an advanced MG concept in which a network is formed using several adjacent MGs. Fig. 2.2 illustrates a typical NMG in a distribution network. The goal of such network is to provide mutual power sharing with neighbouring MGs to increase the reliability of an MG network and to reduce operational costs. The network also enables restoring service to customers after a fault/deficient power condition occurs, efficient use of renewable energy resources (RESs) in the network, providing mutual support in island operation and reducing the burden on the main grid in grid-connected operation. Several similar concepts for defining NMG exist in the literature. Multi-microgrid (MMG), MG cluster and interconnected MGs are the most frequently

used terminologies in the literature to represent a network of MGs connected through an electrical power network to achieve power exchange amongst them.

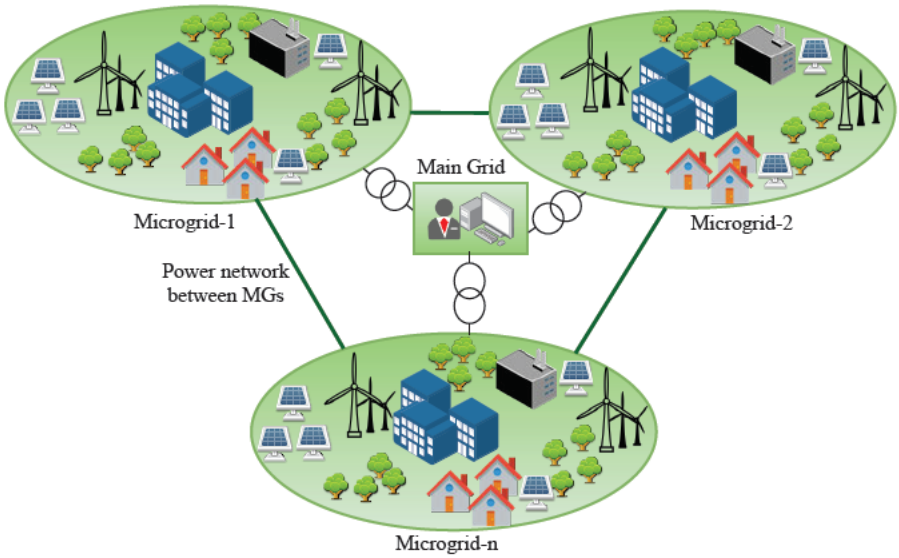

Fig. 2.2 A NMG in a distribution network

However, energy sharing between MGs creates a new challenge because multilevel optimisation is essential in energy management systems (EMSs). Moreover, the parallel operation of multiple MGs will raise the issue of controlling voltage and frequency throughout an NMG. Furthermore, delays in the communication network significantly impact the stability and performance of an NMG [8, 9]. A feasibility study of NMGs was conducted in [10–12] by focusing on the potential benefits and challenges of a network. Moreover, a review of the classification of NMGs based on AC/DC, voltage and phase-sequence constitutional forms was provided in [13]. A summary of NMG projects worldwide was also provided in this article. A comprehensive review of the control of DC MGs and DC MG clusters was included in [14]. The operational feasibility of DC MG clusters was discussed in the literature without an extensive discussion of control methods. In addition, a review of NMGs architecture, control, communication and operation was conducted in [15]. However, control and optimisation methods for NMGs were not included in this review. Meanwhile, the operation and control of NMGs were reviewed in [16] without focusing on control and optimisation methodologies. In addition, a survey on the distributed control and communication strategies for NMGs was presented in [17]. Different types of distributed control strategies and communication network reliability were discussed in this article. A survey on EMSs for NMGs based on EMS objectives, timescale and scheduling optimisation was also conducted in [18]. This research focused on optimisation methods under a distributed EMS structure. Hence, a review of

methods for obtaining optimised control and energy sharing in NMGs remains lacking. Studies have applied different methods and algorithms for the control and optimisation of energy in NMGs. This article discusses a typical classification of NMGs based on network formation. Thereafter, a summary of

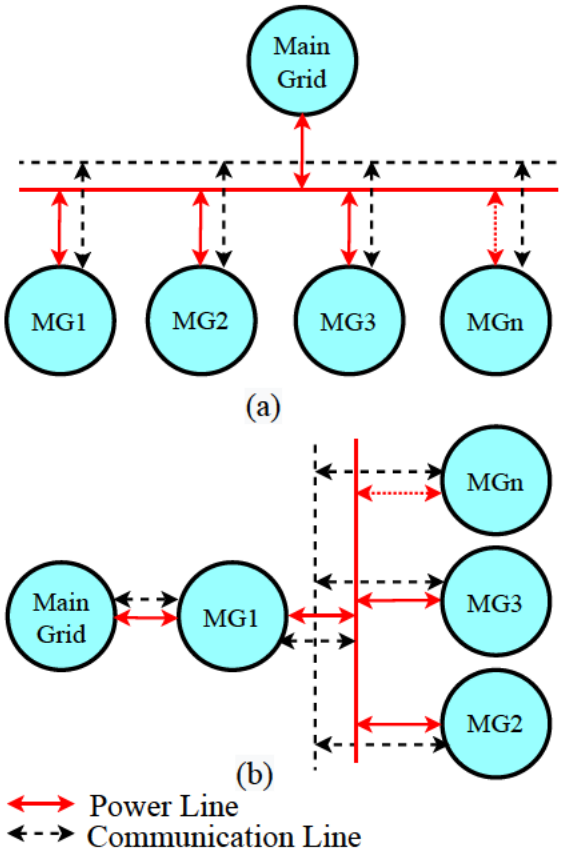

Fig. 2.3 Star-connected NMG

control structures and methods in different networked operation scenarios is reviewed. Furthermore, different EMS structures used in the energy optimisation of NMGs are discussed. In addition, a review of applied algorithms for achieving optimal energy management in networked operation is presented. Lastly, the major advantages and challenges of the networked operation of MGs are described for future research suggestions regarding this highly potential concept.

2.2 Power Flow Control of Microgrids

Due to stochastic nature of RESs and load, importance of power flow control and energy management in an MG is crucial for system stability and its performance. In addition, real time energy management system (EMS) in an MG needs fast response compared to conventional power systems [19]. The power

flow equation of an MG is the power balance equation between supply and demand. Equation (2.1) represents the EMS equation for a typical MG.

$$\sum P_{Load} = \sum P_{gen} + P_{ESS} + P_{grid} \qquad \forall t \tag{2.1}$$

Where P_{Load} is consist of critical and non-critical load of an MG, P_{gen} includes renewable and non-renewable energy resources of an MG, P_{ESS} is the energy storages to supply critical load in island or emergency situation and P_{grid} is the amount of grid support needed to balance the supply and demand in grid-connected operation.

The key objectives of power flow control and EMS in an MG are to define optimal set points for different controllable units inside an MG, cost optimization by economic aspects of the grid, smoothing the grid profile and reliability of customer service. Research has been conducted several ways to obtain the objectives of an MG such as demand side management, control of generation units, control and management of ESSs or combination of them. Based on the MG structure and requirement, appropriate control elements has been chosen during control and management of an MG. For example, demand side management described in [20, 21] to minimize the operating cost of an MG . R. Palma-Behnke et al. [20] presented the rolling horizon strategy for determining the set points of generation units and signals for customers based on demand side management. Similarly, in [21], the operating cost of an MG was minimized by 3.06% by controlling water pump and other electric loads in demand side management. On the other side, for maximizing the MGs profit, a day ahead optimal planning of generation units was made in [22] by keeping the system constrains in secure limit. Besides that, to minimize the cost of MG, receding horizon technique for optimal scheduling of battery was adopted in [23] where wind turbine is the key support for local load. Similarly, adaptive modified firefly algorithm is used in [24] to reduce the operating cost of MG considering the stochastic nature of RESs and load demand. In [25], to support the rapid fluctuation of demand in an MG, a composite ESS was used to allocate steady load to battery and dynamic load to ultra-capacitor. Y.-K., Chen et al. [26] deploys fuzzy logic in EMS where selling the electricity to the connected grid was the main priority of the control algorithm along with satisfying the demand of an MG. In addition, different methods and strategies are chosen for optimal operation of the MG based on the MG structure & predefined objectives. The following subsections discuss different power flow control methods of single MGs used in various studies.

2.2.1 Rule and Fuzzy Logic-based Power Flow Control

A. Rule-based Control

A rule-based power flow control method is a low cost and low complexity method implemented in EMS of an MG. In a rule-based method, several rules has been set up depending on the structure and control objectives of an MG. However, rule-based methods can not provide optimal solution for a complex system and can easily effected by system uncertainties. Several studies use rule-based method to obtain the operational objective of an MG. A rule-based control method is applied in [27] to monitor and control the active power flow in a smart MG system. The objectives of the EMS were to maximise the use of RES and to obtain maximum economic benefits. A rule-based model predictive controller was designed in [28] to set the binary decision variables using if-else rule. A single level control structure was employed using different sampling time for optimal operation of an MG. In [29], a rule-based EMS was proposed that optimized using grass-hopper optimization algorithm to obtain an efficient long-term capacity planning in an island MG. In [30], a rule-based EMS was applied using electricity price through out the day to obtain the peak shaving, and a smart ESS was used to provide a cost-benefit to the customers. Moreover, a rule-based centralised MG control system was implemented in [31] to keep the battery state of charge (SoC) within a predefined limit. The supply reliability to the customers and efficient use of RESs were ensured by controlling the tie-line power in grid-connected mode. Seamless transition control to island mode and reconnection to the main grid were also discussed in this article. In [32], a rule-based energy management was used to reduce the dependency on the main grid during power shortage inside an MG. The algorithm was implemented in a laboratory environment using dSPACE 1104 real-time operating system. An offline dynamic programming-based optimisation and a real time rule-based power flow control method was applied in [33] for energy scheduling of an MG.The proposed method was implemented in a magnetically coupled hybrid renewable energy system connected to the load using a multi-winding magnetic link. In [34], a rule-based dispatch algorithm was used in a hybrid MG by prioritising system buses and components. In [35], a comparative study between a rule-based and a MPC-based EMS was presented targeting the cost effective-benefit analysis of the methods in a office building MG. The results demonstrated better performance using the optimising method in compare with the rule-based method.

B. Fuzzy Logic-based Control

A fuzzy Logic is an extension of multivalued logic whose objective is approximate reasoning rather than exact solution. A fuzzy logic block consists of three functional blocks such as fuzzification block, interface engine and defuzzyfication block. The ideal procedure to design a fuzzy logic controller (FLC) based system is summarized as follows:

1. Design the membership functions (MFs) of inputs and outputs.
2. Set the rules to determine crispy output.
3. Adjust the membership functions and rules to optimize the performance parameters.

A fuzzy logic control is a widely acceptable method for power flow control and management of an MG. In [26], a fuzzy logic was deployed in EMS of an MG and the main priority of the control algorithm was to sell the electricity to the main grid along with satisfying the demand of an MG. Besides that, a fuzzy logic based coordinated control between a dispatch-able distributed generation and a ESS was proposed in [36] to adjust the active power reference of the battery based on SoC and targeted active power from battery to minimize the grid power in grid connected mode. In [37] , a fuzzy logic-based EMS was applied to increase the profit of an investment in a polygeneration MG included the electricity, transport and water. In [38] , partially management of the battery was presented using FLC and grid power is determined by filtering the high frequency component from the difference between MG net power and FLC output. A different strategy was implemented in [39], where the amount of power assigned to the grid was computed as a sum of two components. First one was the average value of net power demand calculated by a moving average filter and second one was the modifying term of the grid power calculated by a FLC to increase, decrease or maintain grid power and to maintain the battery SoC within secure limit. A FLC-based EMS was developed in [26] to optimize the energy distribution in an MG and to maintain the battery health. A RS-485/ZigBee network was used to conduct the data collection from system and then the developed fuzzy control method was implemented in an intelligent management system. Besides that, a battery management system was developed in [40] using a FLC to decide the charging/ discharging of battery based on power distribution cost and system loss. A fuzzy interface system was develop in [41] to reduce the tie-line fluctuations and to increase the life-time of the battery. To improve an MG economic efficiency, a FLC was designed in [42] to apply in battery management system. A genetic algorithm (GA) was used in this study to optimize the fuzzy design parameters. A fuzzy logic expert system was used in [43] for scheduling the battery of an MG based on forecasted

generation profile. A comparison with heuristic flowchart battery scheduling method was demonstrated to show the performance of the fuzzy system in term of cost minimisation and reduced emission level. Furthermore, a fuzzy logic based battery management system was designed in a supervisory control scheme of an isolated MG to maximise the use of RESs and to keep the battery SoC with in limit [44]. Several scenarios had been demonstrated to show the effectiveness of the battery management system. In [45] , a fuzzy based expert system was developed to control the output power of the battery

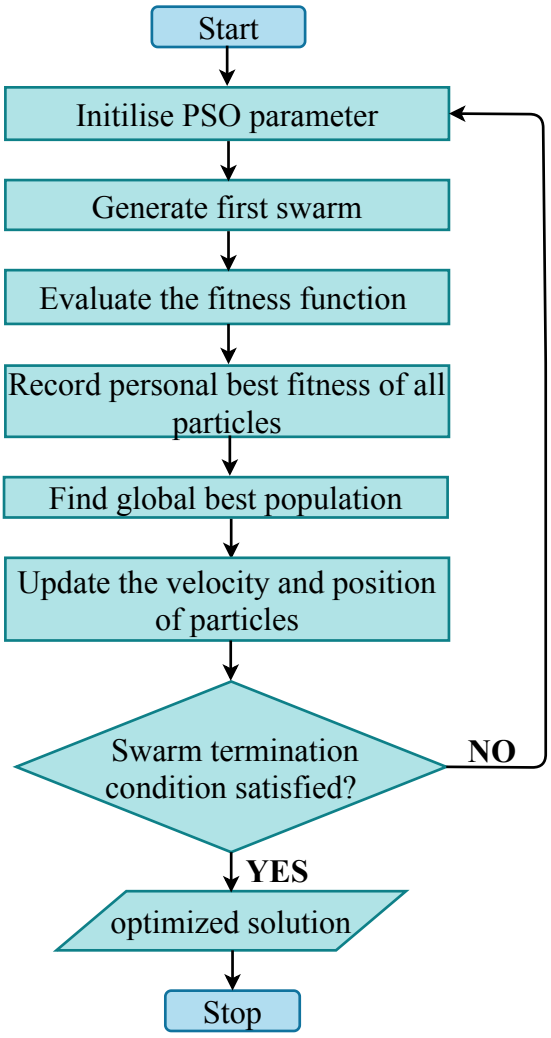

Fig. 2.4 Flow chart to solve the optimisation problem using particle swarm optimisation algorithm

to achieve reduced operation cost in an MG. Two GAs were engaged in the system to optimize the membership functions and fuzzy rules. A fuzzy logic based EMS was employed in [46] and the FLC was optimised by an artificial bee colony algorithm to increase the system energy saving efficiency and to reduce the operation cost of an MG. In [47], a fuzzy logic based EMS was presented with a hybrid

energy storage system to improve the economic performance of an MG. To maximise the duration of power supply to the customers, a fuzzy logic based approach was implemented in [48] in an island MG based on availability of RESs and ESS.

2.2.2 Heuristic Algorithm-based Power Flow Control

A. Particle Swarm Optimisation

A particle swarm optimisation (PSO) determines the position and velocity of all particles in a search space using a mathematical formulation to find the solution of an optimisation problem . Fig. 2.4 shows the routine process for obtaining an optimised solution using PSO algorithm. PSO algorithm is widely used to solve the optimisation problem in an MG. A modified PSO was used in [49] to solve the optimal dispatch problem of an MG. The results demonstrated the lower operating cost and less carbon emission on the application of the proposed method. An efficient PSO approach was presented in [50] to minimise the total energy and operating cost of an MG. The weibull and normal distributions were used to model the system uncertainties. After that, the operation and management of the DERs ans ESSs were done by maintaining the system constrains. A new model of a hybrid MG was presented in [51], and an canonical differential evolutionary PSO was applied to optimise the energy inside the MG. In [52], an adaptive EMS was implemented using advanced metering infrastructure to reduce the system operational cost. A new concept "operation value factor" was introduced to improve the overall system performance and a PSO algorithm was applied to solve the optimisation problem. A two stage stochastic management approach was used in [53] to achieve faster computation, smaller conservative bounds and lower operational costs. The optimal power of the MG was obtained by applying affine arithmetic and stochastic weight tradeoff PSO algorithm. Besides that, an adpative modified PSO based on a chaotic local search mechanism and a fuzzy self adaptive structure was employed in [54] to solve the multi-objectives optimisation problem in an MG. The objectives of the optimising problem were to minimise the operating cost and net emissions in a renewable energy-based MG. A comparison with GA and conventional PSO algorithm was performed to show the effectiveness of the proposed structure. In [55], an improved PSO-exterior point method was used to solve the multi-objectives scheduling problem in an island MG. The evaluation indexes indicated better performance of the proposed energy scheduling method compared with a single objective solution. The generations and demand forecasting errors were counted in [56] and a modification inertia weight of the PSO algorithm was applied to solve optimal scheduling problem of an MG. An optimal power problem was formulated in [57] to minimise

the operating cost and emission in an MG. A bird swarm optimising algorithm was used to solve the optimisation problem and the proposed solution was implemented using a IEEE 30-bus testing system. A power flow controller was designed in [58] to control the power flow between an MG and main grid during the load change conditions. A PSO algorithm was applied for real time tuning of the active and reactive power to share the MG load with main grid. A fuzzy optimisation model was presented in [59] and solve using binary PSO algorithm to minimise the total cost and network losses in an MG. In [60], a modified multi-objective PSO algorithm was proposed to minimise the operation cost and emission using a real-time EMS. A comparison with multi-objectives GA was presented in the article that showed the faster computation time using PSO algorithm to solve the optimisation problem. Furthermore, a day ahead optimal scheduling was done in [61] using PSO and GA. In the optimisation problem, a dynamic pricing scheme was considered to minimise the cost paid by the customers.

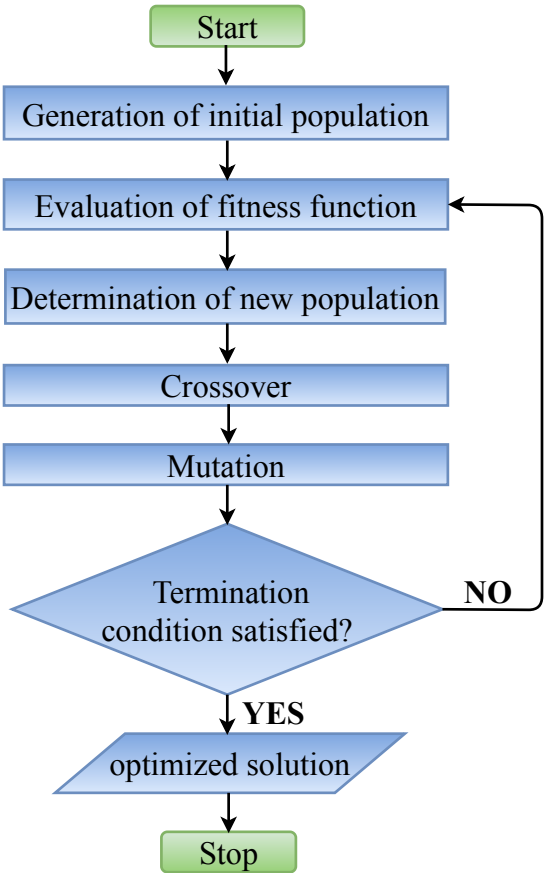

Fig. 2.5 Flow chart to solve the optimisation problem using genetic algorithm

B. Genetic Algorithm

A GA is a search heuristic algorithm that is motivated from natural evaluation theory. There are five steps in a GA algorithm such as initial population, fitness function, selection, crossover, and mutation to search for an optimal solution. Fig. 2.5 shows the routine process for obtaining an optimised solution using genetic algorithm. Several studies used GA algorithm to solve the power flow optimisation problem in an MG. An energy and reverse scheduling problem was discussed in [62] under a high performance EMS to obtain the optimal switching sequence of DERs and responsive load. The uncertainty of generations and load was considered in the optimisation framework and a GA was used to solve the optimisation problem. A memory-based GA was applied in [63] to minimise the energy production cost of an MG. A centralised EMS was used to gather all information and decided the generation set points between a number of DERs. Moreover, a comparison with conventional GA and PSO was presented to show the superiority of the proposed method. A optimal dispatch model of MG EMS was presented in [64] to minimise the operating cost, emission as well as maximise the utilisation of RESs. The optimisation problem was solved using a GA algorithm under variable load conditions. An energy trading model was developed in [65] based on the forecasted generation of RESs in an MG and a GA was used to decide the energy trading with the main grid. A GA-based optimal power flow control was employed in [66] to minimise an MG set up cost including PV and battery system. In [67], a smart EMS for an MG was proposed that consists of forecasting and optimisation module. First, a day ahead forecasting was presented based on different weather variations. After that, a matrix real-coded GA was used to decide the optimal economic operating point of the MG.

C. Other Heuristic Algorithms

A day-ahead energy scheduling model was formulated in [68] and a hybrid harmony search algorithm with differential evolution was applied to solve the energy optimisation problem. The proposed model and algorithm were validated using IEEE 9-bus, IEEE 39-bus and IEEE 57-bus systems MGs. In [69], the experimental design and validation of a home-based MG operating in island mode was presented using a central EMS structure. The central EMS was combined with forecasting module and real-time management system to minimise the cost margin and to provide plug-and-play functionality of the MG. The EMS problem was solved using multi-period artificial bee colony algorithm. Moreover, a comparison with mixed-integer non-linear programming was presented to show the effectiveness of the proposed algorithm. A multiperiod artificial bee colony optimization algorithm was also used in [70] to implement

the economic dispatch of an MG considering demand response. An artificial neural network combined with a markov chain method was adopted in this study to forecast the uncertainty of RESs and customer demand. In [71], an intelligent dynamic EMS was adopted using a action-dependent heuristic dynamic programming for energy scheduling of a RES dominated MG. A comparison with decision tree approach based EMS was presented to illustrate the MG operation in different ESS conditions. An optimal operation of a grid-connected MG was discussed in [72] and a new recurrent neural network was applied to minimise the grid power over a week horizon. A gravitational search algorithm was used in [73] to solve the energy optimisation problem in an MG to achieve improved economic dispatch, peak-shaving and generation cost minimisation. In [74], a modified bacterial foraging optimisation algorithm was employed under an intelligent EMS to find the optimal set points of DERs in an MG. A multi-layer ant colony optimization algorithm was used in [75] to figure out the optimal operating point of DERs in an MG. The results showed that the proposed method had reduced the energy cost of the MG by 5% in comparison with PSO algorithm. A reinforcement learning algorithm was applied in [76] for scheduling the battery power though continuous interaction with customer agents for reward optimisation. A distributed EMS was proposed in [77] to set the optimal power regulation of DERs in an MG. An alternating Direction Method of the multiplier was used to solve the power management problem.

2.2.3 Model Predictive Control

In [23], a model predictive control (MPC) framework was used in EMS of an MG to utilise the battery during peak period and to support the local load using RESs. The proposed method was simulated using real weather and load profile in a test-bed MG. An MPC-based online resource scheduling was done in [78] for an island MG to improve RESs utilisation, system efficiency and battery life time. A comparative study had been carried out with fuzzy-based EMS to show the improved result for MPC-based EMS. A two-stage MPC optimisation strategy was adopted in [79] for a rural area MG consists of diesel generator, RESs and battery. At the first stage, real time forecasting of the future power profile was done to calculate the optimal power dispatch. At the second stage, the output power of the diesel generator was adjusted using a boundary value problem to reduce the forecasting error. In [80], an EMS problem was solved using an MPC algorithm that ensures faster computational time for a large MG. A lithium-ion battery was used in the MG to reduce the peak demand during grid-connected mode and to support deficient power during island mode. A power dispatch optimisation had implemented in [81] using an MPC to control the each sub-system in an MG. All sub-systems coordinated each other through a central management system to minimise the cost of the whole system. An MPC-based DC-AC

inverter was designed in [82] to regulate the grid power flow in an DC MG. Besides that, a hybrid ESS consists of battery and super-capacitor was used to suppress high and low frequency variation in the MG for achieving an effective EMS. A lyapunov-based hybrid MPC was used in [83] to deal with energy management problem in an MG. The results demonstrated the recursive feasibility and closed-loop stability of the system in more effective manner. A coordination strategy between RESs and charging/discharging of electric vehicle was implemented in [84] using a robust MPC to provide economic optimisation in an MG. A number of scenarios had been demonstrated to show the probabilistic guarantee of EV constrains satisfaction. An MPC-based home EMS was presented in [85] to minimise the operating cost of an MG. An mixed-integer linear programming (MILP) algorithm was used to solve the optimisation problem considering the forecasting uncertainty of RESs and load. Several case studies had been conducted to illustrate the benefit of the proposed method compared with traditional benchmark. In [86], a three-layer coordinated scheduling system was presented using an MPC framework, and a GA was combined with an MPC to solve the optimisation problem of an MG. In [87], MPC approach was employed to solve the energy optimisation problem of a RESs dominant MG. A hybrid ESS was used to control the power exchange with the main grid considering operational cost, degradation issues, and associated constraints. An MPC based operation optimisation technique was proposed in [88] to minimise the cost of energy taken from grid. The performance comparison of the MPC method had been performed with a rule-based method for a labscale MG and a commertial MG.

2.2.4 Linear/Non-linear Programming

A mathematical model of the EMS problem was formulated in [89] by considering power flow constrains and system unbalance in an island MG. The EMS problem was decomposed into a mixed-integer linear programming (MILP) and a non-linear programming to reduce the computational time. The proposed method is tested using CIGRE medium-voltage benchmark system. A demand-response programming was used in [90] to obtain peak shaving by using a peak-time rebate scheme. An optimal EMS was used to control the battery, DER and shifting load so that both MG and man grid can be benefited from the scheme. In [91], an MILP approach was used to model the EMS problem in an MG and to minimise operating cost subject to economical and technical constraints. To minimise the operational cost of an island MG an EMS was proposed in [92] by using the droop characteristics of DERs. An MILP was used to solve the optimal power flow control problem that ensured maximum utilisation of the system assets. A mixed mode EMS was presented in [93] for efficient use of ESSs and an MILP method was used to solve the EMS problem. Besides that, optimal sizing of the ESSs was done using PSO technique

to minimise the installation and operating cost of an MG. An EMS problem for a real life residential MG consists of several apartments were addressed in [94]. An MILP method was used to solve the energy optimisation problem considering several system constrains. The results demonstrated energy cost saving solution for an MG community. In [95], three different scheduling were employed for an MG that included customer driven, MG operator driven and MG operator driven with utility constraints. A gradient-based search method was adopted to solve the optimisation problem. Moreover, a comparative analysis amongst three scheduling method was also presented in terms of network loss and customer benefits. An EMS model for a residential MG consists of vehicle to grid system was presented in [96] by separating the household load into three different profiles. The results demonstrated a reduction of the energy cost by 10% per day for a typical Spanish house. An optimised EMS was used in [97] to reduce the fuel cost by effective use of the battery in a remote military base MG. An MILP method was used to solve the optimisation problem by considered the effect of battery sizing on overall economic benefit of the MG. Furthermore, an MILP-based EMS was formulated in [98] for a three-phase residential MG to minimise the operational cost by taking into count system constrains. The results showed that proposed method method provide accurate solution compared with non-linear formulation of the optimisation function. A demand response programming was used in [99] for component size optimisation in an MG. The analysis showed that component sizing will also provide relevant cost saving of the MG system.

2.2.5 Dynamic Power Flow Control of Microgrids

Dynamic control and management of an MG in a crucial issue for real-time operation and control of an MG. The stability of the whole system also effects on dynamic operation of an MG. P-Q and droop control have been used in several studies to implement the dynamic operation and control of an MG. In [100], a smooth transition between different operation modes of an MG was the main focus of the research. A small signal model of an MG was presented including droop controller, network and load. A GA algorithm was used to find the optimal settings of the key control parameters in MATLAB simulink environment to show the enhanced dynamic performance of the MG. A dual-layer control was used in [101] for autonomous control and optimisation of an DC MG under system disturbances and mode transition. First, droop gains of DERs updated using an event-driven scheme for simultaneous load sharing and system optimisation. After that, an adaptive voltage droop scheme had implemented in primary level for effective load sharing between DERs. The proposed control was implemented through simulation and lab experiment to show the validity of the control method. In [102], a voltage-frequency $(V - f)$ and an active and reactive power $(P - Q)$ control method was applied in PV unit of an

MG to obtain an integrated control with the aid of the battery. In island mode, voltage-frequency control was used to obtain coordinate control between maximum power tracking control and battery charging/discharging control. On the other side, $P-Q$ control was used for coordinate operation in grid-connected mode. In [103], a coordinate control method was also employed in a hybrid MG for effective transition of MG in various operating mode. A $V_{dc}-Q$ or $P-Q$ control was adopted for grid-connected operation of interlink inverter to implement the power exchange between AC and DC system. Similarly, a $V-f$ control method was adopted in island mode for achieving system wide stability and power flow control of an MG. A new power sharing method was introduced in [104] by integrating a superconducting magnetic energy storage with a battery to obtain the primary frequency control in an island MG. An MG test bed based on Uligam Island of Maldives was developed in PSCAD and a comparative analysis with a hybrid ESS was presented using a dynamic droop control approach. A dynamic model and operation strategy for a RESs dominant MG was used in [105] to explore the system-wide performance during RESs, local AC load and grid power variations . The study used a multiple input DC-DC converter to integrate RESs into the main DC bus. In [106], a control strategy was proposed for inverter oriented DERs to improve MGs transient response during fault condition. A reactive power control method was demonstrated in [107] to maintain the bus voltage near nominal value for an island MG. An MPC-based scheme was used to predict the future behaviour of the bus voltage and to compensate the difference between generation and demand of reactive power. Several case studies had been conducted to validate the system performance using the proposed control method. In [108], a small signal model of an MG was presented that consists of a RES, a synchronous generatora and an ESS. Model of each element of the MG was developed individually and combined using a global reference axil frame. The eigenvalue-based stability analysis of the developed model had been conducted to see the sensitivity of the model in different operating modes and control strategies. An enhanced control strategy for a superconducting magnetic energy storage was developed in [109] to improve the power flow control and the system stability in a wind power oriented MG operating in island mode.

2.3 Control of Power Flow in Networked Microgrids

NMGs control is a challenging issue in regulating the voltage and frequency of the network under different operating scenarios and system architecture. Optimal power sharing amongst DERs is another challenge in an NMG. The control of single MGs was discussed in several articles [110–115]. However, control in NMGs has recently become the focus because of the increasing interest in NMG research. Hierarchical

and distributed control structures are used in research to achieve the control objectives of NMGs. The hierarchical control structure used in [116, 117] demonstrated the operational feasibility of NMGs in a distribution system. Meanwhile, a distributed control structure was presented in [118, 119] for a network of MGs operating in island mode. Figs. 2.6(a) and 2.6(b) illustrate the control pyramids of NMGs that use hierarchical and distributed control structures. In a hierarchical control structure, primary level control implements droop control, island detection and local protection in an MG. Meanwhile, the secondary level control performs voltage and frequency regulation due to primary level deviation, grid synchronisation, optimal operation of DERs in an MG/NMG and real-time energy management to maintain the power balance of individual MGs in the network. Tasks in secondary level control can be performed using three controlling concepts: centralised, decentralised and distributed. In the centralised control approach, an MG central controller collects information from all the measurement units of the system through a communication link and performs optimal scheduling of DERs and load in an MG. The central controller also communicates with DNO or other MGs to implement tertiary level control. Centralised control is the most applied approach to power systems due to its implementation flexibility. The major drawbacks of the central control approach are single point of failure, high bandwidth requirement and hindering of the plug-and-play functionality. Decentralised and distributed controls can be implemented using local information to eliminate the necessity of a central controller. Decentralised control does not consider information sharing with neighbouring nodes and uses only local information to accomplish an optimal decision. Droop control can be used to implement decentralised control. The

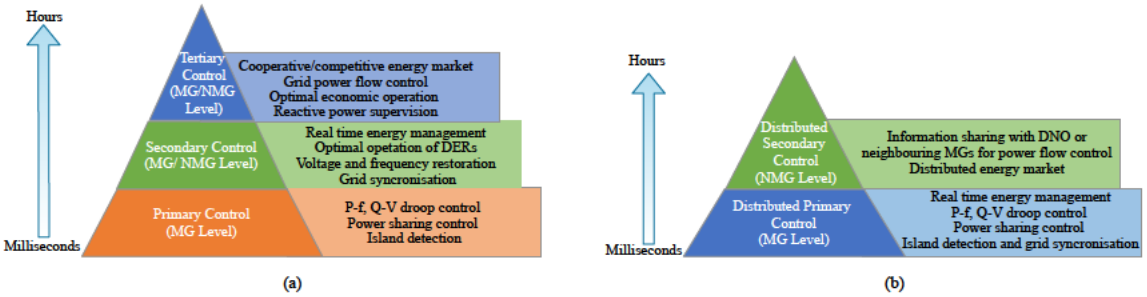

Fig. 2.6 (a)Hierarchical and (b) Distributed control structure of NMGs

major drawback of decentralised control is its poor system performance due to lack of communication. The distributed control approach uses information sharing with neighbouring DERs to overcome the downside of centralised and decentralised controls. DERs in an MG/NMG send/receive information with adjacent nodes to perform optimal operation and power sharing amongst DERs. Distributed control exhibits plug-and-play capability, low bandwidth requirement, high flexibility and system side

Table 2.1 Summary of recent studies on the control of NMGs

Main Research goal	Major Remarks	References
Voltage and frequency control	• Distributed secondary control • Pinning based PQ and droop control • ESS is not counted	[120]
	• Hierarchical control • Large signal model • Uncertainty of RES is not considered	[117]
	• Power exchange control • Model predictive control • Generation uncertainties has ignored	[121]
	• Distributed control • Adaptive neural network • ESS is not counted	[118]
	• Distributed control • Droop control • RES and ESS are not considered	[122, 123]
	• Distributed control • Cluster-oriented control • Double-layer communication network	[124]
	• Primary frequency control • Reinforcement learning • No experimental validation	[125]
Voltage stabilisation and generation cost minimisation	• Hierarchical control • Finite-time consensus algorithm • Uncertainty of RES is not considered	[126]
System stability margin	• Power exchange control • Adaptive fuzzy droop control • Uncertainty of RES is not considered	[127]
	• Dynamic assessment • Reachable set computation • No real time simulation	[128]
	• Genetic Algorithm • Dynamic Droop • No experimental validation	[129]
V-I controllability	• Design robustness • Probability index • No real time simulation	[130]
Steady state error	• Primary control • Feed-forward and robust feedback control • Uncertainty of RES is not considered	[131]
Active and reactive power control	• Virtual impedance • Genetic Algorithm • ESS is not counted	[132]
	• Tertiary control • Graph theory • ESS is not counted	[133]
	• Hierarchical communication graph • Building MG-community • EES is not counted	[134]
	• Distributed secondary control • MAS • Networked depended control	[135]

performance enhancement. Tertiary level control performs market operation with DNO. Each MG in the network shares its buy/sell information, such as price signal and reserve capacity, with DNO. On the basis of the information shared by individual MGs, DNO performs optimal market operation to facilitate network-wide power sharing. In cooperative island mode, MGs in the network can share information with a dominant MG instead of sharing information with DNO based on the previous consensus. The dominant MG performs market and system stability operations in island operation mode. Meanwhile, distributed control structure consists of two levels: distributed primary control and distributed secondary control. In distributed primary level control, each MG performs voltage, current and frequency regulation, island detection, grid synchronisation and load power management in an MG. In secondary level control, MGs share the necessary information for power sharing or maintaining system-wide control to neighbouring MGs or DNO. On the basis of network information, each MG determines the necessary actions to achieve the individual/network objectives based on the previous consensus between MGs and the DNO. Table 1 summarises recent studies on NMG control based on the primary research objectives. Meanwhile, several methods have been applied to control NMGs under different operating conditions. The following subsections discuss the main control methods applied in recent studies.

A. Droop Control

Droop control is a well-established method for load sharing in parallel connected inverters in an MG [136, 137]. The characteristics of conventional droop control, i.e., $P-\omega$ and $Q-E$, can be represented using Equations (1-2) and Fig. 2.7.

$$\omega_k = \omega^* - m_k P_k \tag{2.2}$$

$$E_k = E^* - n_k Q_k \tag{2.3}$$

Where P_k, Q_k, m_k, n_k, ω and E are the output active power, output reactive power, frequency coefficient, voltage coefficient, rated frequency and rated voltage of the kth inverter, respectively. Droop control techniques can be divided into three types:

1. conventional droop control,
2. virtual impedance droop control,
3. adaptive droop control.

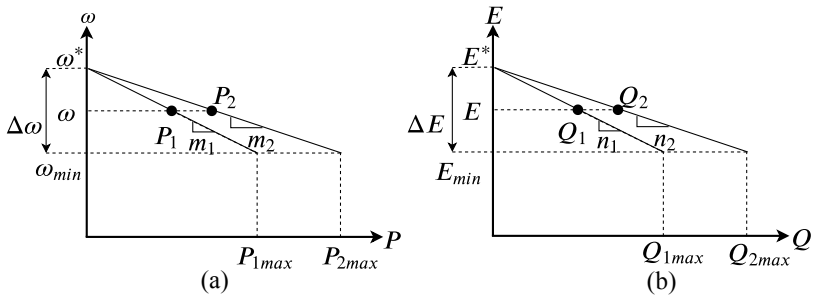

Fig. 2.7 (a) P-ω and (b) Q-E droop

Conventional droop control is useful for maintaining voltage and frequency in parallel connected inverters by avoiding critical communication links. The major drawback of conventional droop control is a slow transient response and poor harmonic load sharing amongst inverters under line impedance mismatch and nonlinear load conditions. Virtual impedance-based droop control overcomes the line impedance mismatch problem through improved reactive power sharing amongst parallel-connected inverters. The major drawback of virtual impedance droop control is the degradation of voltage regulation. However, adaptive droop control is applied to address slow transient response and achieve accurate power sharing amongst inverters by maintaining system-wide voltage and frequency within an acceptable limit.

Droop control can also be used to control voltage and frequency in an NMG. A distributed secondary control was applied in [120] for achieving coordinate operation between droop-controlled and PQ-controlled DERs in an NMG. Coordination was realised on the basis of pinning control and a group consensus algorithm. Primary and secondary controls were implemented in [122] using a distributed control framework. At the primary control level a droop controller was used to facilitate proportional load

sharing among DERs in the network. And, at the secondary control level voltage deviations due to load change and adjusting power generation of DERs to facilitate the power exchange among MGs. In [126], a droop function was modified by adding voltage deviation and average marginal cost in secondary and tertiary levels in a cluster of DC MGs.The objective of the control was to maintain a stabilised voltage throughout the network and reduce generation cost. A two-layer power flow model was introduced in [138] using a hierarchical control structure to regulate the critical bus voltage and frequency after a disturbance. Coordinate control of RES-dominant MGs was presented in [139] to achieve network operation in grid-connected and interconnected island modes. Droop control was used to realise network power sharing in interconnected operation mode. Moreover, an improved droop control strategy was implemented in [140] to reduce voltage and frequency fluctuations in MMG environment. In addition, pinning-based control method is highly suitable for MGs with a large number of DERs. A pinning-based DER cluster-oriented tertiary control was used in [123, 124] to generate a voltage/frequency reference based on power mismatch amongst MGs in a cluster. A distributed secondary droop control was implemented on the basis of the generated reference for maintaining the voltage and frequency of MGs in a cluster along with optimal power sharing. Virtual impedance control is an improved version of the droop control method that can increase reactive power sharing between parallel inverters by adding virtual impedance to the control loop. In [132, 141], a virtual impedance controller was designed to minimise global reactive power sharing between MGs in a network of MGs. An adaptive droop control-based coordinated control scheme was presented in [140] to achieve power-sharing amongst MGs and boost frequency and DC voltage stability in a DC/AC NMG.

B. Model Predictive Control

Model Predictive Control (MPC), also known as receding horizon control, is widely recognised as an optimal control strategy that exhibits high performance [142, 143]. Optimised control is achieved on the basis of future behaviour predicted by a linear model of the entire system [144]. The general equations for MPC are presented as Equations (3–4).

$$\Delta x(k+1) = A\Delta x(k) + B\Delta y(k) + C\Delta u(k), \tag{2.4}$$

$$0 = D\Delta x(k) + E\Delta y(k) + F\Delta P(k). \tag{2.5}$$

Where x denotes the dynamic state variables, y denotes the algebraic variables outside each MG, u denotes the control variables (voltage, frequency or power) and P denotes the uncontrolled variable of

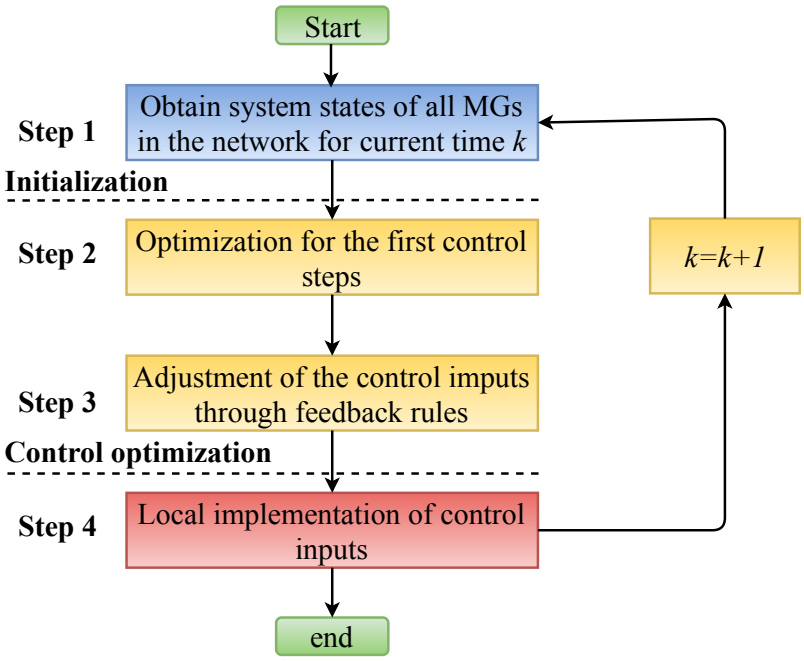

Fig. 2.8 Procedure for implementing the MPC method in an NMG

the system (DERs/load). (A–F) are the system matrices of the linear system model. The ideal procedure to implement the MPC methods in an NMG are illustrated in Fig. 2.8.

*Step*1 : Each MG in the network determines its linear model, measures the local states $x(k)$ and allows states of neighbouring MGs.

*Step*2 : Each MG determines the optimal control sequence for generating the first control effort.

*Step*3 : The control inputs are calculated, and the results are implemented in the local controllers.

*Step*4 : The sampling time index $k = k + 1$ is increased, and the preceding steps are repeated.

The major advantage of MPC is predicting system disturbance to perform an upcoming control action and improve the transient responses of a system. An accurate system model is a prerequisite for implementing this control method. Moreover, the possible cost of the controller is another downside of the MPC method. MPC-based control is a prominent method for controlling voltage and frequency in a networked of MGs. In [128], an MPC method was used to regulate the voltage and frequency of DERs in an island MG connected to an adjacent grid-connected/fully island mode MG. An MPC method was also applied in [145] for controlling frequency in an NMG by adjusting the voltage of voltage-sensitive loads and maintaining voltage constraints. A distributed economic MPC was presented in [146] for coordinated stochastic power sharing amongst MGs.

C. Graph Theory-based Control

A graph is a set of nodes that are connected through a set of edges [133]. Graph theory-based distributed secondary and tertiary controls were mentioned in the research to reduce power mismatch between MGs and DERs in NMGs. A two-layer hierarchical communication graph was presented in [134] to utilise a thermostatic control load in a building MG community. The inner and intra building communication graph ensured that power regulation and dispatch orders are at satisfactory levels. A graph theory-based tertiary control was proposed in [133] to regulate power sharing in a DC MG cluster. Cooperation amongst MG agents determined the voltage set point for the proportional sharing of networked load within the MG cluster. A two-layer distributed control method was implemented in [135] by using two subgraphs. The first graph ensured demand–supply balance, and the second graph reassigned controllable DERs for optimal power dispatch.

D. Artificial Intelligence Control

Artificial intelligence (AI) control methods are widely used for controlling single MGs [147, 148]. AI control methods can be easily applied to solve the control problem in a complex power network, such as an NMG. Long processing time and excessive memory are the major drawbacks of implementing AI-based control methods in a real application. Several studies have also applied AI-based methods to control voltage, frequency and power in NMGs. Adaptive primary and secondary voltage and frequency controllers were developed in [118] for inverter-based DERs in an island NMG. The controllers were designed using neural networks and distributed cooperative control theory to reduce the dependency of the controllers on system dynamics and to achieve PQ power sharing amongst DERs in a network. An adaptive deep dynamic programming scheme consisting of three deep neural networks was applied in [149] to achieve integrated frequency control in a network of MGs. This control replaces conventional load frequency control and generation command dispatch to minimise frequency deviation and generation cost in an MG network. Meanwhile, an adaptive fuzzy interface system was implemented in [127] to regulate the droop coefficient in a network of DC MGs, increasing system stability margin and power allocation precision. In [150], a genetic algorithm-based control method was used to enhance system stability in photovoltaics (PV) MG clusters by addressing oscillation due to the dynamic nature of PV. The effect of a large transient due to inverter switching and end-user load on system dynamic stability was analysed in [125] for a RES-dominant NMG. A reinforcement learning-based trained controller was adopted to avoid considerable frequency deviation by reducing system voltage set point. Moreover, a reinforcement

learning-based distributed secondary control was implemented in [151] via reward feedback pinning for the selected distributed generators in an MMG system. In [131], a robust feedback voltage control strategy was applied to suppress system disturbance caused by DER output in MMG. An alternating direction method of multipliers (ADMM)-based tertiary control was implemented in [152] to solve the optimal power flow problem and provide real and reactive power references for secondary control level in an NMG.

2.4 Advantages and Challenges of Networked Operation of Microgrids

The operation of an NMG has several advantages and challenges. This section presents the major advantages and challenges of NMGs.

2.4.1 Advantages of Networked Microgrids

A. Cost Effectiveness of Networked Microgrids

One of the primary purposes of NMGs is to gain economic benefits via mutual energy sharing amongst MGs [153, 154]. In this concept, one or more MGs in a network exhibits excess generation or has a resource that can generate more power. By contrast, one or more MGs in the same network exhibits a shortage of power generation for a short/long period. In such case, excess power or capacity can be sold to overcome the power shortage of a network. The additional income resulting from this power sharing will provide economic benefit for MGs with excess generation. Meanwhile, MGs with a power shortage may reduce operation cost if the power price of a neighbour MG is less than the power price of the main grid. The coordinated dispatching of ESSs/DERs can be cost-effective operation for a RES-dominant NMG [155]. A competitive bidding market amongst MGs is a highly attractive solution for energy trading amongst MGs to realise a cost-effective operation of individual MGs. A distributed or hierarchical EMS framework can be used to implement a market bidding facility amongst MGs. However, the cost-effectiveness of the entire network is occasionally more important than that of individual MGs in a community-based MG [146, 156]. In such cases, cooperative resource sharing amongst MGs is the most effective approach for obtaining a cost-effective network.

B. Utilising Resources in Networked Microgrids

The networked operation of MGs provides the opportunity to utilise the excess generation or capacity of an MG. MGs with excess generation/capacity can share power with MGs experiencing power shortage [157]. Such sharing will reduce the grid dependency of MGs. It will also help to utilize green energy from RESs. RESs in an MG are variable in nature and can generate excess power for a certain period. The excess generation in an MG is typically sold to the main grid with nearly zero economic benefits. If the excess generation from RESs in an MG can be sold to other MGs in the network through a cooperative power exchange amongst MGs, then that MG will gain economic benefits. Moreover, utility-owned RESs outside an NMG can supply power to an NMG at a competitive price to support the shortage of power in an NMG. Resource utilisation may be achieved via an NMG controller [158, 159]. Moreover, the previous consensus between MGs and an NMG controller will require to maximise the utilisation of resources in a network.

C. Increasing Reliability in Networked Microgrids

Reliability is one of the important issues in NMGs that should be assessed during the planning stage of NMGs [160]. Networked operation amongst MGs provides an opportunity to increase the supply reliability of MGs in a network [161, 162]. Cooperative operation amongst MGs can minimise system restoration time under a fault or power deficiency condition. It also ensures an efficient operation of demand response. The result increases customer satisfaction through economic benefits. Supply reliability also depends on the structure of NMGs. The mesh structure NMG is a more reliable network compared with other structures due to the redundant power link for power exchange amongst MGs. Besides that, networked operation of MGs in emergency/autonomous island mode can increase power supply reliability for the critical load of each MG by using DERs or battery storage [163]. The supply for critical load can be short/long term depending on the requirement and availability of resources in a network. The reliability of supply can be controlled by the NMG controller/dominant MG in the network though a common bus or a private power network between MGs. However, a previous agreement between MGs or a DNO is required to execute the emergency power sharing strategy.

2.4.2 Challenges of Networked Microgrids

A. Control and Stability Issues

Control and stability issues in an NMG are more complex than those in a single MG. Appropiate power electronics devices are important for power flow control amongst MGs in different operating modes. Networked operation in island mode is more challenging when two or more MGs operate in island mode but intend to resume cooperative mode. Voltage and frequency stability are difficult to achieve in such a network. Adaptive and robust power electronic devices should be developed to facilitate power exchange amongst MGs. A master–slave approach can be a suitable solution in which one MG will act as the master and will be responsible for setting voltage and frequency references. Other MGs in a network will work as slaves by following the master MG to minimise voltage and frequency deviations. In this approach, the master MG is responsible for maintaining the stability of the overall system. However, the privacy of MGs may be required to be sacrifice. Meanwhile, the NMG controller can send voltage, frequency and power references to individual MGs based on information from the network and each MG. However, this process may increase computational complexity. Thus, a robust control architecture should be developed to avoid control and stability issues in networked operation. Further quality research is anticipated in this area.

B. Dependency on Communication Network

The networked operation of MGs depends on communication amongst MGs in a network of MGs. The power-sharing decision amongst MGs requires information from neighbouring nodes. Such information sharing is based on modern communication networks. Therefore, the requirement of a redundant communication network should be evaluated in the design stage by considering the amount and frequency of information and future extension [12]. Moreover, maintaining a secure communication network is a challenging task because of possible cyberattacks in a communication network. Communication networks based on different information and communication technologies (ICT) may lead to possible cyberattacks in NMGs. A control structure based on a hierarchical or distributed framework should share information with neighbouring nodes for the optimal control of a network. Such networks typically connect to several ICT networks. Thus, a hierarchical or distributed control structure of NMGs is more vulnerable to possible cyberattacks. By contrast, in a central controller structure, all the nodes in a network send/receive information from/to the central controller to perform the desired control action. The central controller in an NMG broadcasts the control command to the all nodes through one-to-one

communication protocol. Thus, the central control structure is less vulnerable and more resistant to cyber-attacks. Cybersecurity in NMGs addressed in [164–166] because of the network dependency of the control structure in an NMG. A cyberattack-adoptive distributed control structure was incorporated in [167] wherein each node detects and isolates the defected nodes to exhibit optimal operation for other MGs in the network. Three types of possible attacks, namely, a communication link, a local controller and an MG controller, were considered to demonstrated the performance of the control strategy. Additional research is required in the future to avoid possible cyber attacks and communication failures in an NMG.

C. Protection Complexity

The protection scheme of NMGs differs from that of a single MG due to various possible system structures in a network [168–170]. The system structure in an NMG changes depending on the operation mode and optimal flow path in a network. A dynamic change of the system structure will change the current rating/direction of the breakers. Consequently, false tripping or malfunctioning of the breakers may occur at a certain point in the network. Accordingly, the setting of protection devices should be modified to respond to the revised structure of a network to maintain system reliability. An adaptive protection scheme should be developed to meet the protection requirements for an NMG. Additional contribution is necessary to develop adaptive protection schemes that can support various protection structures of NMGs. Moreover, fault analysis within private power networks between MGs should be addressed in the future.

2.5 Conclusions

This chapter first presents an introduction about MGs and NMGs in distribution networks. After that, it classifies NMGs into star, ring and mesh structures based on network formation. A comprehensive review on methods and algorithms for power flow control of MGs is demonstrated. Besides that, a summary of the control structures and methods for regulating voltage, frequency and power in NMGs under different operation scenarios is presented. In addition, the advantages and challenges of the networked operation of MGs are provided in this chapter. The summary of recent studies indicates that compared with dealing with the power flow optimisation problem; minimal quality research has been conducted on power flow control in NMGs. The effect of MGs cooperative operation on distribution network stability and quality should be addressed in the future. Moreover, the effects of communication networks and

protection issues on MGs and NMGs performance should be the focus in future research to utilise the advantages of NMGs in a distribution network. Furthermore, suitable power electronic devices and energy trading guidelines should be developed to control power flow though power networks amongst MGs. In conclusion, this chapter intends to provide an extensive review of MG and NMG research to direct interested researchers and professionals in developing suitable control and optimisation models of MGs and NMGs for promoting smart grid technologies in future power system networks.

Chapter 3

Power Flow Fluctuation Control using Rule and Fuzzy-based Methods

Chapter Contribution Declaration

This chapter addresses the tie-line fluctuations in a RES-dominant MG. A fuzzy logic controller-based power flow control method is proposed to reduce the tie-line fluctuations of a grid-connected MG due to dynamic nature of RESs and load. The designed controller is employed to control the ESS in an MG. A comparison with other two rule-based methods is demonstrated in simulation experiment to show the effectiveness of the proposed fuzzy controller.

This chapter includes a co-authored paper. The bibliographic details of the co-authored paper, including all authors, are:

Islam M, Yang F, Ekanayek C, Amin M. Grid power fluctuation reduction by fuzzycontrol based energy management system in residential microgrids. Int Trans Electr Energ Syst. 2019;29:e2758. DOI: https://doi.org/10.1002/etep.2758

My contribution to this paper involved: conceptualization, system modelling, controller design, simulation experiment and analysis, the original draft writing, revising and proofreading.

Signed: _____ Date: *23.01.2021*

PhD Candidate: Mojaharul Islam (Principle Author)

Countersigned: _____ Date: *23.01.2021*

Principle Supervisor: A/Prof. Fuwen Yang (Corresponding Author)

Countersigned: _____ Date: *23.01.2021*

Associate Supervisor: Prof. Junwei Lu

Countersigned: _____ Date: *23.01.2021*

External Supervisor: Dr. Chandima Ekanayeke

Countersigned: _____ Date: *23.01.2021*

External Supervisor: A/Prof. Mohammad Amin

3.1 Abstract

Smoothing grid profile plays a crucial role in dynamic operation of microgrids. This chapter focuses on reducing the grid power fluctuation in a grid connected microgrid due to stochastic nature of renewable generations and its impact on the stability and quality of a distribution network. To achieve this, the control strategies are designed to control the charging/discharging of battery storage system based on the difference between generations of renewable energy resources and load demand as well a battery state. Fuzzy logic controller is applied in energy management system of a microgrid by considering dramatic behavior of renewable energy resources while maintaining the battery state within secure limits. A comparison with time based constant and variable charge/discharge control of battery presents in simulation experiment to demonstrate the effectiveness of the proposed fuzzy controller in a residential AC microgrid.

3.2 Introduction

The worldwide commitment to the reduction of fossil fuel drives the power system to incorporate green/renewable energy resources (RESs) into the grid to meet the future power demand. The adaptation of these RESs in the distribution network has a reflection in terms of economic benefits from the customer level to the core system level for future smart grid networks. Microgrid (MG) is one of the leading features of smart grid which integrates distributed energy resources (DERs) and energy storage system (ESS) to create a grid that feeds different loads on a low voltage network and can operate either grid-connected or islanded mode [1, 2]. Luida et al. [3] demonstrates a review of existing MG test networks around the world. Jackson et al. [4] investigates the feasibility, control and management strategies of AC and DC MGs consists of RESs, ESS and load. Due to stochastic nature of RESs and load, importance of energy management system (EMS) in MG is crucial for system stability and its performance. Moreover, EMS in MG needs fast response compared to conventional power systems [19].

The key objectives of EMS are to define optimal set points for different units of MG, cost optimization by economic aspects of grid, smoothing the grid profile and reliability of customer service. Based on the MG structure & predefined objectives, different methods and strategies are chosen for optimal operation of the MG. For example, demand side management describes in [20, 21] to minimize the operating cost of MG . R. Palma-Behnke et al. [20] presents the rolling horizon strategy for determining the set points of generation units and signals for customer based on demand side management. Similarly, in [21],

the operating cost of MG is minimized by 3.06% by controlling water pump and other electric loads in demand side management. On the other side, for maximizing the MG profit, a day ahead optimal planning of generation units is made in [22] by keeping the system constrains in secure limit. In [45], a day ahead optimal scheduling of MG is determined using genetic algorithm based on load demand, wing generation and electricity price. The article is also used genetic algorithm for optimal setting of fuzzy system that are used to control the battery power. Besides that, to minimize the cost of MG, receding horizon technique for optimal scheduling of battery is adopted in [23] where wind turbine is the key support for local load. Similarly, adaptive modified firely algorithm is used in [24] to reduce the operating cost of MG considering the stochastic nature of RESs and load demand. In [25], to support the rapid fluctuation of demand in a MG, a composite ESS is used to allocate steady load to battery and dynamic load to ultra-capacitor. Y.-K., Chen et al. [26] deploys fuzzy logic in EMS where selling the electricity to the connected grid is the main priority of the control algorithm along with satisfying the demand of a MG.

However, smoothing grid profile is an important objective of EMS in a grid connected MG to reduce the effect of stochastic nature of RESs and load on grid as well as to maintain the stability and quality of the distribution network. Researchers proposed different control methods to obtain smooth grid profile through the EMS of MG. Considering the forecasting of the MG future power, a mixed linear program is used in [171] to obtain the smooth grid power along with minimising the operation cost of battery and energy usage. Besides that, forecasting method is used in [172, 173] to reduce the grid fluctuation in a residential MG operation. Centralized moving average strategy [172] and fuzzy logic [173] based control has taken into the count to reduce the forecasting error by maintaining the battery state of charge (SoC). However, without forecasting, a coordinate control between demand response and battery storage is proposed in [174] to smooth the grid power service. Similarly, EMS with a coordination algorithm between battery and diesel generation is considered in [175] to reduce the impact of solar variation on grid. Besides that, a fuzzy logic based coordinated control between dispatch-able distributed generation and ESS is proposed in [36] to adjust the active power reference of battery based on SoC and targeted active power from battery to minimize the grid power in grid connected mode. In contrast, the study concentrates on a residential MG where MG depends on the main grid to maintain service reliability in any condition and EMS in MG operates without forecasting or controlling of generations and loads. In [38] , partially management of battery is presented using fuzzy logic controller (FLC) and grid power is determined by filtering the high frequency component from the difference between MG net power and FLC output. A different strategy is implemented in [39], where the amount of power assigned to the grid

is computed as a sum of two components. First one is the average value of net power demand calculated by a moving average filter and second one is the modifying term of the grid power calculated by a FLC to increase, decrease or maintain grid power and to maintain the battery SoC within secure limit. Both articles adopt grid operator control approach to perform the energy management of MG. However, in this framework, instead of using grid control approach of EMS, the study focuses on management of battery storage system only to reduce the grid power fluctuation in a residential MG.

Aiming to this, a fuzzy logic controller (FLC) is designed to control the battery storage system to obtain the reduced grid power fluctuation in a residential MG connected in direct integration to the grid. The design takes MG net power demand and battery SoC as input of the fuzzy system to determine the charging/discharging of battery as output by maintaining the reliable supply to the load and securing the battery constrains in all conditions. The target of the new FLC based design is only to control the charging/discharging of battery to reduce the grid fluctuation rather than controlling the grid power in the EMS. Thus, eliminates the necessity of filter used in previous works. Besides that, lithium-ion battery is used as ESS due to its performance efficiency in grid connected PV application and longer life cycle compare to other types of battery. Furthermore, battery SoC is maintained in a limit to reduce capacity failure and maximize the use of battery resource. Moreover, the chapter designs a residential MG consist of PV panel and battery storage system based on yearly load demand of a residential building and statistical weather information. Stochastic nature of PV panel is obtained based on real weather information for several days. Moreover, the dynamic nature of residential load is illustrated considering the peak and off-peak hours of the day. After illustrating the dynamic behavior of an MG, a FLC is designed based on membership functions and rules by using two inputs and one output. The design is optimised for the performance parameters, define as peak grid power and root mean square value of grid power fluctuation for one day. Finally, a typical AC MG with PV array, battery storage system and dynamic residential load connected to the grid has considered in building the system using Simscape Electrical™tool in MATLAB Simulink. To evaluate the performance of the proposed FLC based control, a comparison with two others EMS without FLC are discussed to obtain the same objective by maintaining the battery SoC in secure limit.

The rest of the chapter is organized as follows: section 3.3 describes the architecture of study MG, section 3.4 describes power flow equations and performance parameters, section 3.5 illustrates three different power flow control strategies to reduce grid fluctuation, section 3.6 simulation result and comparison among the methods, section 3.7 concludes the chapter.

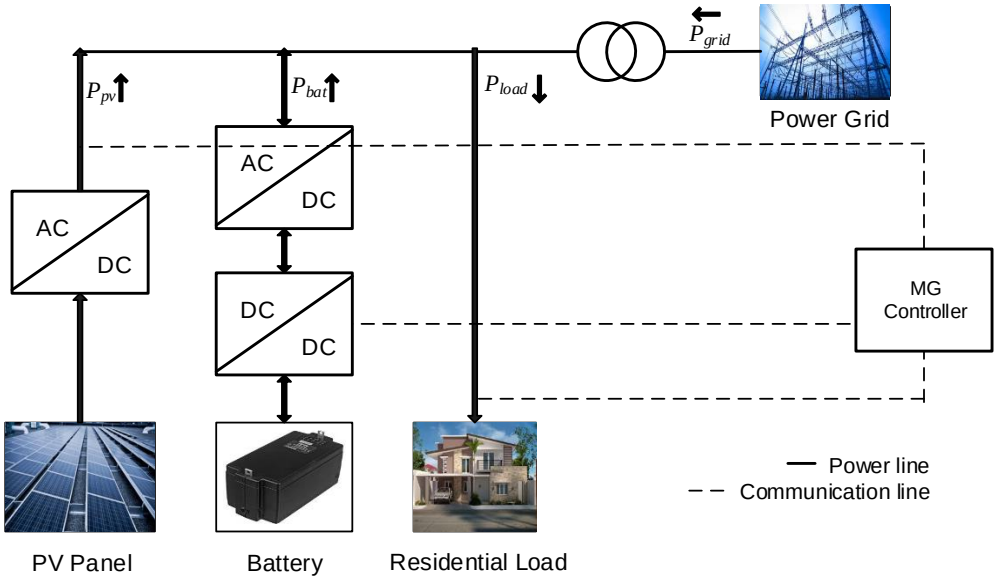

Fig. 3.1 Typical structure of grid-connected residential AC MG

3.3 Microgrid Architecture

The study considers a typical grid connected residential AC MG structure with a PV panel as RES, a battery as an ESS and a residential load. The PV panel and the battery are connected in direct integration to the grid. The PV panel connects to the grid through an inverter inbound of a maximum power point tracking (MPPT) controller. The battery storage system interfaces in the MG through DC-DC bidirectional converter and a bidirectional inverter. Fig. 3.1 depicts the MG for the system under study. The size of the PV panel and the battery is designed based on the load profile in a residential building. According to the statical weather information of Brisbane, Australia, 1 KW of PV can generate approximately 1550 KWh energy per year [176]. Besides that, the average energy demand in the study MG is assumed as 10000 KWh per year. Considering the power loss inside the MG, the total energy demand is roughly assumed as 11000 KWh per year. Based on the above information, the capacity of the solar panel is determined as 7.2 KW. However, the size of the battery for a specific microgrid depends on the average load demand and the battery backup time[177] . The average load of the study microgrid during a 24 hours duration is 2.2 KW. Considering the loss in the system, the actual load to the system is assumed as 2.5 KW. Moreover, to longer the battery life time, the study considers to use 60% of the battery capacity [178, 179]. So, the system assumes a battery size of 350 Ah to support an average load of 2.5 KW for 12 hours assuming the power from PV panel is unavailable during this time.

Table 3.1 System Configuration

Parameter	Value
PV module	7.2KW(15 series module, 2 parallel module)
Battery Module	350Ah, 120V
Load Demand	11000KWh/per year
DC voltage	400V
AC voltage	240V (rms)
Frequency	50 Hz

Besides that, the system assume a robust communication structure between different units of study MG. The outline of different parameters of MG is illustrated in Table.3.1.

3.4 Power Flow in Microgrid

3.4.1 Power Flow Equations and Constrains

To drive the power flow equation for the MG architecture under study, positive power direction of each unit is given in Fig. 3.1. The equation of MG demand power and grid power can be illustrated as,

$$P_{net} = P_{load} - P_{pv} \tag{3.1}$$

$$P_{grid} = P_{net} - P_{bat} = P_{load} - P_{pv} - P_{bat} \tag{3.2}$$

Where P_{net} is the MG demand power, P_{pv} is the power from PV module, P_{bat} is the power from battery module, P_{load} is the load power and P_{grid} is the grid power. The EMS updates the parameters of the Equations (3.1-3.2) in every minute. Fig. 3.2 shows the stochastic nature of PV module output power for the variation of temperature and radiation. The temperature and radiation information was collected from statical weather information of Brisbane, Australia in September 2017 for linear variation day, small variation day, medium variation day and large variation day. Besides that, dynamic load variation is illustrated in Fig. 3.3for 24 hours of the day. Moreover, Fig. 3.4 shows the net demand power of the MG which is the difference between load and PV generation.

However,in the absence of PV generation, battery plays a crucial role to support the main grid to maintain a reliable power supply to the load. So, to extend the lifetime of lithium-ion, battery parameters state of charge(SoC) and depth of dischanrge(DoD) need to keep within secure limits.The

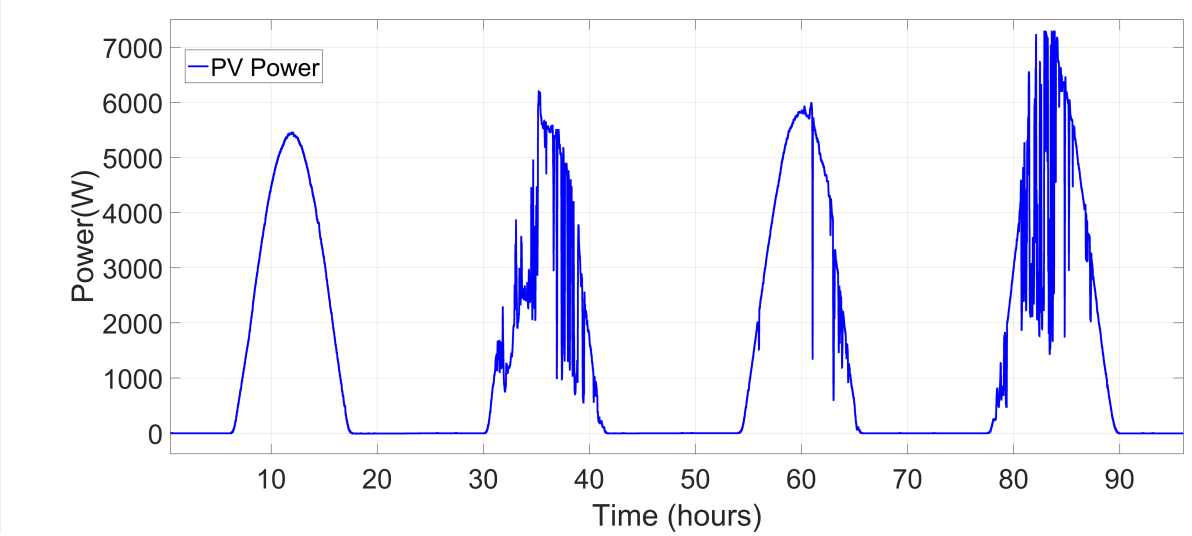

Fig. 3.2 PV power profile for different radiation day of study MG

SoC indicates the available charge of a battery in percentage (0% means battery is empty and 100% means battery is fully charge). The equation to determine the SoC can be written as,

$$SoC(t) = \frac{C_{bat}(t)}{C_{cap}} * 100\% \tag{3.3}$$

Where C_{cap} is the total capacity and C_{bat} is the amount of remaining charge at that time.

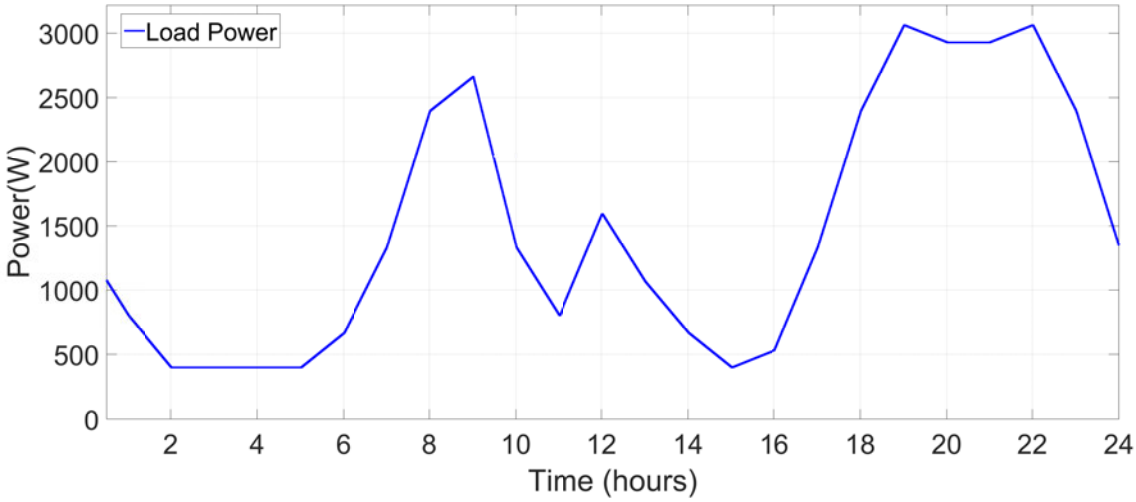

Fig. 3.3 Day long residential load profile of study MG

The DoD depends on maximum and minimum value of SoC. the DoD of a battery can be defined as,

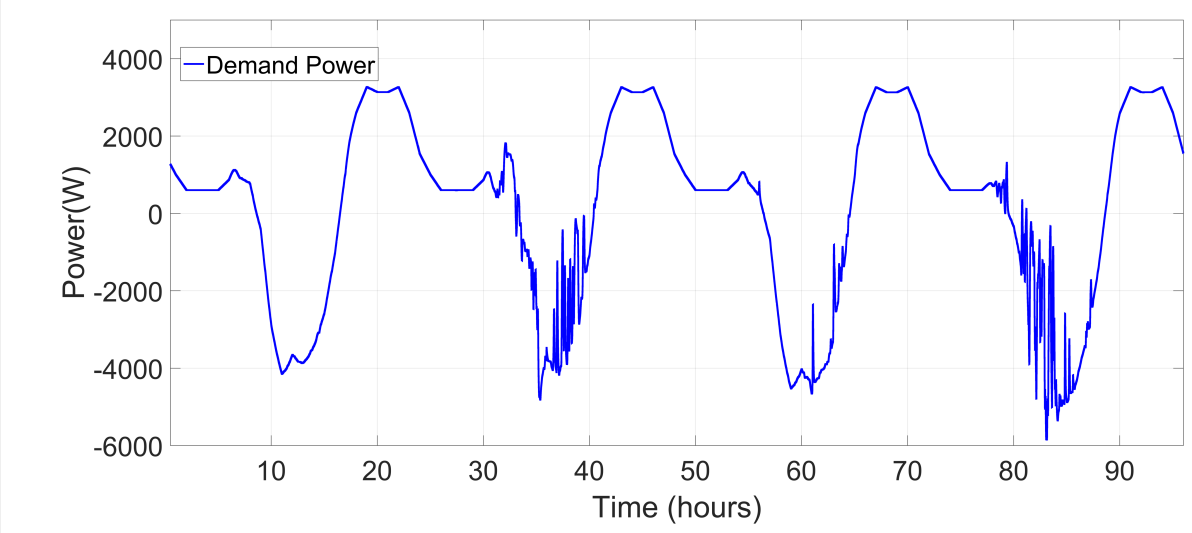

Fig. 3.4 Demand power profile of study MG

$$DoD = \frac{(SoC_{max} - SoC_{min})}{SoC_{max}} * 100\% \tag{3.4}$$

Where $S0C_{max}$ and SoC_{min} is the maximum and minimum SoC respectively.

The high value of DoD leads to reduction in the battery life. On the other hand, low value of DoD leads to capacity loss of the battery. Apart from this, charging/discharging current has a great impact on battery lifetime. Battery current is usually expressed as a rate of nominal capacitance. For example. 10Ah battery is charging at a current of 10A means charging at 1C. For lithium-ion battery, with slow charging rate ($\leq$0.5C) constant/multistage charging method performed better rather than constant power method in terms of capacity fading [180]. In [181], results shows that charging the battery more than 1C degrades the battery life time significantly. However, degradation rate has little impact for a discharging rate up to 1C and DoD 70-100%. Moreover, [179] suggests DoD less than 80% to maintain the longer battery lifetime. Considering the suggestions, this chapter selects a DoD of almost 70% and maximum charge rate of $\leq 0.5C$ to maintain healthy life of battery. Table 3.2 summarizes the battery parameters and other system parameters for the study MG.

3.4.2 Definition of Performance Parameter

Peak Grid Power: Maximum value of power injected to/from the power grid within 24 hours duration.

$$P_{G,max} = MAX|P_{grid}| \tag{3.5}$$

Table 3.2 System Parameter

Symbol	Parameter	Value
SoC_{max}	Maximum value of SoC	90%
SoC_{min}	Minimum value of SoC	30%
SoC_{int}	Initial value value of SoC	40%
DoD	Depth of discharge	66.67%
T_s	Sample time	60sec.
N	Total number of sample per day	1440

Cumulative Root Mean Square: Cumulative root mean square (CRMS) value calculates the grid power fluctuation over a 24 hours duration and can be determined by the following equation,

$$CRMS = \sqrt{\frac{1}{N}\sum_{n=1}^{N} \parallel \{(P_{grid(n)})^2\} \parallel} \tag{3.6}$$

Where $P_{grid}(n)$ is the grid power for nth sample of the day and N is the total number of samples during 24h hours duration. The ideal design is to make the CRMS value to zero within a duration of 24 hours. In this study, samples are taken every minute to determine the fluctuation of grid power.

3.5 Power Flow Control Strategies of Microgrid

This section describes three different power flow control strategies to reduce grid power fluctuation in a day by controlling the power of the battery storage system. In this study, battery control has achieved by controlling the DC-DC converter of the battery storage system.

3.5.1 Constant Control Method

The constant control method maintains a constant charging/discharging of battery storage system depending on the availability of solar power. The EMS takes time of the day, solar power and battery SoC as input to determine the charging/discharging of battery as output. The battery will charge at a constant rate of $K_{p1} * C_{cap}$ from 5AM to 5PM if P_{pv} is greater than 1500W and $SoC(t) < SoC_{max}$. Similarly, battery will discharge at a constant rate of $k_{p2} * C_{cap}$ from 5PM to 5AM if P_{pv} is less than 500W and $SoC(t) > SoC_{min}$. On the other case, the power from the battery will be zero. Equation (3.7-3.8) represent the charging and discharging power of battery for constant control method.The value of K_{p1} and K_{p2} are adjustable up to $0.5 * C_{cap}$ depending on maximum load demand of MG.

From 5AM to 5PM if $P_{pv} > 1500W$ and $SoC(t) < SoC_{max}$,

$$P_{bat}(n) = -K_{p1} * C_{cap} \tag{3.7}$$

From 5PM to 5AM if $P_{pv} < 500W$ and $SoC(t) > SoC_{min}$,

$$P_{bat}(n) = K_{p2} * C_{cap} \tag{3.8}$$

Based on the system parameter, the value of K_{p1} and K_{p2} are set as 0.1 and 0.08 respectively, so that the battery can charge enough during day time and support the local load at night along with grid supply.

After determining battery power, grid power is calculated using the following equation.

$$P_{grid}(n) = P_{load}(n) - P_{pv}(n) - P_{bat}(n) \tag{3.9}$$

3.5.2 Variable Control Method

The variable control method determines the battery power based on net demand power of MG and battery SoC. In stead of using solar power, the method uses MG net power demand to determine the charging/discharging of battery. From 5AM to 5PM, the battery will charge only if the value of the net power demand is negative and $SoC(t) < SoC_{max}$. Similarly, From 5PM to 5AM, battery will discharge if the net power demand is positive and $SoC(t) > SoC_{min}$. The equation of battery power is illustrated in Equation (3.10).

$$P_{bat}(n) = K_p * (P_{net}(n)) \tag{3.10}$$

Where K_p is a proportional constant. The value of K_P is set to 1.2 for optimising the performance parameters by maintaining battery constrains. Similar to constant control method, the EMS use the Equation (3.9) to determine the grid power. The main drawback of the design is the time dependency of the control.

3.5.3 Fuzzy Control Method

To overcome the time dependency of control and to simplify the design, a fuzzy logic controller(FLC) is designed by using only two inputs and one output. The advantage of this design is to reduce the number of inputs to determine the same output. MG net power demand and battery SoC are the inputs of the

controller to determine the power of the battery as output. The output power from FLC is used to calculate the grid power using Equation (3.9). The block diagram of the FLC based power flow control is illustrated in Fig. 3.5.

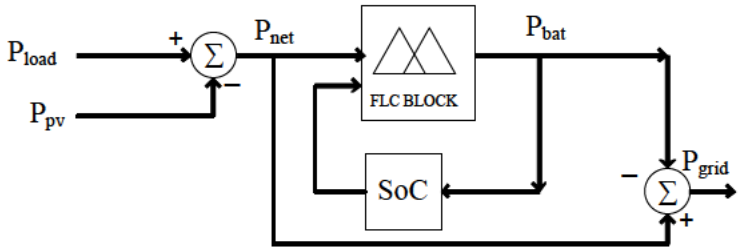

Fig. 3.5 Block diagram of fuzzy controller

The design constrains is set in Equation(3.11-3.14) to determine the battery power using FLC.

$$P_{net}(min) \leq P_{net} \leq P_{net}(max) \tag{3.11}$$

$$SoC_{min} \leq SoC \leq SoC_{max} \tag{3.12}$$

$$-0.5C_{cap} \leq P_{bat} \leq 0.5C_{cap} \tag{3.13}$$

$$P_{bat} = Fuzzy(P_{net}, SoC) \tag{3.14}$$

The FLC in this design uses mamdani based controller, rules with minimum value and centroid technique for defuzzificaion. There is no unique method to design the membership function of a fuzzy logic controller. Different shapes can be used to design the fuzzy membership function based on user choice. Among them, triangular shape membership function is most encountered one in practice. At first, the membership functions are designed for each input and output using several triangular shapes by equally dividing them within the design contains. Then, rules are applied to map between inputs and output. After that, the adjustment of fuzzy parameters (e.g., Membership Functions number, type, mapping, and rule-base) is performed by an off-line adjustment procedure to minimise the performance parameter.

The ideal procedure to design a FLC based system is summarized as follows:

1. Design the membership functions (MFs) of inputs and outputs.

2. Set the rules to determine crispy output.

3. Adjust the membership functions and rules to optimise the performance parameters.

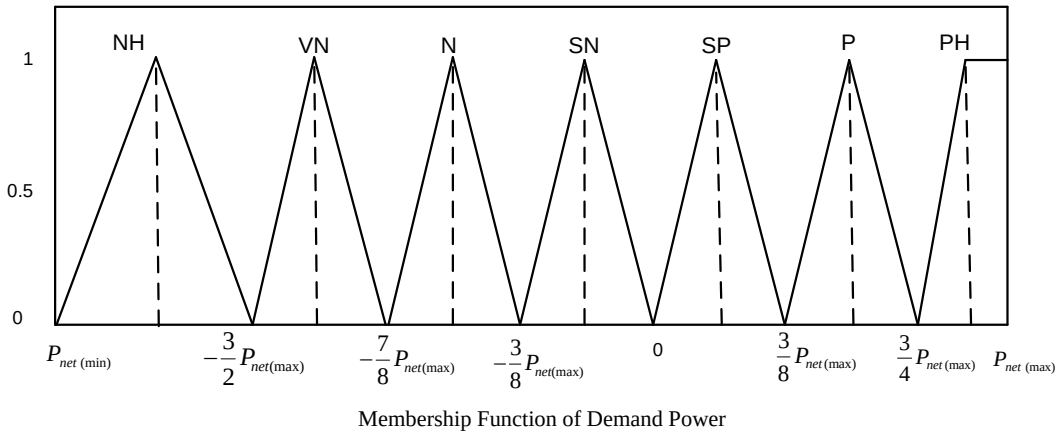

Fig. 3.6 Membership function of demand power

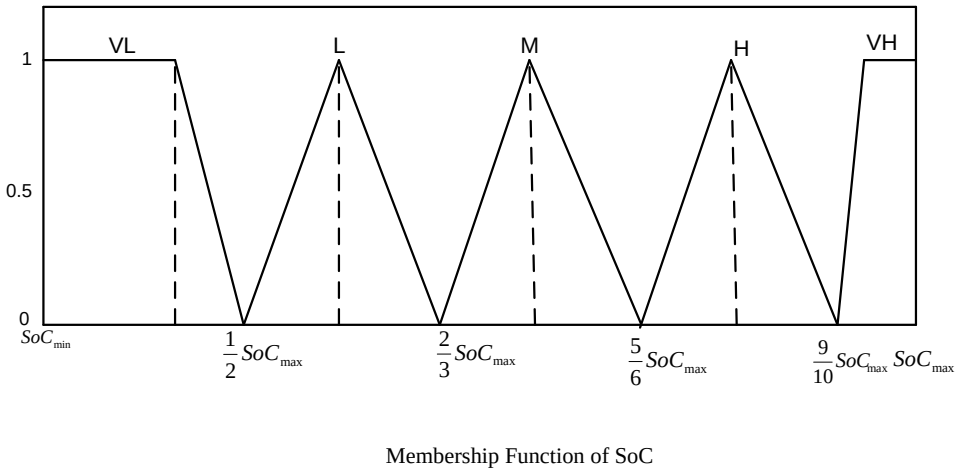

Fig. 3.7 Membership function of SoC

The proposed FLC defines the demand power MF using six triangular and one trapezoidal MFs: VH(negative high), VN (very negative), SN (small negative), N (negative), SP (small positive), P(positive)

and PH (positive high). Similarly, the SoC MF shapes using three triangular and two trapezoidal: VL (very low), L (low), M (medium), H (high), and VH (very high). In the same way, the battery power MF is figured out using five triangular and two trapezoidal: VHC(very high charge), HC (high charge), MC (medium charge), SC (small charge), NO (no charge/discharge), SD (small discharge), MD (medium discharge), HD (high discharge). The MFs are designed based the system constrain defined in Equation (3.11-3.14). The MFs of demand power, battery SoC and battery power are depicted in Fig. 3.6, Fig. 3.7 and Fig. 3.8 respectively.

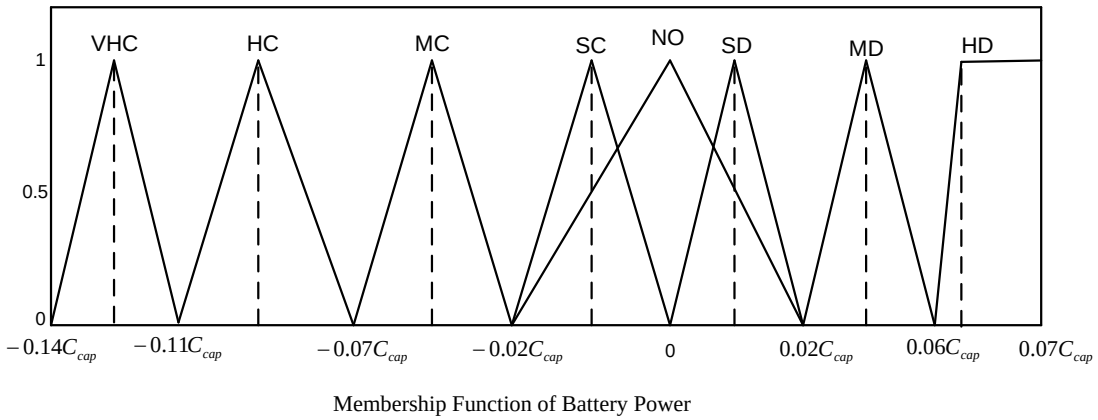

Fig. 3.8 Membership function of battery power

After that, rules are defined based on the MG behavior. For example, if the demand function value is a negative high (P_{net} is NH) and the battery SoC is low (SoC is L), then the battery will charge in high rate (P_{bat} is VHC). So, the rule can be written as,

IF P_{net} is NH and SoC is L THEN P_{bat} is VHC.

Similarly, when the demand function value is small positive and battery charge is high, then the battery will discharge in small rate. And the rule can be written as,

IF P_{net} is SP and SoC is H THEN P_{bat} is SD.

The rules and membership functions of the FLC design are optimised using off-line optimised procedure for the performance parameters. The performance parameters of this design are peak value of the grid power and cumulative root mean square (CRMS) value of the grid power. The optimised rules of the FLC are illustrated in Table.3.3.

Table 3.3 Optimised fuzzy rules

P_{bat}		SoC				
		VL	L	M	H	VH
P_{net}	NH	VHC	VHC	VHC	VHC	NO
	VN	HC	HC	HC	HC	NO
	N	MC	MC	MC	MC	NO
	SN	SC	SC	SC	SD	SD
	SP	SD	SD	SD	SD	SD
	P	MD	MD	MD	MD	MD
	PH	MD	MD	HD	HD	HD

3.6 Result and Comparison

In this section, a simulation model of the MG is developed in MATLAB SIMULINK using Simscape Electrical™tool. The system parameters in Table 3.1 & Table 3.2 are used to develop the simulation model. Simulation is run for 96 hours (4 days) using historical weather data for different radiation day on September 2017 of Brisbane, Australia. The EMS strategies are implemented to calculate

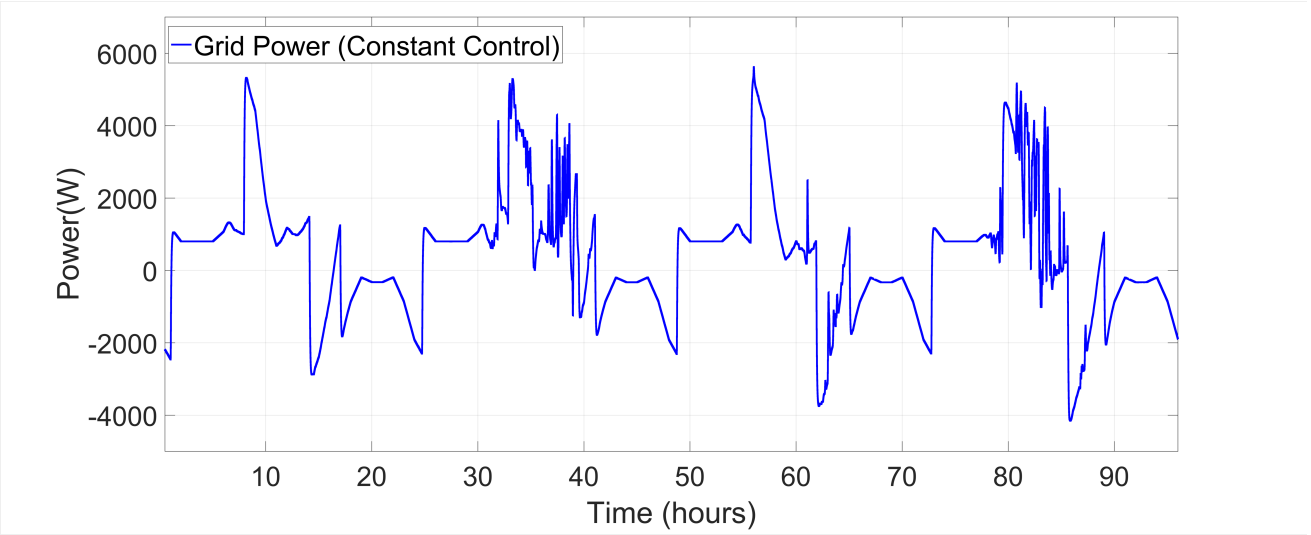

Fig. 3.9 Grid power profile for constant control

the performance parameters defined in section 3.4.2. To design the fuzzy logic controller based EMS, MATLAB fuzzy logic designer tool is used to design the membership functions and to set the rules as described in Fig. 3.6, Fig. 3.7, Fig. 3.8 and Table 3.3 respectively.

Fig. 3.9 shows the grid power profile and Fig. 3.10 shows the CRMS value of grid power fluctuation for constant control method. The result shows that grid power has a peak of 5.7kW and average value of CRMS grid power for four consecutive of the simulation is 1557.

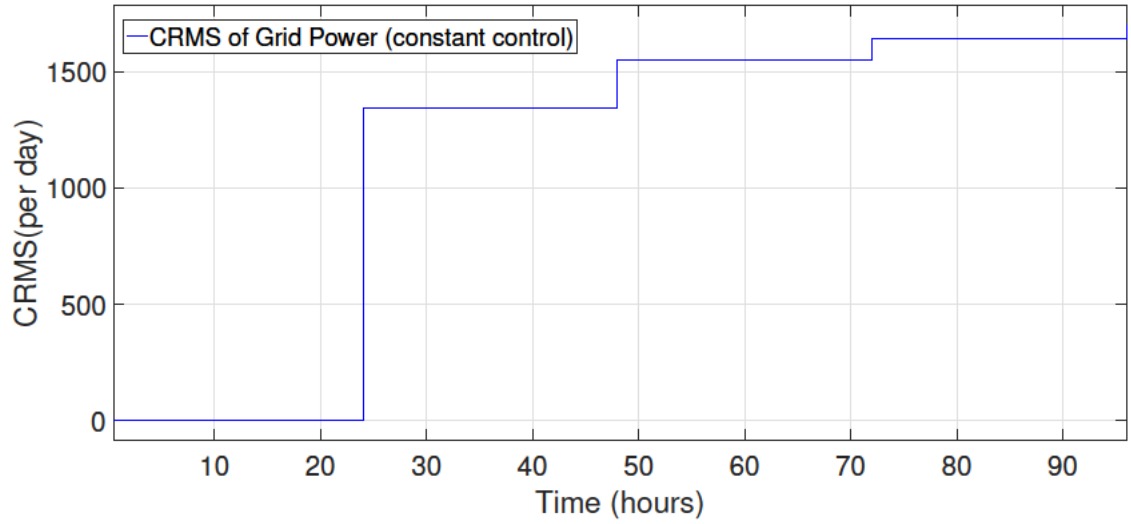

Fig. 3.10 CRMS grid power for constant control

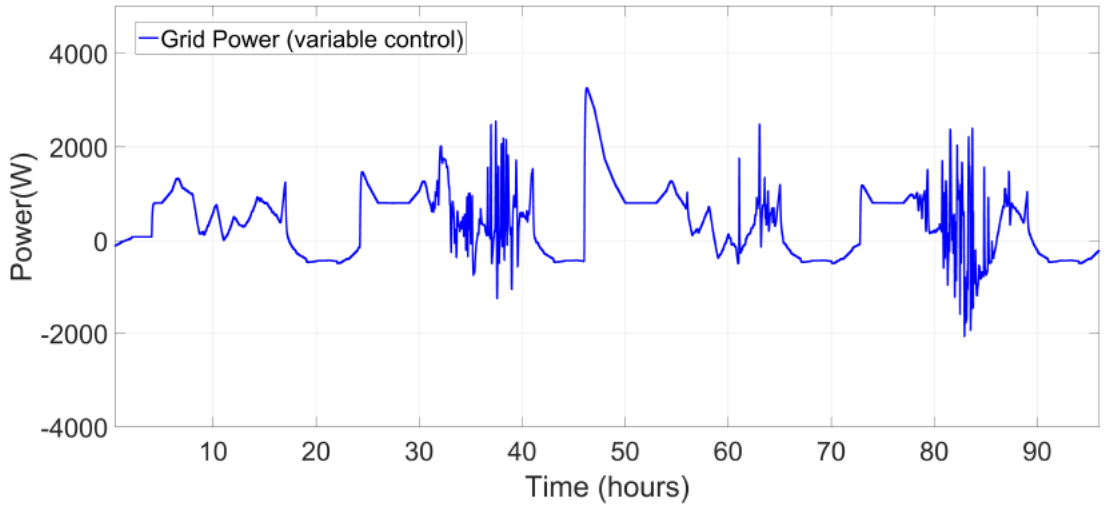

Fig. 3.11 Grid power profile for variable control

Besides that, Fig. 3.11 and Fig. 3.12 show the grid power profile and CRMS grid power respectively for variable control method. The results in simulation show the significant improvement of performance

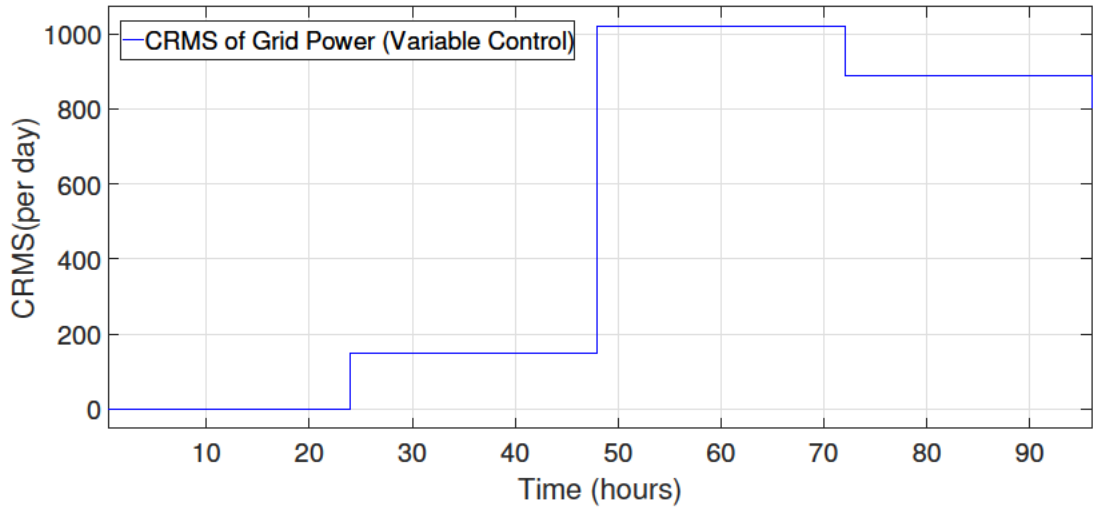

Fig. 3.12 CRMS grid power for variable control

parameters compare to constant control method. The maximum grid power is reduced to 3.2kW where as the average value CRMS of grid power fluctuation is reduced to 715. Similarly, Fig. 3.13 and Fig. 3.14 show the grid power profile and CRMS of grid power for fuzzy control EMS.

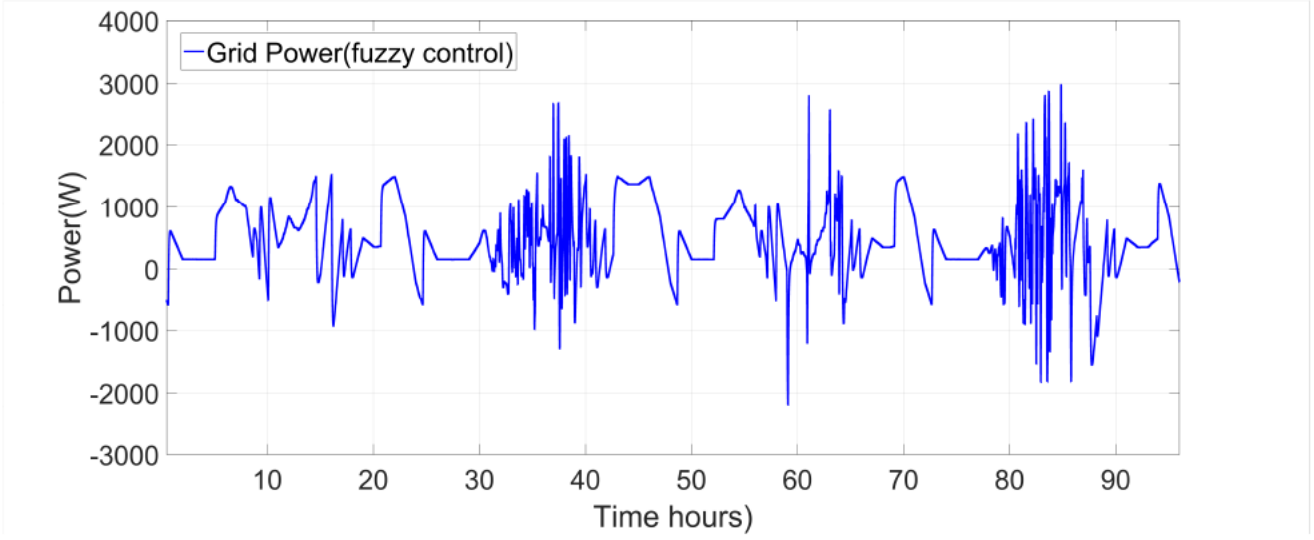

Fig. 3.13 Grid power profile for fuzzy control

The peak value of the grid power is reduced to 3kW and the average value of CRMS grid power for the simulation period is 175.

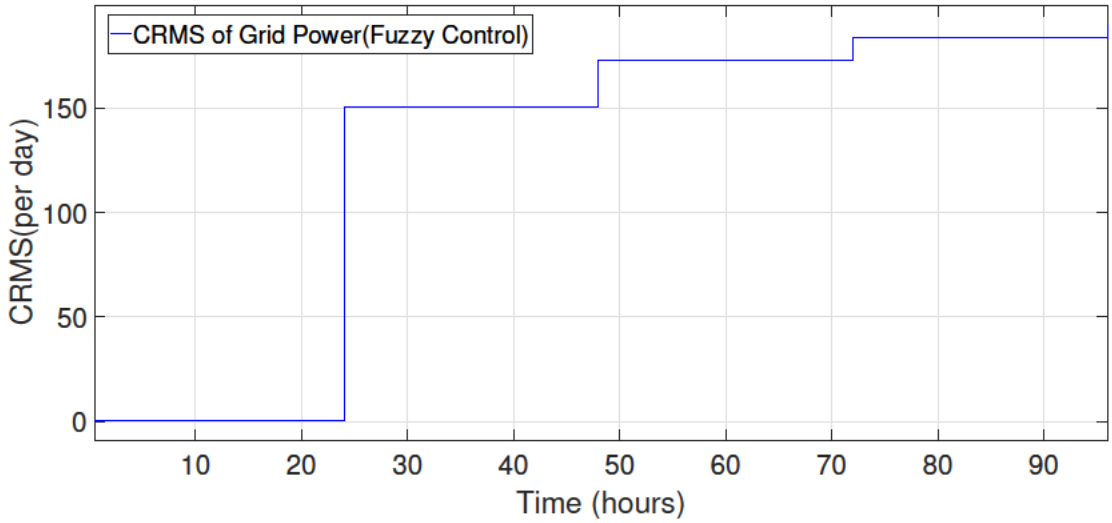

Fig. 3.14 CRMS grid power for fuzzy control

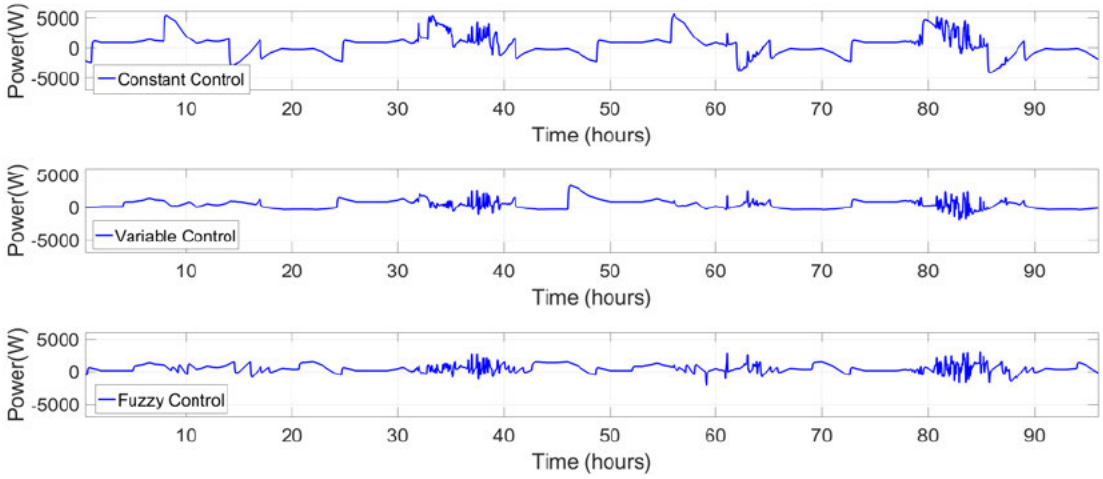

Fig. 3.15 Comparison of grid power profile

Table 3.4 Comparison of performance parameter

EMS strategy	Peak value of grid power	Average value of CRMS
Constant Control	5.5 kW	1557
Variable Control	3.2 kW	715
Proposed FLC	3 kW	175

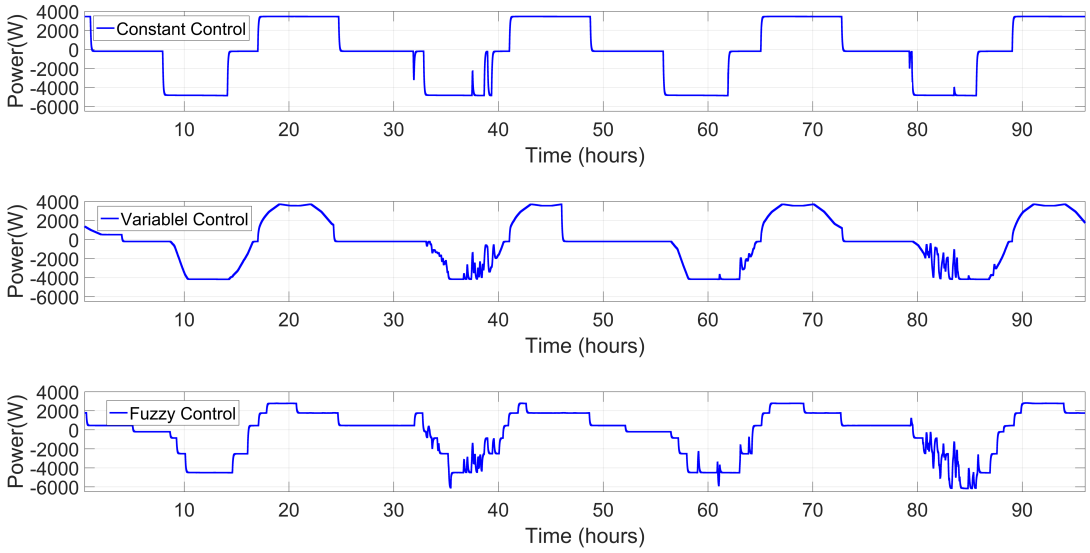

Fig. 3.16 Comparison of battery power

Fig. 3.17 proves the battery SoC remains in secure limits for three different methods as discussed in section 3.5. Moreover, Fig. 3.18 compares the CRMS grid power for constant control method, variable

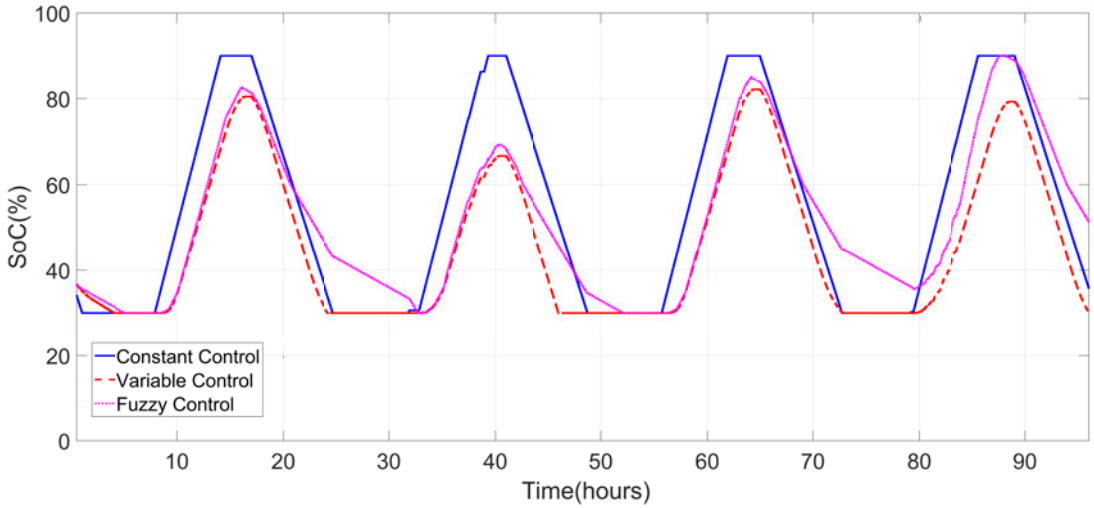

Fig. 3.17 Comprison of battery SoC

control method and FLC based method. The result highlights the lowest value of CRMS grid power for FLC based EMS compare with other two methods.

Furthermore, Fig. 3.15 shows a comparison of grid power profile between three different methods. The FLC based EMS is showing improved grid profile in terms of peak reduction compare with other two methods. In addition, Fig. 3.16 shows the battery power of three different methods. The result

shows that fluctuation of battery power has increased as an impact of grid fluctuation reduction. The result of the quality parameters for three different methods are summarized in Table 3.4.

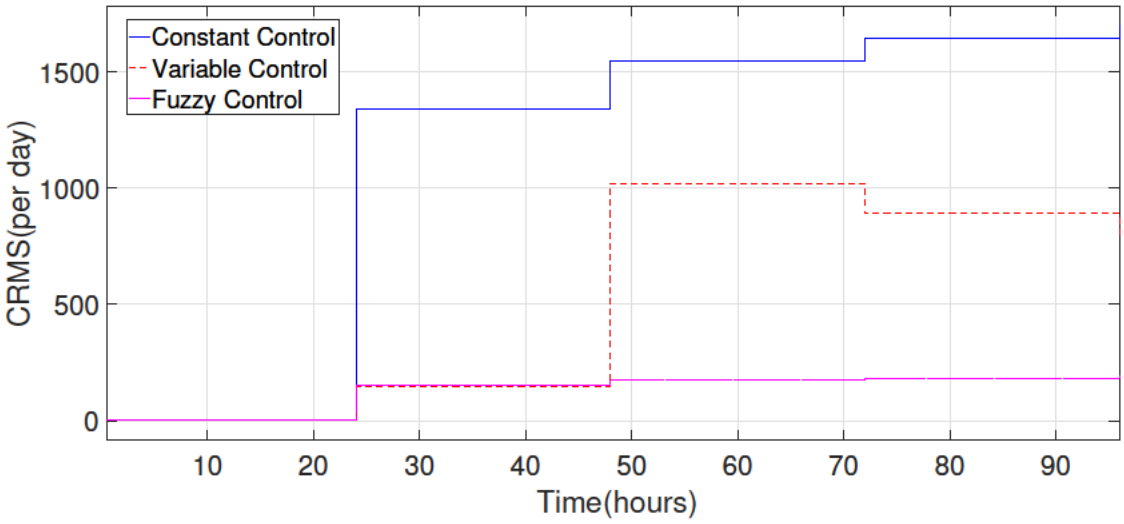

Fig. 3.18 CRMS grid power for three different methods

3.7 Conclusions

The chapter designed a FLC based power flow control strategy for reducing the grid power fluctuation in a residential MG. The FLC has designed by taking net power demand and battery SoC as input to determine the battery power as output to reduce impact of dynamic nature of PV panel and load on gird power. The design is optimised to improve the predefined of quality parameters. Moreover, Battery parameters like charging/discharging current, SoC and DoD are kept within secure limits for minimising the capacity failure of battery with time and maximizing the use of battery storage. The results demonstrate a better grid profile for the FLC based control compare with other two approaches having the same goal. The results signify the FLC design for a grid-oriented MG for reducing the active power drawn from the grid.

Chapter 4

Power Flow Fluctuation Control using Non-linear Programming Optimisation Method

Chapter Contribution Declaration

This chapter addresses a power flow control method to minimise the tie-line fluctuations in a grid-connected MG. A golden section search-based nonlinear programming method is used to control the battery power in a dynamic EMS. The designed parameters are optimised through offline optimisation method to minimise the pre-defined performance parameters. The designed power flow control method is validated using simulation experiment to achieve a minimised grid power by keeping battery state of charge in limit. A comparative study with two other rule-based power flow control methods aiming to achieve the same objective is presented to demonstrate the performance of the proposed power flow control method.

This chapter includes a co-authored paper. The bibliographic details of the co-authored paper, including all authors, are:

M. Islam, F Yang, J Hossain, C. Ekanayeke, UB. Tayab. Battery management system to minimize the grid power fluctuation in residential microgrids. 28th Australasian Universities Power Engineering Conference, 2018.

DOI: 10.1109/AUPEC.2018.8758005.

My contribution to this paper involved: conceptualization, system modelling, battery management system design, simulation experiment and analysis, the original draft writing, revising and proofreading.

Signed: _____ Date: *23.01.2021*

PhD Candidate: Mojaharul Islam (Principle Author)

Countersigned: _____ Date: *23.01.2021*

Principle Supervisor: A. Prof. Fuwen Yang (Corresponding Author)

Countersigned: _____ Date: *23.01.2021*

Associate Supervisor: Prof. Junwei Lu

Countersigned: _____ Date: *23.01.2021*

External Supervisor: Dr. Chandima Ekanayeke

4.1 Abstract

The stochastic nature of renewable resources and loads leads to a large fluctuation of grid power in a grid-connected microgrid (MG) operation. Integrate battery energy storage system in an MG is popular way to handle the stochastic nature of renewable resources to feed the stochastic load. In this chapter, a battery power management system is proposed using golden section search algorithm to minimise the grid power fluctuation by securing the battery constraints. The algorithm is applied in energy management system (EMS) of an MG to minimise the grid peak power and grid power variation within a 24 hours duration by considering the random nature of renewable generations. The proposed battery power management system is verified through the simulation experiment in a grid-connected residential MG.

4.2 Introduction

A microgrid (MG) is defined as a cluster of distributed generations, energy storage systems and loads in a low/medium voltage network that can operate in both grid connected and island mode [1, 2]. An energy management system (EMS) in a MG plays a key role for reliable and stable operation of MGs. Minimise the grid power fluctuation is one of the main objectives of MG EMS. Researchers apply different methods and algorithms to minimise the grid fluctuation through the EMS of MGs.

A mixed linear program is used in [171] with consideration of the forecasting of an MG future power to manage the smooth operation of power grid and minimise the operational and maintenance cost of available power generation resources in MG. Besides that, a coordinated control between demand response and battery storage is proposed in [174] without the forecasting of generations and loads to smooth the grid power service. Similarly, EMS with a coordination algorithm between battery and diesel generation is included in [175] to handle the stochastic nature of solar power in an MG. In this context, some researchers considers a residential MG where the MG solely depends on the main grid for service reliability, and the battery storage system is the only controlling unit of an MG to minimise the grid power fluctuation.

A combination of fuzzy logic controller and moving average filter was used in a residential MG by Arcos-Aviles et. al., to remove the high frequency component from the grid power and transferred it to a battery to obtain a smooth grid power [38, 39]. In contrast, this chapter focuses on the management of a battery storage system in a residential MG without controlling the grid power in the EMS. Moreover, the

nonlinear nature of renewable generations and loads suggest the nonlinear control approach of battery storage system because the rule-based EMS such as fuzzy system is unable to provide optimal solution for non-linear control. In addition, a fuzzy logic controller take high computational time.

In this chapter, a battery management strategy is designed using a non-linear optimising algorithm to minimise the grid power fluctuation in a grid-connected residential MG. The decision of battery charging, and discharging are taken based on the MG net power demand and battery state. Golden section search algorithm is applied to control the battery power to minimise the grid power considering the dynamic nature of a PV panel based on real weather information over several days. Moreover, battery constraints are kept in secure limit for extending battery lifetime.

Finally, a typical AC MG consists of a PV panel, battery storage system, residential load and main grid which is considered for building the system using Simscape Electrical™tool in MATLAB Simulink. The performance of the proposed method is evaluated in simulation to verify the effectiveness of proposed approach.

The rest of the chapter is organized as follows: section 4.3 describes the details architecture and power flow of the study MG, section 4.4 presents the power flow control techniques, section 4.5 illustrates the simulation results and discussion and finally section 4.6 draws the conclusion.

4.3 Architecture and Power Flow of Microgrid

4.3.1 Architecture of a Residential Microgrid

The residential MG system in this study illustrates in Fig. 4.1 consists of a PV panel, a battery storage system and a residential load tied to the main grid through an isolation transformer. The MG depends on the main grid to maintain a reliable supply to the load. The PV panel connects to the grid through an inverter inbound of a maximum power point tracking (MPPT) controller. The battery storage system interfaces in the MG through DC-DC bidirectional converter and a bidirectional inverter. The PV panel is designed for a residential area having an average energy demand of 11000 KWh in a year. From the statistics of Brisbane, Australia, 1 KW of PV can generate approximately 1550 KWh energy in a year [176]. So, a capacity of 7.2 KW PV panel is needed to build the system. Moreover, the system designs a battery size of 42 KWh to support an average load of 2.5 KW for 12 hours. Besides that, the system assumes a robust communication structure for a reliable operation of MG EMS.

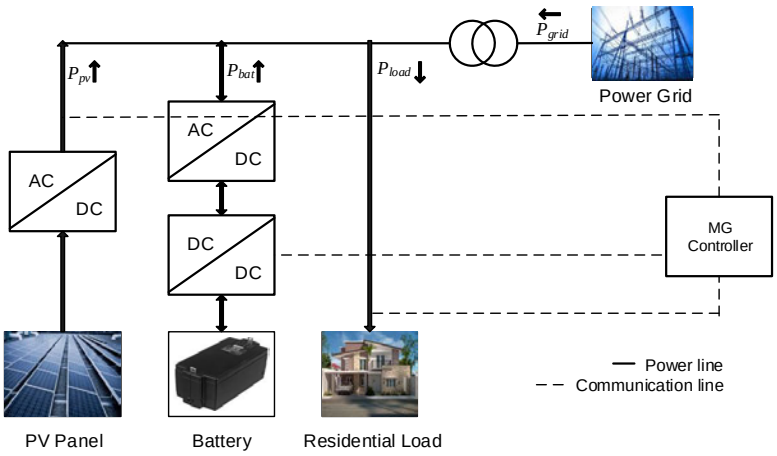

Fig. 4.1 Typical structure of a grid-connected residential MG

4.3.2 Power Flow of Microgrid

The power flow equation is the power balance equation between MG units. The power flow equations of the MG are described in Chapter 3 Equations (3.1-3.2). The EMS updates the parameters of the equations to determine the grid-power in every minute.

However, a battery plays a crucial role to support the load to minimise the grid power. So, the battery parameters like state of charge (SoC), depth of discharge (DoD) and charging/discharging current need to keep within secure limits to extend the battery lifetime . The high value of DoD leads to reduction in the battery life and low value of DoD leads to capacity loss of the battery [179]. Apart from this, the charging/discharging current has a great impact on battery lifetime [180][181]. So, this chapter chooses a DoD of 70% and maximum charge rate of $\leq 0.5C$ to maintain a healthy life of the battery.

4.3.3 Definition of Performance Parameters

Peak Grid Power: Maximum value of power injected to/from the power grid within 24 hours duration.

$$P_{G,max} = MAX|P_{grid}| \tag{4.1}$$

Cumulative Root Mean Square: Cumulative root mean square (CRMS) value calculates the grid power fluctuation over a 24 hours duration that can be determined by the following equation,

$$CRMS = \sqrt{\frac{1}{N}\sum_{n=1}^{N} \parallel \{(P_{grid(n)})^2\} \parallel} \tag{4.2}$$

Where $P_{grid}(n)$ is the grid power for nth sample of the day and N is the total number of samples during a 24h hours duration. The ideal design is to make the CRMS value to zero within a duration of 24 hours. In this study, samples are taken every minute to determine the CRMS value of the grid power.

4.4 Power Flow Control Techniques Analysis and Design

This section analyses the three different power flow control techniques to reduce the fluctuation of grid power in one day period by regulating the battery power. In this analysis, the battery power has accomplished by controlling the DC-DC converter of battery energy storage.

4.4.1 Power Flow using Constant Control Method

Depending on the availability of solar power, the constant control approach ensures a constant charge and discharge of the battery storage system. To decide the charging and discharging of battery as output, the EMS uses solar power, time of the day, and battery SoC as input. When the P_{pv} is greater than 1500 W and $SoC(t) < SoC_{max}$, the battery will charge at a constant rate of $K_{p1} \times C_{cap}$ from 5 AM to 5 PM. On the other hand, when the P_{pv} is less than 500 W and $SoC(t) > SoC_{min}$, the battery will discharge at a constant rate of $K_{p1} \times C_{cap}$ from 5 PM to 5 AM. Other than these conditions, the battery power will be zero.

From 5 AM to 5 PM, when the P_{pv} is greater than 1500 W and $SoC(t) < SoC_{max}$:

$$P_{bat}(n) = K_{p1} \times C_{cap} \tag{4.3}$$

From 5 PM to 5 AM, when the P_{pv} is less than 500 W and $SoC(t) > SoC_{min}$:

$$P_{bat}(n) = K_{p1} \times C_{cap} \tag{4.4}$$

The value of K_{p1} and K_{p2} are set as 0.1 and 0.8 based on system parameters to maintain the enough charging of battery during day time so it can meet the load demand during night time along with grid supply. After calculating the battery power, the grid power will be calculated by using the following

equation:

$$P_{grid}(n) = P_{load}(n) - P_{pv}(n) - P_{bat}(n) \tag{4.5}$$

4.4.2 Power Flow using Variable Control Method

The variable control approach calculates the battery power depend on net power demand of MG and SoC of battery. This control method utilizes the net power demand of MG to calculate the charging and discharging of battery. When the value of demand for net power is negative and $SoC(t) < SoC_{max}$ than the battery will charge from 5 AM to 5 PM. Similarly, if the net power demand is positive and $SoC(t) > SoC_{min}$ than from 5 PM to 5 AM the battery will discharge. The power of battery can be calculate as follows:

$$P_{bat}(n) = K_p \times P_{net}(n) \tag{4.6}$$

Here, K_p is proportional constant which is set be 1.2 to achieve the optimal performance parameters with consideration of battery constraints.

4.4.3 Power Flow using Golden Section Search Optimisation Method

The golden section search method is a non-linear programming (NLP) method to solve the single variable optimization problem with non-linear relationship [182]. The mathematical formulation of the algorithm is illustrated as,

$$\min_{x} f(x) \quad \text{subject to} \quad x_l < x < x_u \tag{4.7}$$

Where x is the decision variable, x_l is the lower limit of x, x_u is the upper limit of x and $f(x)$ is a non-linear function.

In golden search method, iteratively consider the function value at four carefully spaced points:

1) Assume a unimodal function

2) Leftmost x_l is always a lower bound on the optimal value x^*

3) Rightmost x_u is always an upper bound on the optimal value x^*

4) Points x_1 and x_2 fall in between. The points x_1 and x_2 are taken as:

$x_1 \equiv x_u - \gamma[x_u - x_l]$

$x_2 \equiv x_u - \gamma[x_u - x_l]$

Where γ= 0.618 a fraction known as golden ratio.

For choosing the interactive point, Case 1:$f(x_1) < f(x_2)$, Case 2: $f(x_1) > f(x_2)$

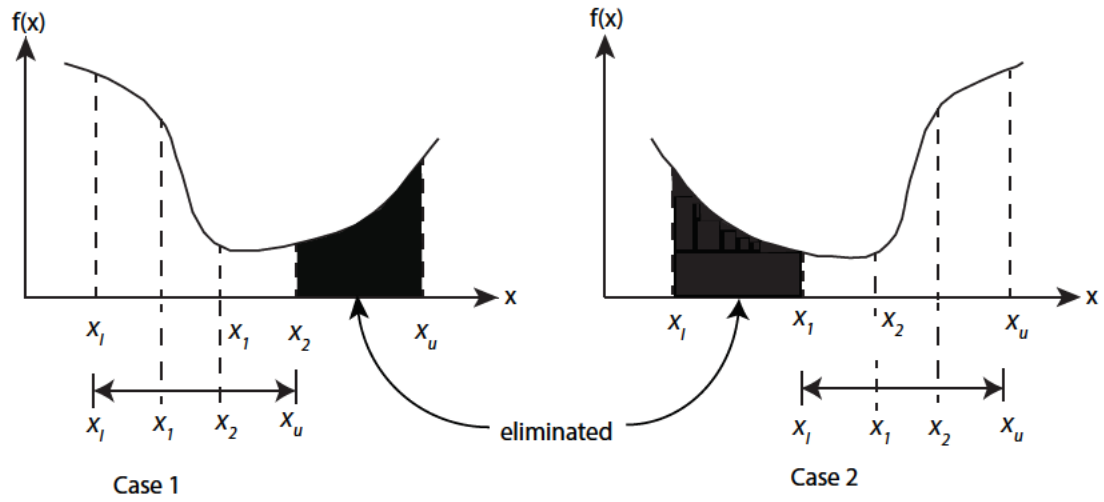

Fig. 4.2 Finding minima using golden section search method

The following steps will follow to determine the consecutive iterations:

Step 0: Initialization

Choose lower and upper bounds, x_l and x_u that brackets x^*, as well as stopping tolerance $\varepsilon > 0$. Set, $x_1 \leftarrow x_u - \gamma[x_u - x_l]$ and $x_2 \leftarrow x_l - \gamma[x_u - x_l]$.

Step 1: Stopping if $x_u - x_l < \varepsilon$, stop- report $x^* = 1/2[x_u - x_l]$ as an approximate solution.

Step 2a: Case $f(x_1) < f(x_2)$ (optimum left)

Narrow the research by eliminating the rightmost part:

$x_u \leftarrow x_2, x_2 \leftarrow x_1, x_1 \leftarrow x_u - \gamma[x_u - x_l]$

and evaluate $f(x_1)$ -return to step 1

Step 2b: Case $f(x_1) > f(x_2)$ (optimum right) Narrow the research by eliminating the leftmost part:

$x_l \leftarrow x_1, x_1 \leftarrow x_2, x_2 \leftarrow x_l - \gamma[x_u - x_l]$

and evaluate $f(x_2)$ -return to step 1

Fig 4.2 presents the process to find the minima using golden section search method in consecutive iterations.

In the proposed EMS strategy, the battery charging/discharging criteria has set to keep the battery SoC within predefined limits. The battery will discharge only if the net demand power of the MG is more than the γ percentage of the rated load power $P_{load(rated)}$. On the other case, the battery will charge based on the net power demand of MG. After that, the golden section search method is applied to minimise the grid power fluctuation of MG through the EMS. The grid power fluctuation problem

in Equation (4.10) is represented as a single control variable optimizing problem. The target of the optimization is to set an optimal value of the battery power to minimise the grid power at any instance of time by maintaining the battery constrains. But, the decision variable (battery power) depends on another independent variable of the optimizing function defined as net power demand (P_{net})) of MG which is highly stochastic in nature. Thus makes the problem non-linear in nature. So to apply the algorithm in the EMS, the boundary conditions (upper and lower limit) of the battery power is set as a function of net demand power of the MG. The boundary condition need to update every minute to apply the algorithm to the system. So, the optimising algorithm will operate every minute to take the decision of the battery power for a specific value of the net demand power. Considering the above requirements, the objective function and boundary conditions are described in Equations (4.10-4.13) to apply the algorithm in the study system.

$$min(P_{grid}(n)) = min(f(P_{bat}(n))) = P_{net}(n) - P_{bat}(n) \qquad \forall t \tag{4.8}$$

subject to

$$P_{bat}(l) \leq P_{bat}(n) \leq P_{bat}(u) \qquad \forall t \tag{4.9}$$

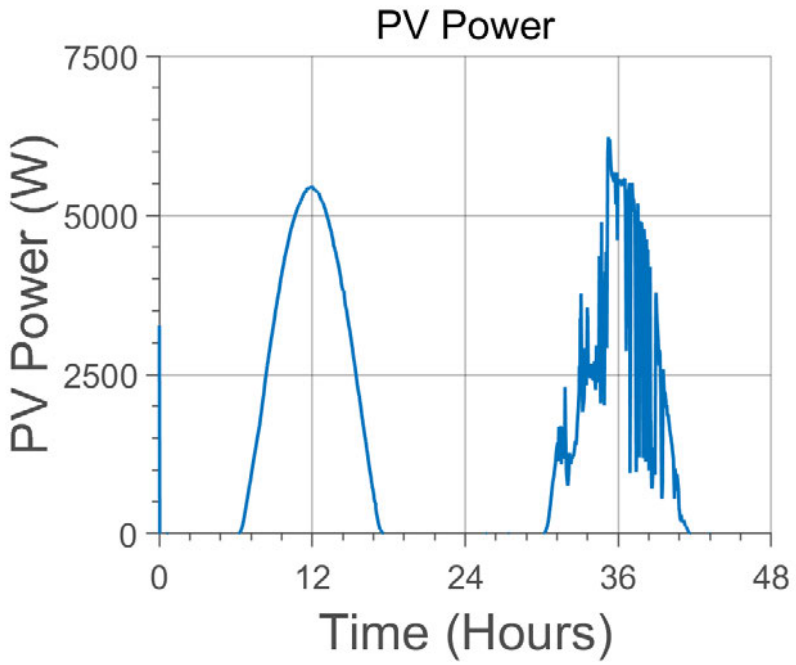

Fig. 4.3 PV power profile for different radiation days

Table 4.1 System Design Parameters

Symbol	Parameter	Value
P_{pv}	Capacity of PV module	7.2KW
C_{bat}	Capacity of battery module	42 KWh
$P_{load(rated)}$	Rated load power	3.2 KW
SoC_{int}	Initial value of SoC	40%
DoD	Depth of discharge	70%
T_s	Sample duration	1 min
N	Total number of sample per day	1440
γ	Charing/discharging decision constant	20%
k	Battery power limit constant	0.001

The value of $P_{bat}(l)$ and $P_{bat}(u)$ in each sample are determined as,

$$P_{bat}(l) = (P_{net}(n) + k * |P_{net}(n)|) \qquad \forall t \tag{4.10}$$

$$P_{bat}(u) = (P_{net}(n) - k * |P_{net}(n)|) \qquad \forall t \tag{4.11}$$

Where $P_{bat}(l)$ is the lower bound of the battery power and $P_{bat}(u)$ is the upper bound of battery power for each combination of P_{net}. k is a constant to determine the maximum and minimum value of P_{bat} for each value of P_{net}. The value of k has to set to a optimal value to minimise the performance parameters defined in section 4.3.

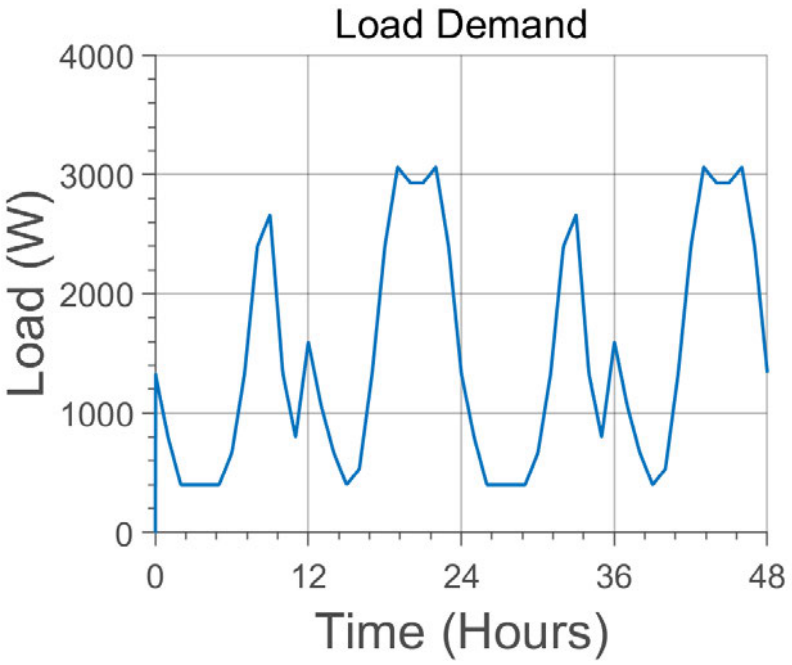

Fig. 4.4 Summer day residential load profile of study MG

4.5 Simulation Result

In this section, a model of the residential MG is developed in MATLAB SIMULINK by using Simscape Electrical™tool. The system design parameters in Table 4.1 are used to develop the simulation model. The simulation is run for 48 hours (2 days) using the statistical data of different radiation days of

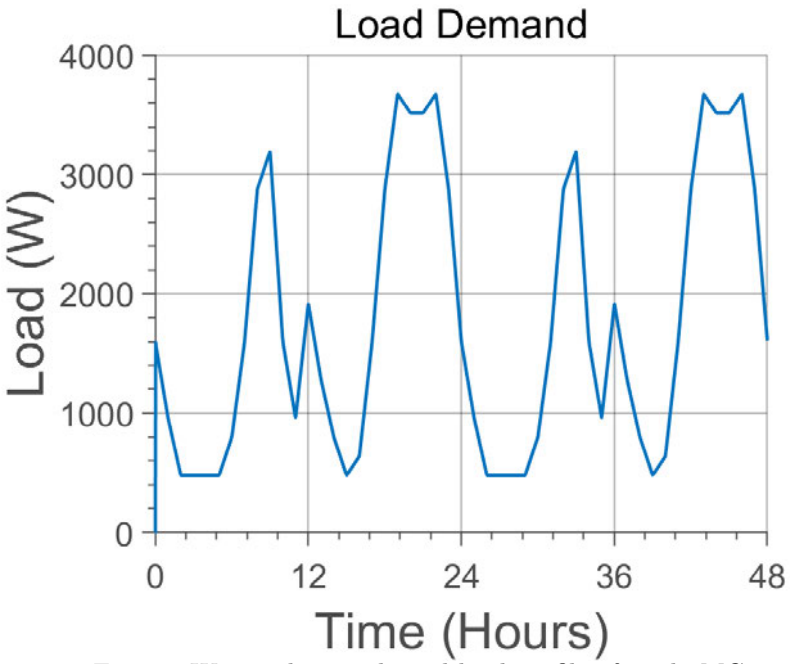

Fig. 4.5 Winter day residential load profile of study MG

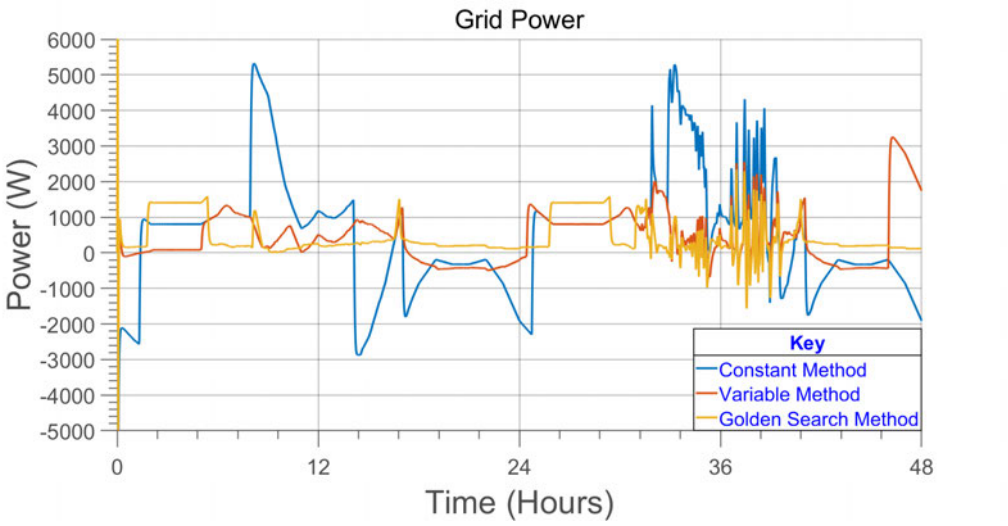

Fig. 4.6 Grid power for simulation period during summer days

Brisbane, Australia. The value of the statical weather is taken in one minute duration. Fig. 4.3 illustrates the stochastic nature of the PV power for the variation of temperature and radiation on September 2017

for linear variation day and large variation day. Furthermore, summer and winter load variation in a residential area for a 24 hours of the day illustrate in Fig. 4.4 and Fig. 4.5 respectively.

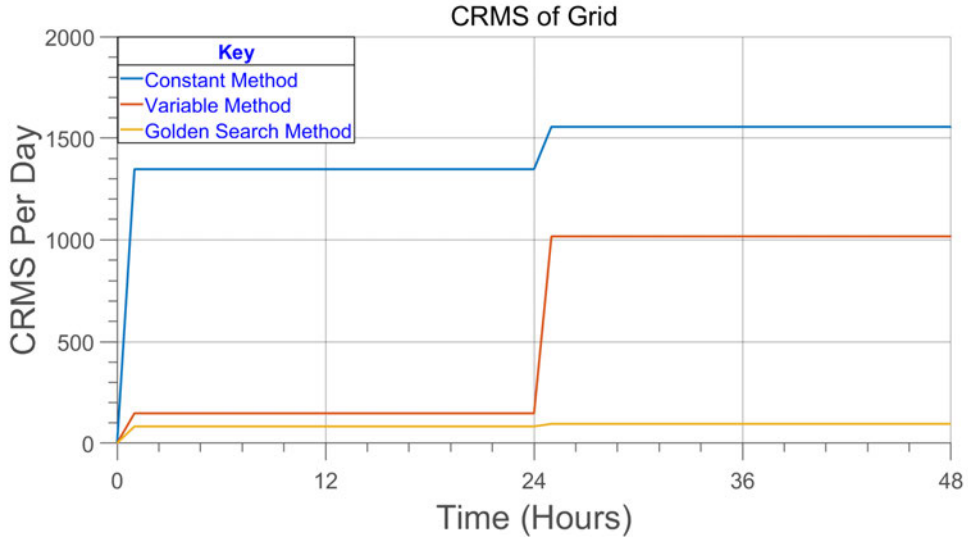

Fig. 4.7 CRMS value of grid power for simulation period during summer days

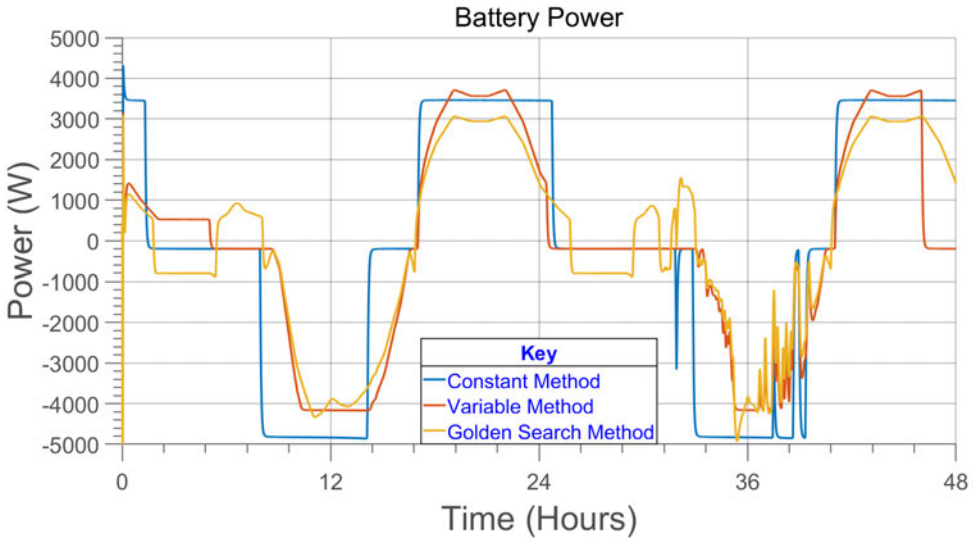

Fig. 4.8 Battery power for simulation period during summer days

The proposed power flow strategies in section 4.4 are applied in an EMS to minimise the grid power fluctuation. Matlab optimization tool box is used to apply the golden section search method to determine the optimal value of the battery power. The simulation runs each algorithms in every minute to determine the battery power for minimising the grid performance parameters. Fig. 4.6 shows the grid power for the simulation period during summer season using constant, variable and golden search method. On other hand, Fig. 4.7 shows the CRMS value of the grid power with three strategies for

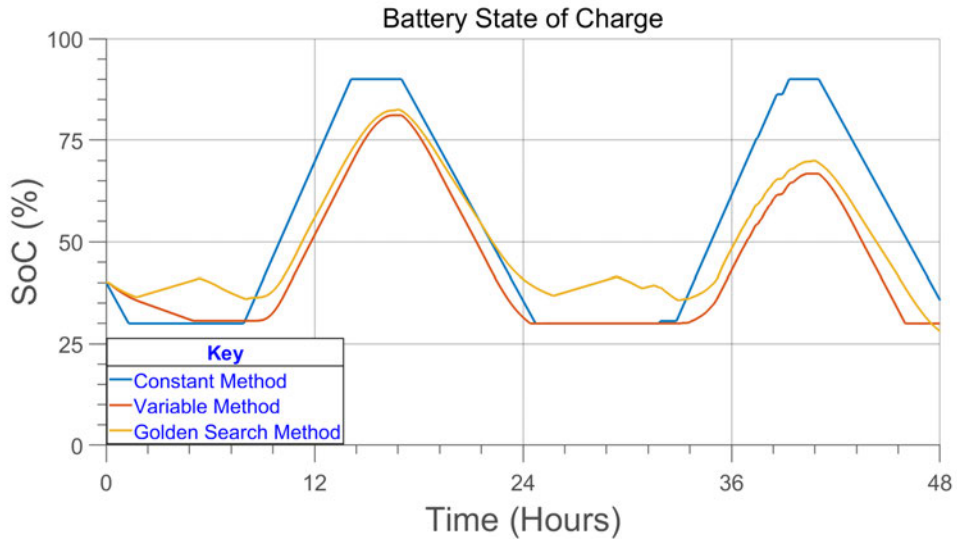

Fig. 4.9 Battery SoC for simulation period during summer days

summer season. The figures show the maximum value of grid power to/from the grid is 2.2 KW and an

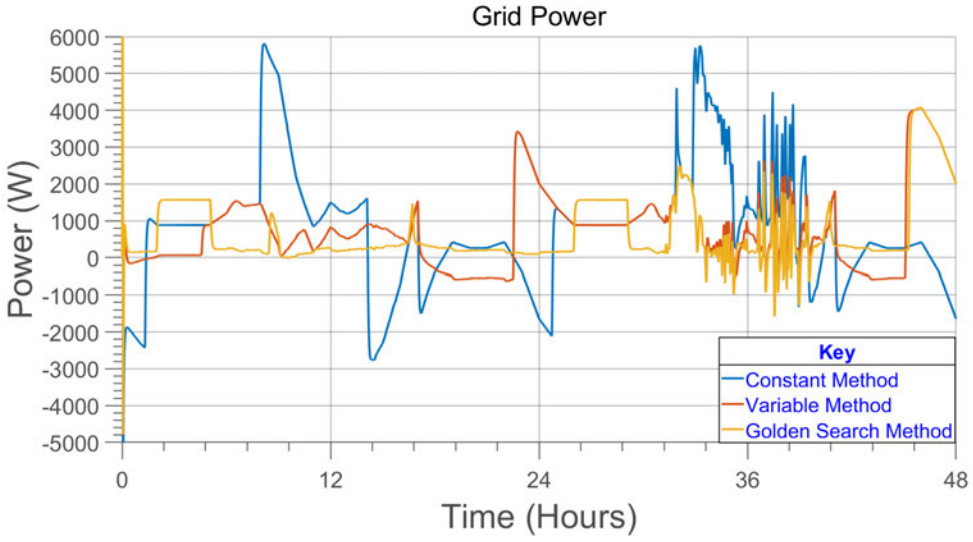

Fig. 4.10 Grid power for simulation period during winter days

average value of CRMS is 89 for the simulation period with the golden search method. However, the peak value of imported/exported power from the grid for constant and variable method is 5.4 KW and 3.2 KW in the same period while CRMS average value for both methods are 1452 and 581, respectively. Besides that, Fig. 4.8 shows a large fluctuation of the battery power as an effect of minimisation of the grid power fluctuation and Fig. 4.9 proofs that the battery SoC is within the predefined limits during the simulation period for presented three strategies. For winter season, the grid power profile is showing in Fig. 4.10 using constant, variable, and golden search method which indicate that peak

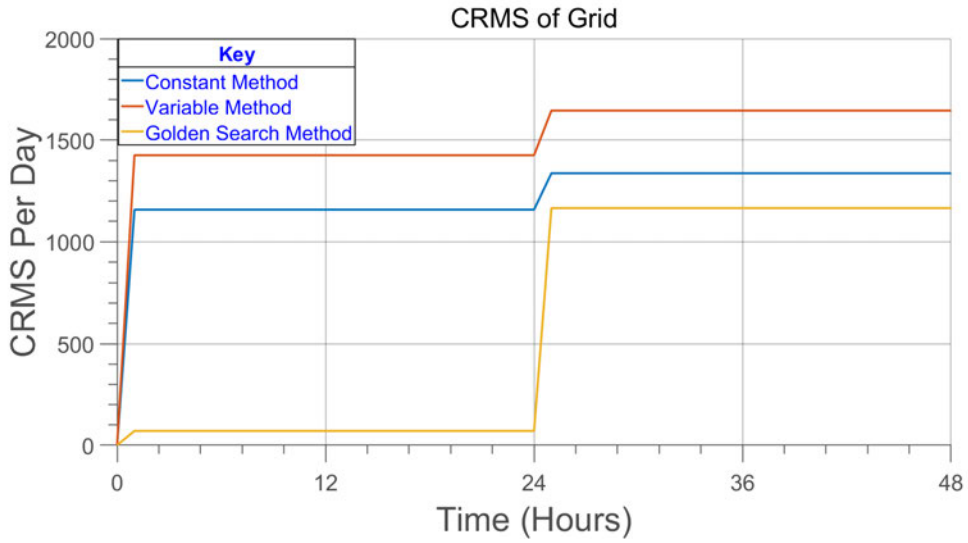

Fig. 4.11 CRMS value of grid power for simulation period during winter days

value of imported/exported power from the grid is 5.8 KW, 4.05 KW and 4.05 KW, respectively. The CRMS average vale for three approaches are 1247, 1535, and 618, respectively are presented in Fig. 4.11. The Fig. 4.12 demonstrates the charge and discharge power of the battery during 48-hours of winter season while the SoC of battery for same period is shown in Fig. 4.13. The outcomes indicate that the

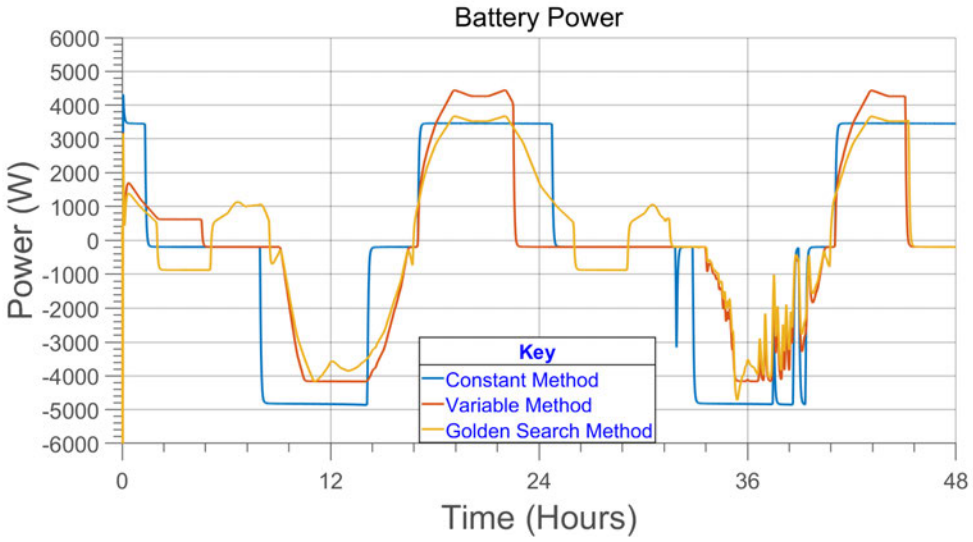

Fig. 4.12 Battery power for simulation period during winter days

fluctuation of battery power has increased due to the effect of reducing grid fluctuation. Compared to the other two methods, the result is showed a major improvement in performance parameters for golden search algorithm-based EMS for winter season which can be seen from Fig. 4.9-4.12. As mentioned in

Section 4.4, Fig. 4.9 and Fig. 4.13 show that the battery SoC remains within secure limits for three different strategies.

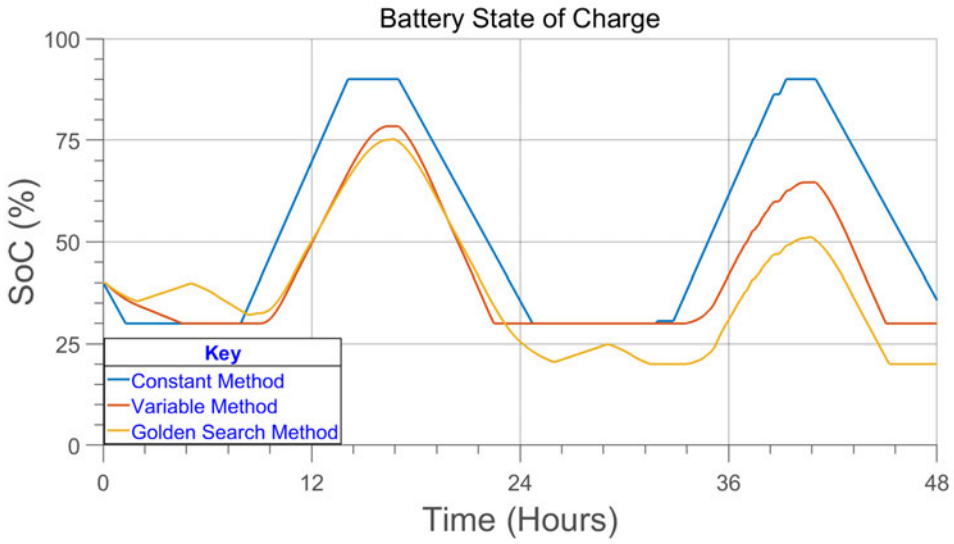

Fig. 4.13 Battery SoC for simulation period during winter days

4.6 Conclusions

This chapter designs a power flow control strategy through the EMS of a grid-connected residential MG for minimising the grid power fluctuation in a residential MG. The golden section search optimisation method is applied to control the battery power as a function of MG net power demand. The design parameters are optimised to minimise the predefined performance parameters of the grid power. Moreover, the battery parameters are kept within secure limits to increase the battery lifetime. The results show that the proposed power flow control method is able to minimise the grid power fluctuation and controls the power flow to/from the main grid as compared to constant and variable method.

Chapter 5

Dynamic Power Flow Control of Interlink Inverters of Microgrids

Chapter Contribution Declaration

This chapter addresses the interlink inverter control to achieve a smooth tie-line power in a grid-connected MG. A grid power controller is designed to maintain a constant tie-line power for typical days of the year. A state-space model is derived from the dynamic model of the MG, and eigenvalue-based stability analysis is done for the variation of system parameters. The proposed control method is verified using real world data through simulation experiment to show the performance of the designed controller. The performance of the proposed control method is compared with a dynamic EMS method to show the effectiveness of the controller.

This chapter includes a co-authored paper. The bibliographic details of the co-authored paper, including all authors, are:

Islam M, Yang F, Amin M. Dynamic control of grid-connected micro grids for tie-line smoothing. Int Trans Electr Energ Syst. 2020;30:e12557

DOI: https://doi.org/10.1002/2050-7038.12557

My contribution to this paper involved: conceptualization, system modelling, controller design, simulation experiment and analysis, the original draft writing, revising and proofreading.

Signed: _____ Date: *23.01.2021*

PhD Candidate: Mojaharul Islam (Principle Author)

Countersigned: _____ Date: *23.01.2021*

Principle Supervisor: A. Prof. Fuwen Yang (Corresponding Author)

Countersigned: _____ Date: *23.01.2021*

Associate Supervisor: Prof. Junwei Lu

Countersigned: _____ Date: *23.01.2021*

External Supervisor: A/Prof. Mohammad Amin

5.1 Abstract

This chapter presents an interlink inverter control method for providing a constant tie-line smoothing service in a grid-connected residential microgrid (MG) to mitigate the fluctuating nature of renewable power generation and load demand. A grid power controller is designed for an MG to keep a constant grid power on typical days of the year by maintaining the charging/discharging of the battery. To achieve this objective, the MG controller sends the reference to the interlink inverter controller based on load dynamics, average PV generation and battery capacity. Moreover, a state-space model is developed from the dynamic model of the MG system, and an eigenvalue-based stability analysis is performed for different system parameters. The proposed control method is verified through extensive case studies by using real irradiance and typical residential customer load data in Queensland, Australia. In addition, a comparison with a dynamic energy management-based method that aims to achieve the same objective is presented to demonstrate the performance of the proposed control method. Results show that the proposed method provides a constant tie-line power for a grid-connected residential MG for typical days of the year.

5.2 Introduction

In the last decades, the integration of renewable energy resources (RESs) into distribution networks has promoted the use of microgrids (MGs) as an attractive and feasible solution for reducing the consumption of fossil fuels in power generation [183]. An MG combines distributed generation (DG) with an energy storage system (ESS) to form a small grid that feeds different loads on a low-/medium-voltage network. An MG can operate in either grid-connected or island mode. Given its economic benefits, an MG has become an attractive solution for customers in recent years. Considerable attention has been given to island MG control [184–188] that focuses on voltage and frequency variation in an island MG. However, tie-line fluctuation is one of the key bottlenecks in a grid-connected MG due to the variations in power from RESs and load demand. Tie-line fluctuation in grid-connected MGs can cause severe stability and quality issues in a distribution network. Previous research has addressed this problem by controlling the power of MG resources, such as non-renewable generation control, demand side control, ESS control or coordinate control through an energy management system (EMS) of the MG [189, 90, 190, 174, 191–193, 175, 194, 195].

Demand side control is one of the approaches for mitigating tie-line fluctuations through direct or indirect (load scheduling, power pricing) control of load demand [189, 90]. A demand side control was presented in [189] by directly and continuously modulating load power consumption in an industrial MG. In [190], a large number of controllable loads were described as virtual energy storage in parallel with battery storage and a fuzzy logic controller was applied to revise the range of the virtual energy storage. Coordinated control between a heat pump and battery storage was proposed in [174] to smooth the tie-line power fluctuations in a group of residential MGs. Similarly, a hybrid electrothermal storage system that uses a battery and a hot water tank was developed in [191] to optimise power exchange with the grid in an electrothermal residential MG. In [192] and [90], a peak power pricing mechanism was used with the short-term forecasting of renewable generation to smooth power exchange with the grid. In the aforementioned studies, a mixed-integer linear programming problem was integrated into a model predictive control framework to reduce forecasting errors. In addition, tie-line smoothing can be achieved through coordinated control among controllable loads, the battery and non-renewable generation. A scheduling method among a diesel generator, battery storage and different controllable loads was performed in [193] through the EMS of an MG to reduce tie-line fluctuations. Coordinate control is also possible between a diesel generator and battery storage wherein demand side control is not allowed. In [175], a power management system was proposed to share the local load with the main grid by controlling the diesel generator with a droop reference estimator and the battery with a current controller. However, demand side control is not possible for most real residential MGs due to service reliability. Moreover, most residential MGs do not have a diesel generator and mostly depend on RESs as their primary resource. Therefore, the tie-line smoothing objective is more challenging for grid-connected residential MGs wherein battery storage is the only controllable unit and ensuring reliability for customers is more important than demand side control. Thus, the aforementioned methods may not be applicable for obtaining a smooth tie-line service in residential MGs.

Previous research has applied different control methods for dealing with the tie-line fluctuation problem in residential MGs based on forecasting or historical weather information. Considering the prediction of MG future power, a mixed-integer linear program was used in [171] to reduce tie-line power fluctuation and minimise the operation cost of the battery and energy usage. A fuzzy logic-based supervisory control was implemented in [196] to minimise the forecast utility power reference by adjusting the set points of DG. A forecasting method was also used in [172] and [173] to smooth tie-line power in a residential MG operation. A centralised moving average strategy [172] and a fuzzy logic-based control [173] were proposed in an EMS of MG to reduce forecasting errors by maintaining battery state

of charge (SoC). In [39], a fuzzy logic-based tie-line smoothing controller was designed for a residential MG without any forecasting by using energy rate of change and battery SoC as inputs to modify the required adjustment of grid power. After the adjustment, the necessary control of the battery was determined using the power balance equation of MG. A hierarchical power scheduling control strategy was proposed in [197] to ensure a flat grid power in a multi-microgrid network consisting of a large number of distributed energy resources (DERs). All the previous studies considers a specific duration, such as 10 min to 1 h to schedule tie-line power. Thus, these methods are difficult to apply in resolving short-term fluctuation problems, i.e. 5 min or less, caused by RESs and load.

A short-term tie-line fluctuation was analyzed in [7], and a fuzzy logic controller was designed in a dynamic EMS to control the battery in a grid-connected residential MG. However, the result showed that the method reduces tie-line fluctuation but is unable to maintain constant tie-line control. Moreover, this previous work did not mention the detailed control architecture nor any dynamic model of the MG. Consequently, it is difficult to design any dynamic controller for mitigating the dynamic behaviour of renewable generation or loads. To the authors' knowledge, the tie-line fluctuation problem in a grid-connected residential MG was not addressed in the previous study by using the dynamic analysis of the system. Therefore, designing a dynamic controller is appealing for resolving this issue. This chapter proposes a grid power control method for the interlink inverter of an MG to maintain constant tie-line power on typical days of the year. The controller is combined with an outer loop droop-based power controller and an inner loop grid current controller. The reference grid power is provided by the MG controller and determined during the design stage based on load dynamics, PV generation and battery capacity. The reference current of the grid current controller is calculated using the reference grid power from the droop controller and grid voltage. The proposed constant power control method can also achieve other tie-line objectives like power smoothing, flat tie-line power, peak shaving and power ramp limitation. The battery module in the MG connects with the PV converter in a hybrid configuration to reduce the number of conversions. The DC/DC converter in the battery module is responsible for maintaining the DC link voltage of the MG through the charging/ discharging operation of the battery in coordination with the proposed current controller. Furthermore, a dynamic model of the MG is developed from the time-average model of a typical grid-connected residential MG. A closed-loop state-space model of the MG system is derived from the dynamic model of the MG, and eigenvalue-based stability analysis is performed for different system parameters. The proposed controller is verified through extensive case studies by using real irradiance and typical residential customer load data in Queensland, Australia. The results show that the proposed controller maintains a constant tie-line

power set by the MG controller through the secure charging/discharging of the battery. Moreover, a comparison with a dynamic-EMS based method to achieve the same objective is presented in a MATLAB simulation. The major contributions of this chapter are as follows.

(1) A constant grid power control method is proposed for the interlink inverter of a grid-connected residential MG to obtain a smooth tie-line service despite the variations in RESs and load demand.

(2) A state-space model is derived from the dynamic model of the MG to analyse the dynamic response of the controller in different case studies.

(3) A comparison with a dynamic EMS method is presented to demonstrate the performance of the proposed control method.

The remainder of this chapter is organised as follows. Section 5.3 describes the system configuration and Modelling . Section 5.4 illustrates control strategies. section 5.5 demonstrates stability analysis of the study MG. Section 5.6 presents the simulation results and the comparisons of different case studies. and Section 5.7 concludes the chapter.

5.3 System Configuration and Modelling

5.3.1 System Configuration

The study considers a typical grid-connected residential AC MG structure with a PV panel as RES, a battery as ESS and a residential load. The PV panel and the battery are connected to the grid in hybrid configuration. A rated capacity of 2.5 kW solar panel and a battery of 17 kWh are installed for supply in a typical single residential house of Queensland, Australia with an average demand of 15 kWh per day. Fig. 5.1 depicts the MG test setup in Griffith for the system under study. Moreover, the system assumes a robust communication structure among different units of the study MG. The system has three converters for fulfilling the control requirements. The boost converter in the PV unit is used to track the maximum power from the PV panel. The buck-boost converter is connected to the battery storage system with the DC link. The converter is designed to maintain the DC link voltage within the reference by charging/discharging the battery. The DC link is connected to the AC bus through an interlink inverter. The interlink inverter control is designed to control the grid power drawn by the MG.

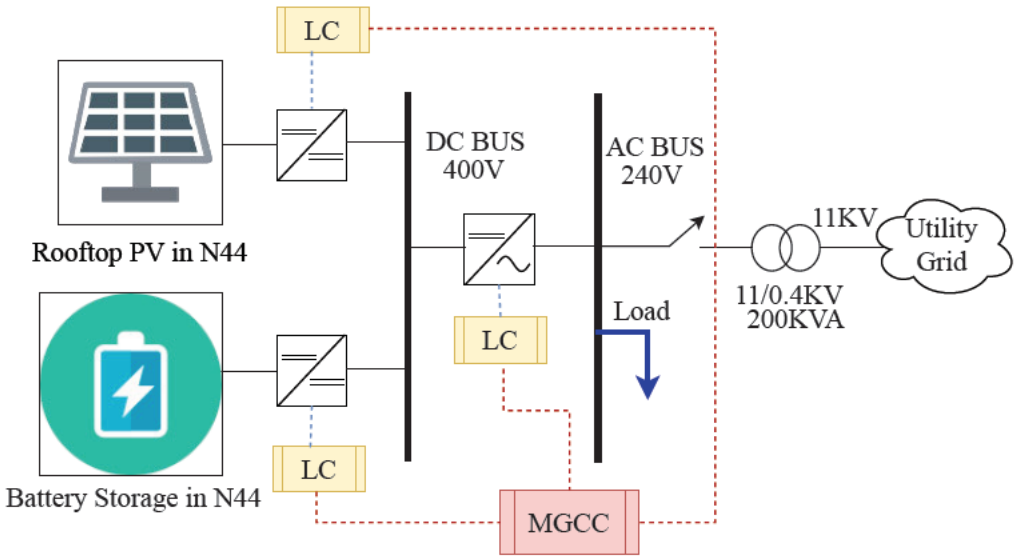

Fig. 5.1 Typical grid-connected residential AC MG setup in Building N44, Griffith University

5.3.2 Modelling of Microgrid

As shown in Fig. 5.1, the PV panel is connected to the DC link through a DC/DC boost converter. The battery module is connected to the DC link through a bidirectional buck-boost converter. The DC link of the MG is connected to the point of common coupling (PCC) through a bidirectional DC/AC inverter and an LC filter. In addition, the MG load is considered as a residential load connected at PCC. However, the MG model shown in the figure can be represented by differential equations to derive an analytical model of the MG.

The voltage and current equations of the DC/DC converters and the DC link are expressed as

$$L_1 \frac{di_1}{dt} = v_{pv} - R_1 i_1 - (1 - d_1) v_{dc} \tag{5.1}$$

$$L_2 \frac{di_2}{dt} = v_{bat} - R_2 i_2 - (1 - d_2) v_{dc} \tag{5.2}$$

$$C_{dc} \frac{dv_{dc}}{dt} = (1 - d_1) i_1 - (1 - d_2) i_2 - d_d i_d - d_q i_q \tag{5.3}$$

Similarly, the AC side voltage and current equations with the inverter can be written in the d-q reference frame as

Inverter loop equations:

$$L_f \frac{di_{fd}}{dt} = v_{id} - R_f i_{fd} + \omega L_f i_{fq} - v_{od} \tag{5.4}$$

$$L_f \frac{di_{fq}}{dt} = v_{iq} - R_f i_{fq} - \omega L_f i_{fq} - v_{oq} \tag{5.5}$$

Grid loop Equations,

$$L_g \frac{di_{gd}}{dt} = -R_g i_{gd} + \omega L_g i_{gq} + v_{od} - v_{gd} \tag{5.6}$$

$$L_g \frac{di_{gq}}{dt} = -R_g i_{gq} - \omega L_g i_{gd} + v_{oq} - v_{gq} \tag{5.7}$$

Equations of filter capacitor,

$$C_f \frac{v_{od}}{dt} = i_{fd} - i_{gd} - i_{Ld} + \omega C_f v_{oq} \tag{5.8}$$

$$C_f \frac{v_{oq}}{dt} = i_{fq} - i_{gq} - i_{Lq} - \omega C_f v_{od} \tag{5.9}$$

5.3.3 Phase Locked Loop (PLL) Control

PLL is necessary to track the actual frequency of the system. The input of PLL is the d-axis component of the voltage across the filter capacitor. Thus, the phase is locked at $v_{od} = 0$ [198]. The Equations (5.10-5.12) illustrate the states associated with PLL.

$$\frac{dv_{odf}}{dt} = \omega_{cPLL} v_{od} - \omega_{cPLL} v_{odf} \tag{5.10}$$

$$\frac{d\phi_{PLL}}{dt} = -v_{odf} \tag{5.11}$$

$$\frac{d\theta}{dt} = \omega_g - k_{pPLL} v_{odf} + k_{iPLL} \phi_{PLL} \tag{5.12}$$

5.4 Control Strategies

In this chapter, a constant grid power control method is proposed to maintain a constant tie-line power on typical days of the year. The detailed control strategies are described in the following subsections.

5.4.1 Maximum Power Point Tracking (MPPT) Control

The boost converter connected to the PV panel is considered as an ideal MPPT controller by using the perturb and observe (P & O) method to track the maximum power from the PV unit [199].

5.4.2 DC Link Voltage Control

The bidirectional buck-boost converter connected to the battery storage is responsible for maintaining the DC link voltage. The idea of using the charge/discharge power of the battery banks to regulate DC voltage (by using a proportional–integral (PI) controller) was introduced in [187, 200]. If the measured DC link voltage is higher than the reference voltage, then the battery will run in buck mode to charge the battery. If the measured DC link voltage is lower than the reference voltage, then the battery will run in boost mode to discharge the battery. Otherwise, the battery will be in rest mode without any buck-boost operation. However, to limit overcharging/overdischarging of the battery, a SoC-based EMS is applied to the system as discussed in Section (2.C). Fig. 5.2 shows the flowchart to decide between buck or boost operation of the converter. Fig. 5.3 presents the block diagram of the DC link voltage controller. The equations of the controller are expressed as Equations (5.13-5.14).

$$d_2 = K_{p1}(v_{dc}^* - v_{dc}) + K_{i1}\gamma \tag{5.13}$$

Where

$$\gamma = \int (v_{dc}^* - v_{dc})dt \tag{5.14}$$

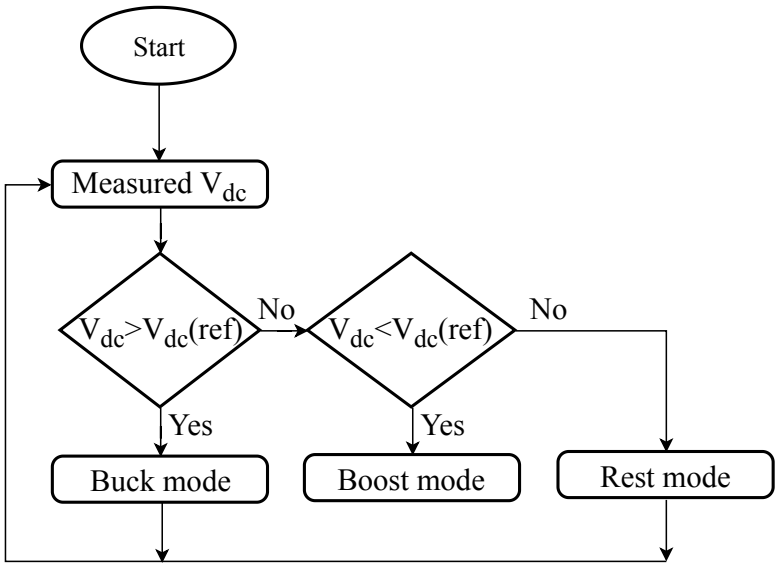

Fig. 5.2 Flow chart of the DC link voltage controller for regulating battery charging/discharging

5.4.3 Proposed Grid Power Control

A DC/AC bidirectional inverter control method is proposed to control the grid power drawn by the MG and obtain a constant tie-line of a grid-connected MG despite the fluctuating nature of RESs and load

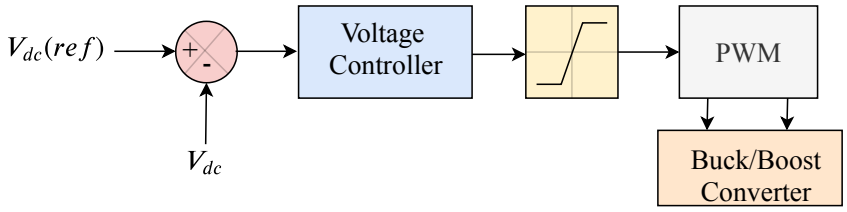

Fig. 5.3 DC link voltage controller

demand. The proposed method follows a three-step hierarchical approach for controlling grid power. In the first step, a process for determining the grid power reference is described to obtain a constant tie-line on typical days of the year. The day-to-day variations in the renewable generation and load demand will change the average daily power drawn by the MG. Commercial software, such as HomerPro, typically uses the statistical data of power generations and demands to calculate the average power shortage of an MG throughout the year. The power shortage should be supplied by the utility grid to balance the power in the MG. On the basis of the system configuration and statistical data of the MG, the software algorithm determines the percentage of the average load needed to be supplied by the utility grid on typical days of the year. The result may vary depending on the available generation capacity, generation type, load dynamics and geographical location of the MG. Thereafter, reference grid power is fed to the MG controller to provide the control reference to the interlink inverter of the MG. In general, an MG controller is responsible for performing different types of activities, such as power flow control, secondary voltage and frequency regulation and economical operation, based on the control requirements of an MG. However, this chapter only focuses on the power flow control of the MG to obtain a constant tie-line power in a grid-connected residential MG. A battery SoC-based EMS is applied to control the grid power and limit the overcharging/overdischarging of the battery. When the battery SoC is within the predefined limit, the MG controller provides a constant reference power determined by the algorithm. If the battery SoC is over SoC_{max} due to overgeneration from the PV panel, then the reference grid power is set to be equal to $P_{pv} - P_{load}$ to transfer excess generation to the grid. If the battery SoC is under SoC_{min}, then the MG controller sets the grid reference power to maintain a reliable power supply to meet the load demand in the MG. In both cases, the grid reference power is set to a value such that the battery will not overcharge/overdischarge to maintain a healthy life of the battery storage system. Fig. 5.4 shows the process for determining the reference gird power to supply to the interlink inverter.

In the second step, a combination of droop control and the current calculation method is introduced to determine the reference grid current from the reference grid power set by the MG controller. A

droop control method is used to control the real and reactive power references in accordance with grid frequency and voltage. The droop control feature also enables the interlink inverter for coordinated operation with other inverters in a multi-microgrid based distribution network. This chapter adopts the conventional droop control method between P-ω and Q-V is illustrated in Equation 5.15.

$$\begin{aligned} \omega &= \omega^* - m(P - P^*) \\ V &= V^* - n(Q - Q^*) \end{aligned} \tag{5.15}$$

The droop co-efficient can be calculated using the equation 5.16,

$$\begin{aligned} m &= \frac{2\pi(f_{max} - f_{min})}{P_{max}} \\ n &= \frac{(V_{max} - V_{min})}{Q_{max}} \end{aligned} \tag{5.16}$$

Given that the reactive power reference of the inverter is typically set to $Q^* = 0$ in grid-connected operation, only P-ω droop is implemented in this chapter. f_{max},f_{min} are selected in accordance with the Australian power system standard, and P_{max} is the rated power of the inverter. The power determined by the droop controller is used to calculate the reference current of the grid current controller.

The real and reactive power equations for a single-phase system in the d-q reference frame can be written as

$$\begin{aligned} P_g &= \frac{1}{2}(v_{gd}i_{gd} + v_{gq}i_{gq}) \\ Q_g &= \frac{1}{2}(v_{gq}i_{gd} + v_{gd}i_{gq}) \end{aligned} \tag{5.17}$$

Equation (5.17) is used to calculate the reference current of the inverter as expressed in Equation (5.18).

$$\begin{aligned} i^*_{gd} &= \frac{2P^*_g v_{ogd} + 2Q^*_g v_{ogq}}{v_{ogd}(v^2_{ogd} + v^2_{ogq})} \\ i^*_{gq} &= \frac{2P^*_g v_{ogd} v_{ogq} - 2Q^*_g v^2_{ogd}}{(v^2_{ogd} + v^2_{ogq})} \end{aligned} \tag{5.18}$$

In the third step, a grid current controller is designed to control the interlink inverter of the grid-connected MG to track the grid current to the reference determined using the second step of the control

method. Fig. 5.5 shows the block diagram of the designed grid current controller with a detailed control structure to determine the duty cycle of the inverter. The equations of the grid current controller are expressed as Equations (5.19-5.22).

$$v_{id} = v_{od} - \omega L_f i_{fq} + R_f i_{fd} + K_{p2}(i^*_{gd} - i_{gd}) + K_{i2}\beta_{id} \tag{5.19}$$

$$\beta_{id} = \int (i^*_{gd} - i_{gd})dt \tag{5.20}$$

$$v_{iq} = v_{oq} + \omega L_f i_{fd} + R_f i_{fq} + K_{p2}(i^*_{gq} - i_{gq}) + K_{i2}\beta_{iq} \tag{5.21}$$

$$\beta_{iq} = \int (i^*_{gq} - i_{gq})dt \tag{5.22}$$

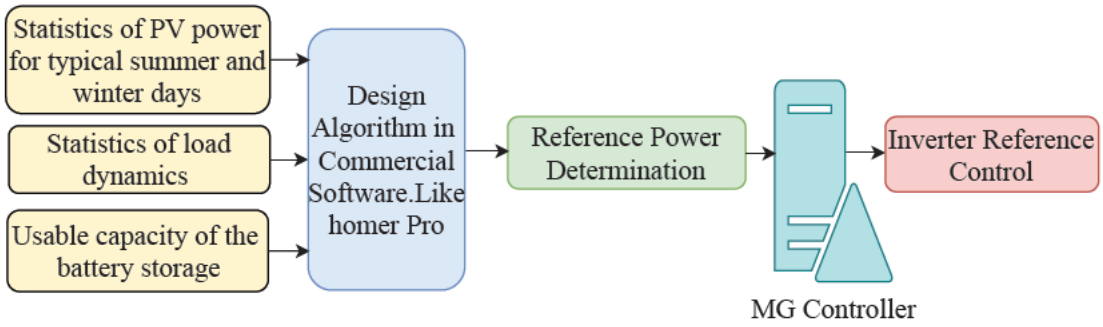

Fig. 5.4 Process for determining the reference power of the interlink inverter

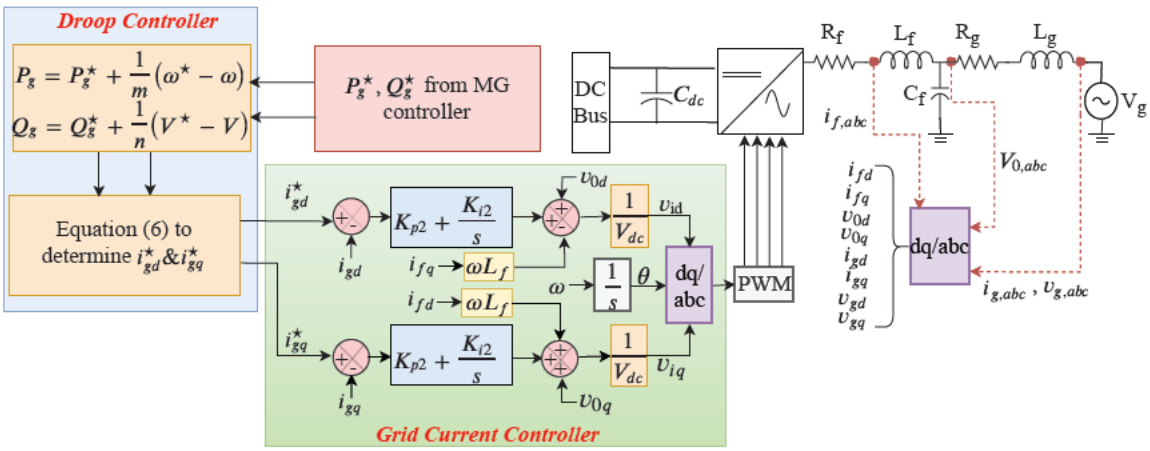

Fig. 5.5 Proposed grid power controller

5.5 Stability Analysis of Microgrid

5.5.1 Small-Signal Model

To derive the small-signal model of the MG and to simplify the analysis, the boost converter and the PV panel are replaced with an ideal variable current source. Accordingly, the DC link voltage equation can be simplified as,

$$C_{dc}\frac{dv_{dc}}{dt} = i_1 - (1-d_2)i_2 - d_d i_d - d_q i_q \tag{5.23}$$

Differential Equations in (5.1-5.14) and (5.19-5.23) are used to derive the closed-loop nonlinear system model of the study MG. The nonlinear system model should be linearised near a steady-state point for the stability analysis of the system. The steady-state operating point of the system can be derived by solving this nonlinear system model with the derivatives terms set to zero. The linearised small-signal model of the MG is represented using the standard state-space equations as,

$$\begin{aligned} \Delta\dot{x} &= A\Delta x + B\Delta u \\ y &= C\begin{bmatrix}\Delta i_{gd}\\ \Delta i_{gq}\end{bmatrix} + D\Delta u \end{aligned} \tag{5.24}$$

Where the state variables Δx and system inputs Δu are represented in Equations (5.25-5.26) and the system coefficients are expressed as Equations (5.27-5.35).

$$\Delta x = [\Delta i_2 \quad \Delta v_{dc} \quad \Delta\gamma \quad \Delta i_{fd} \quad \Delta i_{fq} \quad \Delta\beta_{id} \quad \Delta\beta_{iq} \quad \Delta i_{gd} \quad \Delta i_{gq} \quad \Delta v_{od} \quad \Delta v_{oq} \quad \Delta v_{odf} \quad \phi_{PLL} \quad \theta] \tag{5.25}$$

$$\Delta u = \begin{bmatrix}\Delta i_1 & \Delta v^*_{dc} & \Delta v_{bat} & \Delta i^*_{gd} & \Delta i^*_{gq} & \Delta v_{gd} & \Delta v_{gq} & \Delta i_{Ld} & \Delta i_{Lq}\end{bmatrix} \tag{5.26}$$

$$A = \begin{bmatrix}
-\frac{R_2}{L_2} & A_{12} & \frac{(K_{i1}V_{dc})}{L_2} & 0 & 0 & 0 & 0 & 0 & 0 & 0 & 0 & 0 & 0 & 0 \\
A_{21} & A_{22} & \frac{-(K_{i1}I_2)}{C_{dc}} & A_{24} & A_{25} & \frac{-(K_{i2}I_{fd})}{(C_{dc}V_{dc})} & \frac{-(K_{i2}I_{fq})}{(C_{dc}V_{dc})} & \frac{(K_{p2}I_{fd})}{(C_{dc}V_{dc})} & \frac{(K_{p2}I_{fq})}{(C_{dc}V_{dc})} & \frac{-I_{fd}}{(C_{dc}V_{dc})} & \frac{-I_{fq}}{(C_{dc}V_{dc})} & 0 & 0 & 0 \\
0 & -1 & 0 & 0 & 0 & 0 & 0 & 0 & 0 & 0 & 0 & 0 & 0 & 0 \\
0 & 0 & 0 & 0 & 0 & \frac{K_{i2}}{L_f} & 0 & \frac{-K_{p2}}{L_f} & 0 & 0 & 0 & 0 & 0 & 0 \\
0 & 0 & 0 & 0 & 0 & 0 & \frac{K_{i2}}{L_f} & 0 & \frac{-K_{p2}}{L_f} & 0 & 0 & 0 & 0 & 0 \\
0 & 0 & 0 & 0 & 0 & 0 & 0 & -1 & 0 & 0 & 0 & 0 & 0 & 0 \\
0 & 0 & 0 & 0 & 0 & 0 & 0 & 0 & -1 & 0 & 0 & 0 & 0 & 0 \\
0 & 0 & 0 & 0 & 0 & 0 & 0 & 0 & \frac{-R_g}{L_g} & \omega & \frac{1}{L_g} & 0 & 0 & 0 \\
0 & 0 & 0 & 0 & 0 & 0 & 0 & -\omega & \frac{-R_g}{L_g} & 0 & \frac{1}{L_g} & 0 & 0 & 0 \\
0 & 0 & 0 & \frac{1}{C_f} & 0 & 0 & 0 & \frac{-1}{C_f} & 0 & 0 & \omega & 0 & 0 & 0 \\
0 & 0 & 0 & 0 & \frac{1}{C_f} & 0 & 0 & 0 & \frac{-1}{C_f} & -\omega & 0 & 0 & 0 & 0 \\
0 & 0 & 0 & 0 & 0 & 0 & 0 & 0 & 0 & \omega_{cPLL} & 0 & -\omega_{cPLL} & 0 & 0 \\
0 & 0 & 0 & 0 & 0 & 0 & 0 & 0 & 0 & 0 & 0 & -1 & 0 & 0 \\
0 & 0 & 0 & 0 & 0 & 0 & 0 & 0 & 0 & 0 & 0 & -K_{pPLL} & 0 & K_{iPLL}
\end{bmatrix} \tag{5.27}$$

$$A_{12} = \frac{(K_{i1}\gamma + K_{p1}(V_{dc}^{*} - 2V_{dc}) - 1)}{L_2} \tag{5.28}$$

$$(A_{21} = \frac{-(K_{i1}\gamma + K_{p1}(V_{dc}^{*} - 2V_{dc}) - 1)}{Cdc} \tag{5.29}$$

$$A_{22} = \frac{(K_{p1}I_2 + \frac{(I_{fd}(V_{od}+K_{i2}\beta_{id}+R_f I_{fd}+K_{p2}(I_{gd}^{*}-I_{gd})-L_f I_{fq}\omega))}{V_{dc}^2} + \frac{(i_{fq}(V_{oq}+K_{i2}\beta_{iq}+R_f I_{fq}+K_{p2}(I_{gq}^{*}-I_{gq})+L_f I_{fd}\omega))}{V_{dc}^2}}{C_{dc}} \tag{5.30}$$

5.5.2 Eigenvalue based Stability Analysis

The linearised system model represented by the state-space equation reflects an accurate model of the system. The linearised system model developed in the previous subsection can be used to investigate the eigenvalue-based stability analysis of the system. The system coefficient matrix A is used to determine the states of eigenvalues in all modes of the system. The parameters of the system are listed in Table 5.1. The current controller is tuned on the basis of the symmetrical optimum tuning criteria with a phase margin of 2.59° at crossover frequency of 56.7 rad/s. The eigenvalues of the MG are calculated analytically, and the results are presented in Table 5.2.

The system eigenvalues in Table 5.2 have two poles meeting in the origin and several poles close to the real axis with small damping and low oscillation frequency. Two pairs of complex conjugate poles exist with high oscillation frequency related to the inverter parameters. The system is stable for the parameter in Table 5.1; thus a full range of investigation has been conducted to change the power reference from $-P_{rated}$ to P_{rated}. All other parameters in Table 5.1 are assumed constant except for the steady-state value of the grid power to find the result in Fig. 5.6. The result shows that none of the system poles is moving due to a change in steady-state grid power.

A similar investigation has been performed for the change in PV power within the entire range of operating points from 0 to $P_{pv,max}$ considering that other parameters in Table 5.1 are constant. Fig. 5.7 shows that the poles are nearly constant despite the change in PV operating conditions. A similar analysis can be conducted for other system parameters to determine the sensitivity of the parameters to system pole movement. However, the sensitivity of the controller gain is an essential part of eigenvalue analysis. The sensitivity range of the controller gain exerts a direct impact on system stability. To investigate the sensitivity of eigenvalues to variations in the current controller's proportional gain K_{p2}, the value of K_{p2} is increased from 0.1 to 3. Fig. 5.8 shows the trajectory of the poles with an increase

$$A_{24} = \frac{-(v_{od} + K_{i2}\beta_{id} + R_f * I_{fd} + K_{p2}(I^*_{gd} - I_{gd}) - L_f I_{fq}\omega + R_f I_{fd} + L_f I_{fq}\omega)}{V_{dc}C_{dc}} \tag{5.31}$$

$$A_{25} = \frac{-(V_{oq} + K_{i2}\beta_{iq} + R_f I_{fq} + K_{p2}(I^*_{gq} - I_{gq}) + L_f I_{fd}\omega + R_f I_{fq} - L_f I_{fd}\omega}{V_{dc}C_{dc}} \tag{5.32}$$

in K_{p2} from 0.1 to 3. The result shows that poles with a high imaginary part move to the right half of the axis for a controller gain of more than 2. Thus, controller gain can vary within a wider range, and the system will be unstable for a large controller gain. A similar sensitivity analysis of the system eigenvalues has been performed for the change in DC/DC converter gain. Fig. 5.9 shows the trajectory of the poles with an increase in k_{p1} from 1 to 2.5. The result shows that the poles related to DC/DC converter gain k_{p1} has moved to the right half-plane with an increase in the controller gain of nearly 2 whilst other parameters of the system are fixed. Further investigation of the sensitivity analysis of the eigenvalues can be conducted for other system parameters as long as few parameters are responsible for the stability problem in a specific system configuration. Such investigation is an essential part of the stability analysis of an MG with different parameters, size and number of generations in the system.

5.6 Simulation Results and Comparisons

5.6.1 Simulation Results

The performance of the proposed inverter control method is analysed in the context of Queensland, Australia through the simulation of real residential house load, solar radiation and temperature data. A test MG is designed using available resources in Griffith University, Australia. Fig. 5.1 shows the MG setup in building N44,Griffith University. A SunPower E20 series model PV unit with a peak capacity of 2.5 kW is installed in N44 and used in the simulation. The sun radiation and temperature data of

$$B = \begin{bmatrix} 0 & \frac{(K_{p1}V_{dc})}{L_2} & \frac{1}{L_2} & 0 & 0 & 0 & 0 & 0 & 0 \\ \frac{1}{C_{dc}} & \frac{-(K_{p1}I_2)}{C_{dc}} & 0 & \frac{-(K_{p2}I_{fd})}{C_{dc}V_{dc}} & \frac{-(K_{p2}I_{fq})}{C_{dc}V_{dc}} & 0 & 0 & 0 & 0 \\ 0 & 1 & 0 & 0 & 0 & 0 & 0 & 0 & 0 \\ 0 & 0 & 0 & \frac{K_{p2}}{L_f} & 0 & 0 & 0 & 0 & 0 \\ 0 & 0 & 0 & 0 & \frac{K_{p2}}{L_f} & 0 & 0 & 0 & 0 \\ 0 & 0 & 0 & 1 & 0 & 0 & 0 & 0 & 0 \\ 0 & 0 & 0 & 0 & 1 & 0 & 0 & 0 & 0 \\ 0 & 0 & 0 & 0 & 0 & \frac{-1}{L_g} & 0 & 0 & 0 \\ 0 & 0 & 0 & 0 & 0 & 0 & \frac{-1}{L_g} & 0 & 0 \\ 0 & 0 & 0 & 0 & 0 & 0 & 0 & \frac{-1}{C_f} & 0 \\ 0 & 0 & 0 & 0 & 0 & 0 & 0 & 0 & \frac{-1}{C_f} \\ 0 & 0 & 0 & 0 & 0 & 0 & 0 & 0 & 0 \\ 0 & 0 & 0 & 0 & 0 & 0 & 0 & 0 & 0 \\ 0 & 0 & 0 & 0 & 0 & 0 & 0 & 0 & 0 \end{bmatrix} \tag{5.33}$$

$$C = \begin{bmatrix} 0 & 0 & 0 & 0 & 0 & 0 & 0 & 1 & 0 & 0 & 0 & 0 & 0 & 0 \\ 0 & 0 & 0 & 0 & 0 & 0 & 0 & 0 & 1 & 0 & 0 & 0 & 0 & 0 \end{bmatrix} \tag{5.34}$$

$$D = 0 \tag{5.35}$$

Table 5.1 System Parameters for Study MG

Symbol	Parameter	Value
L_2	Inductor value of the buck-boost converter	9mH
R_2	Resistor value of the buck-boost converter	0.25Ω
C_{dc}	Dc link capacitance	300mF
L_f	Filter inductor	3.2mH
R_f	Filter resistor	0.008Ω
C_f	Filter capacitance	9.67μF
L_g	Grid inductor	0.064 mH
R_g	Grid resistor	0.008Ω
ω_{cPLL}	PLL filter cut-off frequency	25Hz
ω	Rated frequency	50Hz
$P_(rated)$	Rated power of inverter	2.5KW
V_{rated}	Rated voltage	240 V
k_{p1}, k_{i1}	DC link controller gain	1.2, 3
k_{p2}, k_{i2}	Interlink inverter controller gain	0.3, 10

Table 5.2 System eigenvalues of the corresponding states

System states	Eigenvalue ($\lambda_i = \sigma_i \pm j\omega_i$)
λ_1	0+j0
λ_2	0+j0
λ_3	-157+j0
$\lambda_{4,5}$	-265 ± j88825
$\lambda_{6,7}$	-265 ± j88197
$\lambda_{8,9}$	-19 ± j843
λ_{10}	-20+j0
$\lambda_{11,12}$	-47±j30
$\lambda_{13,14}$	-47±j30

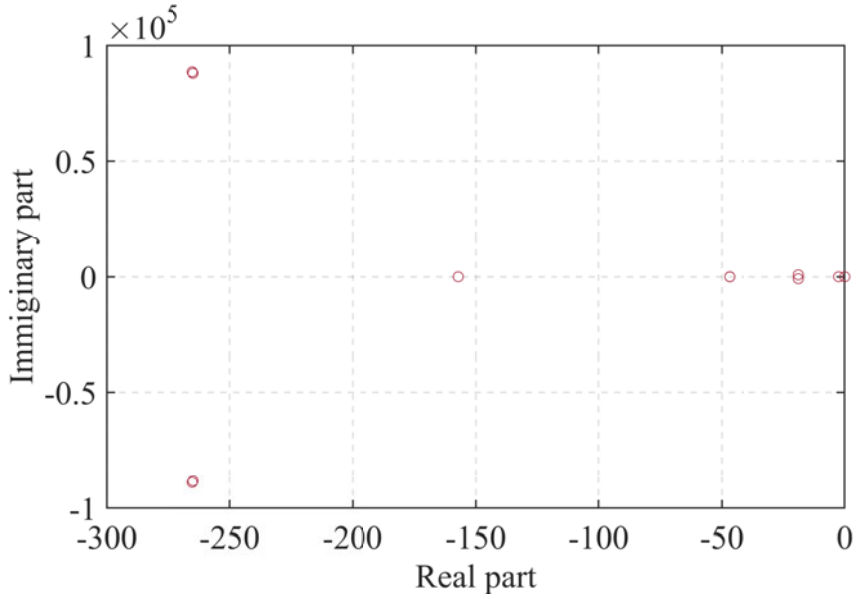

Fig. 5.6 Trajectory of eigenvalues when power P_g^* is changed through the operating range of the inverter

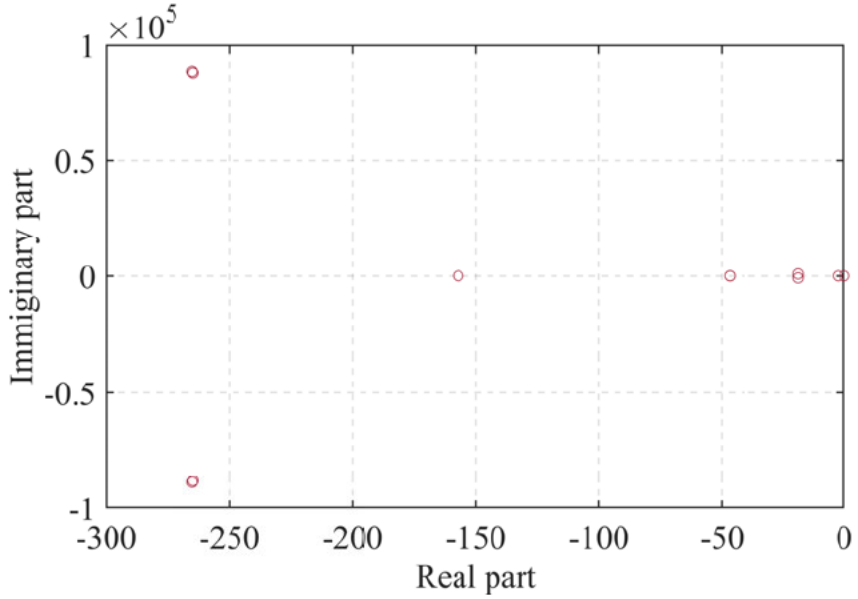

Fig. 5.7 Trajectory of eigenvalues when power P_{pv} is changed through the operating range of the PV

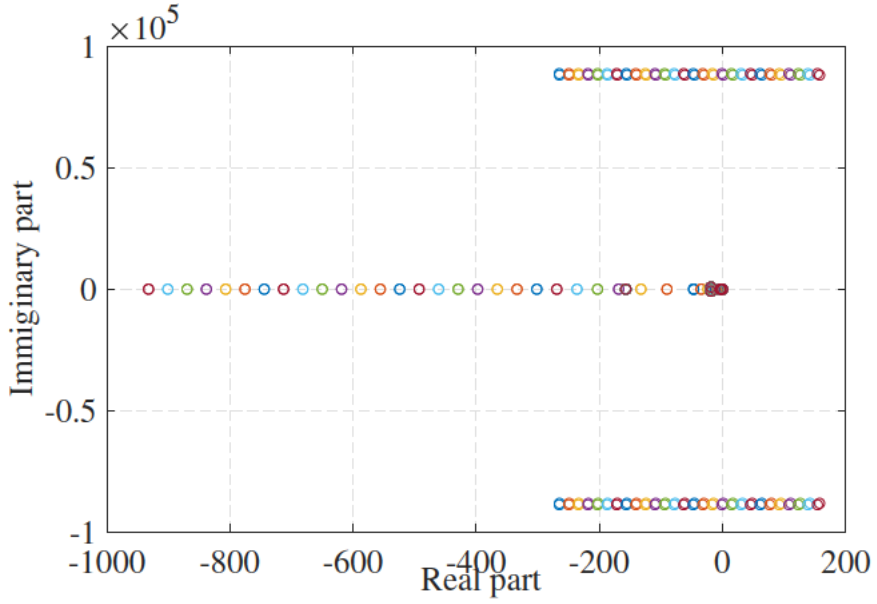

Fig. 5.8 Trajectory of eigenvalues for a change in proportional gain of the inverter

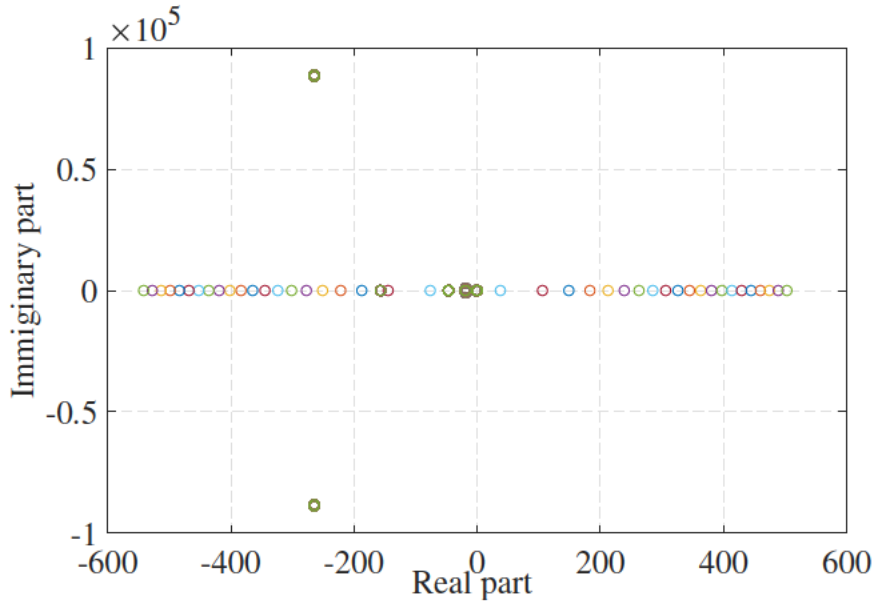

Fig. 5.9 Trajectory of eigenvalues for a change in proportional gain of the DC-DC converter

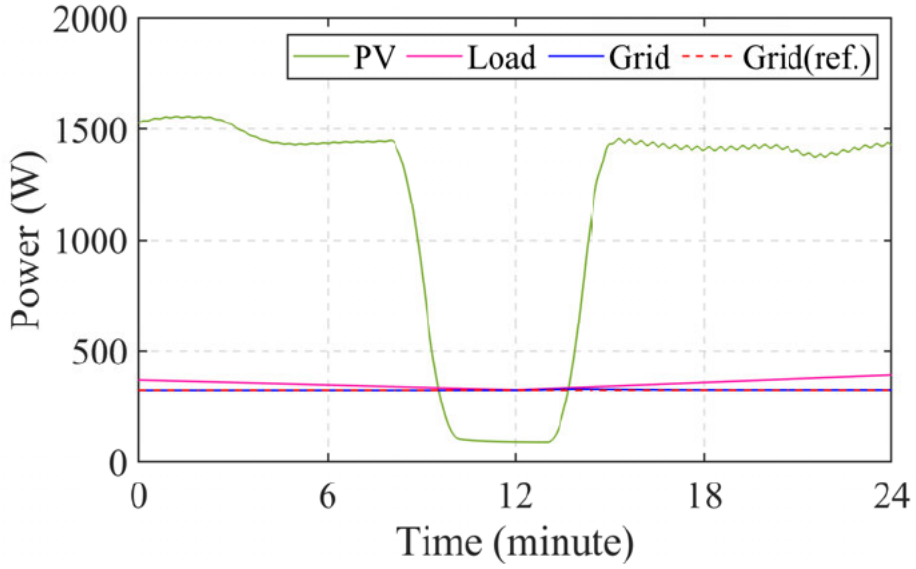

Fig. 5.10 Dynamic response of the controller due to sudden cloud appearance

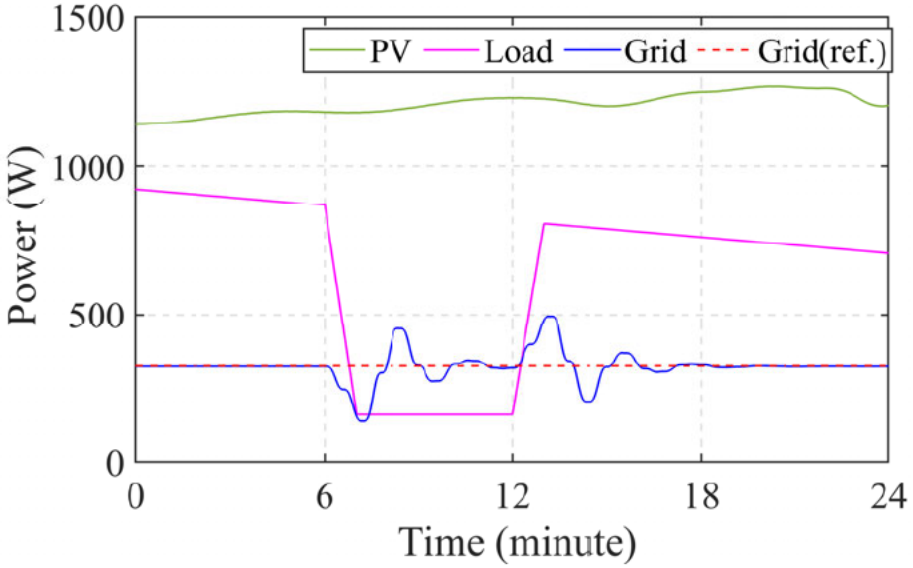

Fig. 5.11 Dynamic response of the controller due to short-term load variation

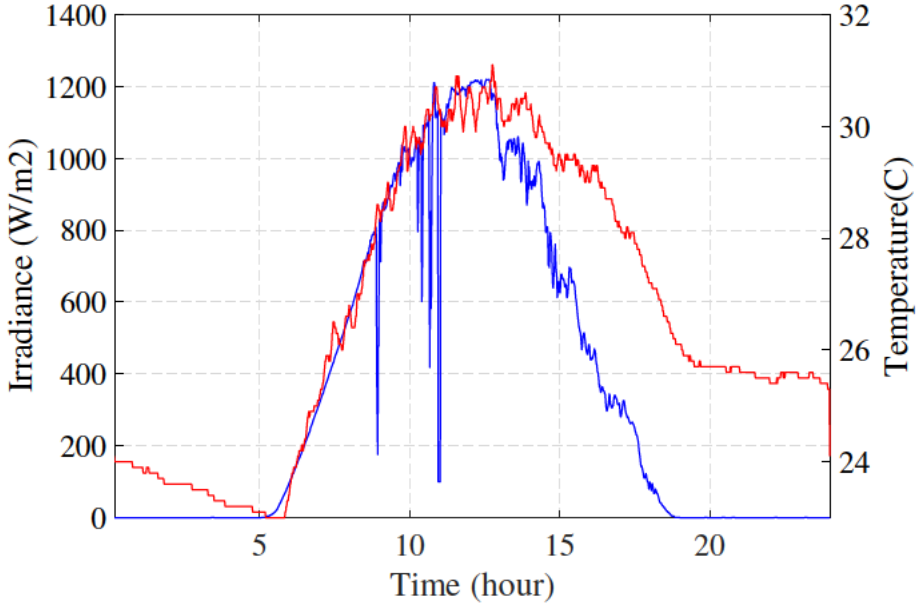

Fig. 5.12 Radiation and temperature on a typical summer day (25th Janunary 2017)

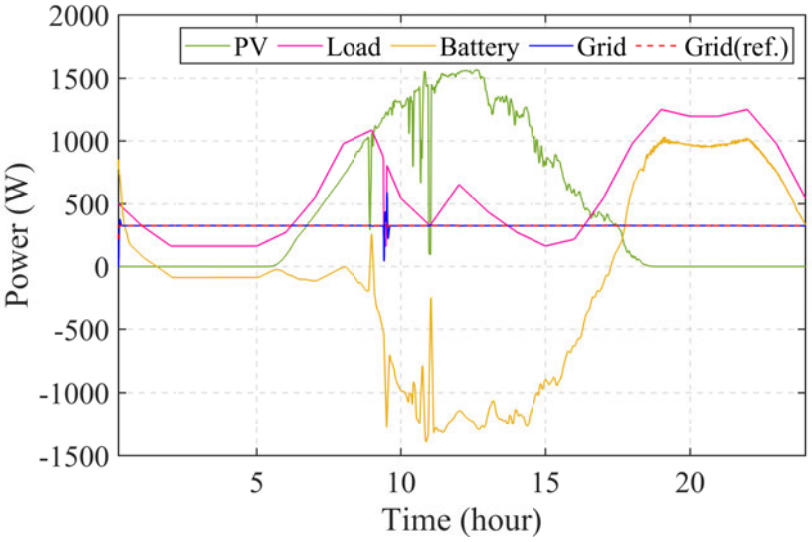

(a)

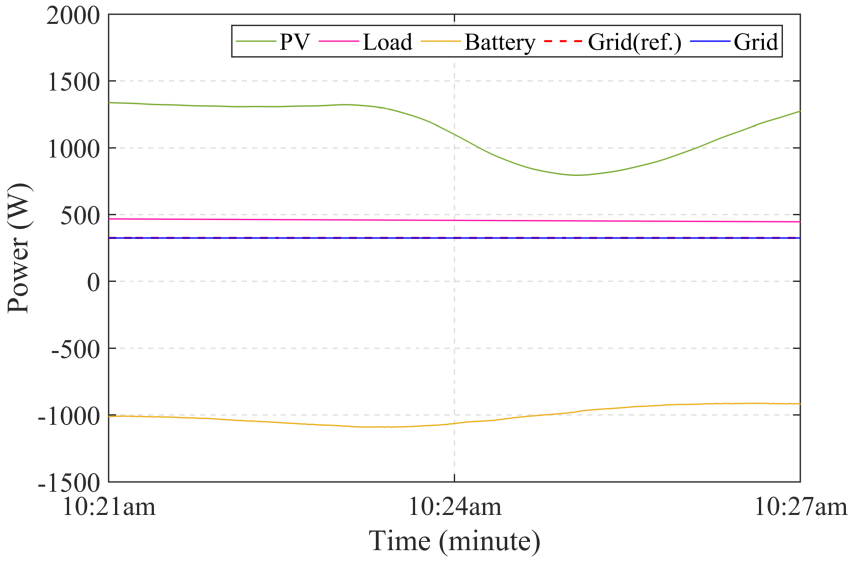

(b)

Fig. 5.13 PV generation, residential load, battery power, grid power and grid power reference on a typical summer day (a) 24 h duration and (b) 6 min duration from 10:21 am to 10:27 am

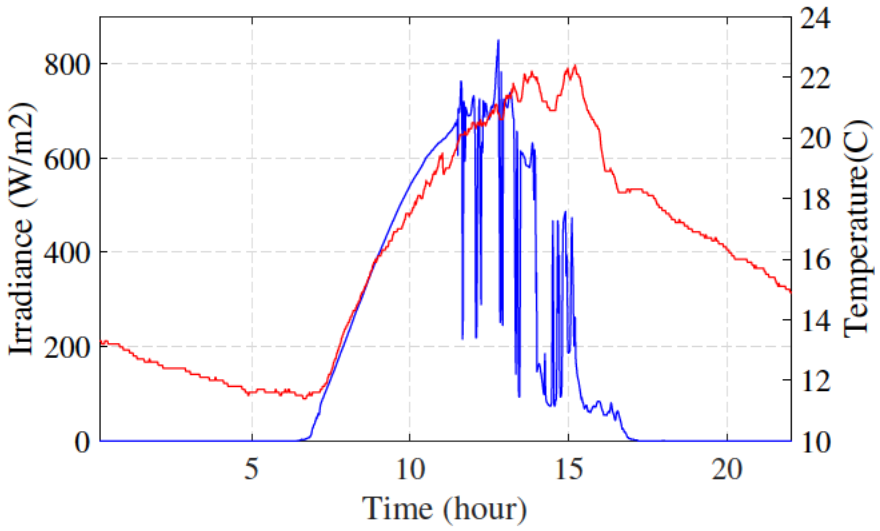

Fig. 5.14 Radiation and temperature on typical winter days (4th June 2017)

Brisbane, Australia in September 2017 are obtained from the statistical weather information database of building N44, Griffith University. The radiation and temperature data are collected from 5 am to 7 pm at 1 min intervals for typical summer and winter days. Furthermore, the load data of a typical residential house in Queensland are collected at 1 min intervals to illustrate the load variation of the MG. Moreover, a lithium-ion battery with a rated capacity of 16 kWh is installed in the system [184]. The depth of discharge (DoD) of the battery storage is set to 90% for residential application. Four different case studies are conducted using weather and load variations to validate the dynamic performance of the controller. Considering system dynamics, the MG controller sets the reference grid power to 13% of the inverter rated power determined during the design stage of the MG. That is, MG will draw a constant power from the grid through the tie-line, which is 13% of the inverter rated power. Moreover, the information in Table 5.2 is used to drive the state-space model of the study MG in MATLAB. The state-space model is used to represent the MG system model. Several case studies are conducted to demonstrate the performance of the controller during short-term changes of input and output system disturbances. In the study MG, the input disturbance is the variation in solar radiation and the output disturbance is load power variation. In addition, controller performance is also shown on typical summer and winter days of the year with variations in weather and load profile. The simulation is run for 24 h with a time step of 1 min.

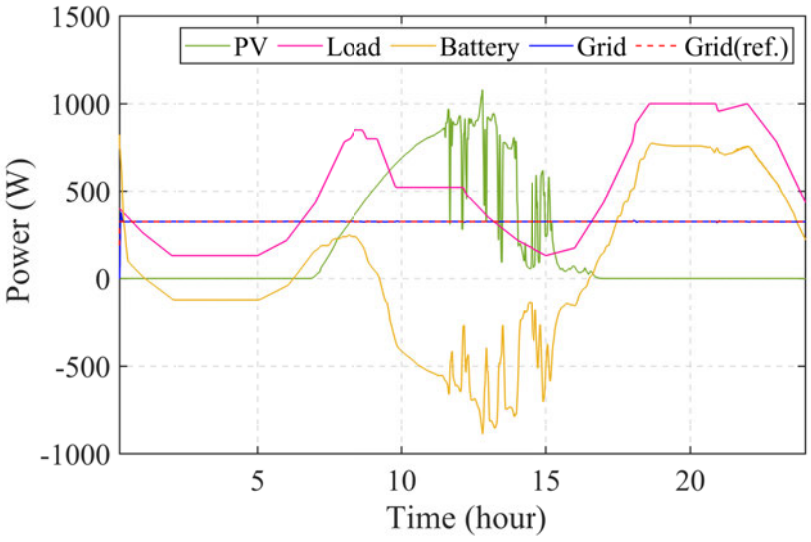

(a)

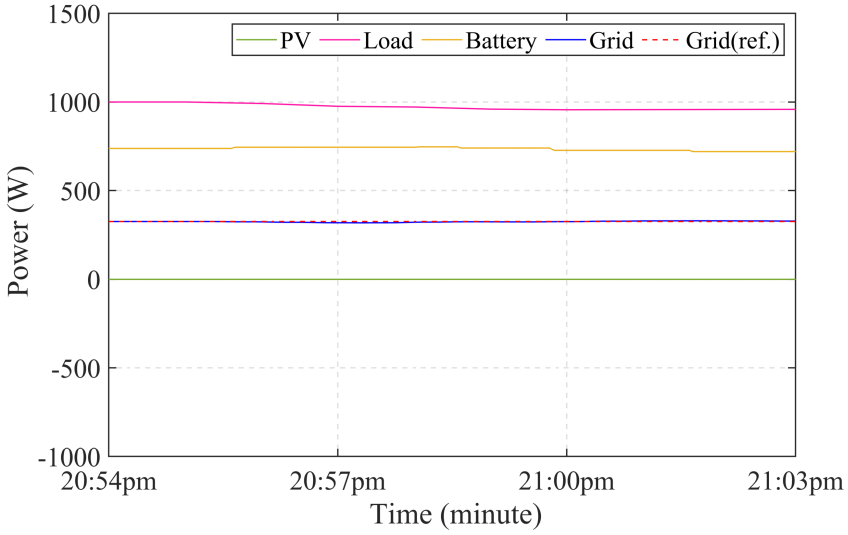

(b)

Fig. 5.15 PV generation, residential load, battery power, grid power and grid power reference on a typical winter day (a) 24 h duration and (b) 9 min duration from 20:54 pm to 21:03 pm

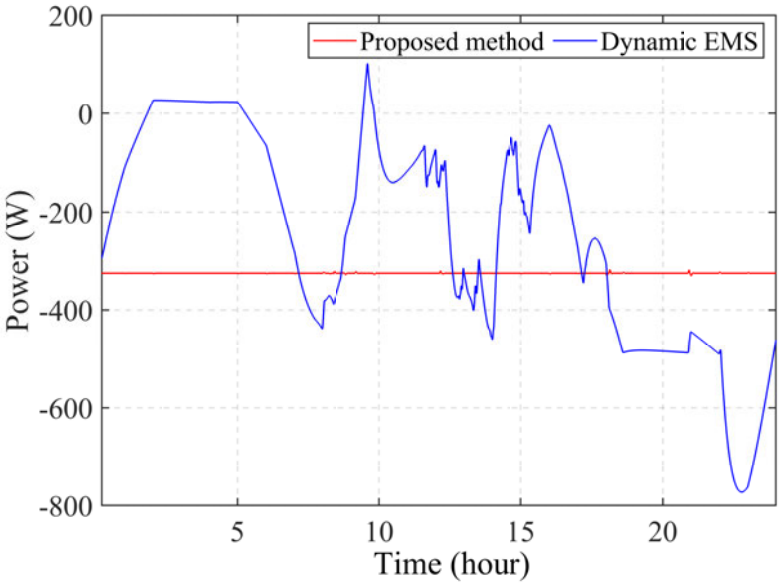

Fig. 5.16 Comparison of grid power on typical winter days

Case I: Effect of Sudden Cloudy Appearance

Weather variations have a direct effect on the power generation of the PV panel. To observe the effect of sudden weather variations on controller performance, Case I illustrates an event of sudden cloud appearance for a short period. During this period, system load is considered almost constant. A typical scenario is illustrated in Fig. 5.10 to show the dynamic response of the proposed grid power controller due to sudden cloud appearance. The figure shows abrupt changes in PV power for 5 min due to the sudden cloudy weather. The figure also shows the grid power, reference grid power and load variation during this period. The result indicates that the measured grid power is following the reference grid power smoothly despite the variations in PV power for a short period. Thus, the robustness of the controller is demonstrated.

Case II: Effect of Abrupt Load Change

Load variation exerts a significant effect on the dynamic performance of the system. In Case II, an abrupt load variation is considered for a short period to observe the effect of load variation on controller performance. During this period, the output power of the PV panel is kept nearly constant. A typical scenario is illustrated in Fig. 5.11 to show the dynamic response of the proposed grid power controller due to abrupt load change (output disturbance). In this scenario, load power suddenly drops for 5 min due to an abrupt load change for a short duration. The dynamic performance of the controller on the

event of abrupt load change is illustrated in the figure. The result shows that the measured grid power is following the reference power with small fluctuations.

Case III: Controller Performance on a Typical Summer Day

To evaluate controller performance for a 24 h duration using summer weather, weather information on a typical summer day (25 January 2017) is selected as the input of the PV panel. Solar radiation and temperature on a typical summer day are illustrated in Fig. 5.12 and used to generate PV power on a typical summer day. In addition, the residential load profile illustrated in Fig. 5.13a is used to represent load dynamics on a typical summer day. Moreover, Fig. 5.13a shows that battery power and grid power on typical summer day follow the power balance equation of the MG. Fig. 5.13b indicates the dynamic response of the controller in minutes to observe the effect of short-term power fluctuations due to renewable generations and load. The results demonstrate that the proposed grid power control method achieves a constant tie-line on a typical summer day despite the variation in PV power and load power. However, battery power fluctuation is increased significantly to realise the objective.

Case IV: Controller Performance on a Typical Winter Day

To verify the performance of the controller for 24 h on winter weather and load variations, a typical winter day (4 June 2017) with variations in temperature and radiation is selected to generate PV output under winter condition. Solar radiation and temperature on a typical winter day are shown in Fig. 5.14. Moreover, PV generation and residential load profile for a typical winter day are presented in Fig. 5.15a. In addition, Fig. 5.15a shows battery power and grid power on a typical winter day. Fig. 5.15b illustrates the dynamic curve and control effort in minutes to observe controller performance during short-term changes of input and output system disturbances. The result indicates that grid power follows the reference for simulation time, and the power balance of the MG is achieved through the required charging/discharging of the battery. The results prove that the MG has drawn a constant power from the grid to obtain a constant tie-line power on a typical winter day of the year.

5.6.2 Comparison

A comparison of the grid power of the proposed inverter control method and a dynamic EMS-based power flow control method [7] is presented in MATLAB to compare the performance of the two control methods. In [7], a fuzzy logic-based dynamic EMS was designed to control the buck-boost current controller of the battery storage system to reduce the tie-line power fluctuation in a residential MG. Fig.

5.16 shows the comparison of the grid power by using the two methods on a typical winter day. The result demonstrates that the proposed inverter control achieves constant grid power on a typical day. By contrast, whereas the dynamic EMS-based method exhibits many fluctuations. That is, the proposed controller achieves robust control to obtain smooth tie-line compared with the dynamic EMS-based control method.

5.7 Conclusions

In this chapter, a constant tie-line power method is proposed to overcome tie-line power fluctuations in a grid-connected residential MG due to RES and load variations. A grid current controller combined with a droop power controller is designed to maintain constant grid power drawn by the MG. The grid power reference is determined during the design stage based on system dynamics. The power flow inside the MG is balanced through the controlled charging/discharging of the battery. In addition, a state-space model of the MG system is derived for a stability analysis of the system with variations in system parameters. Furthermore, a simulation model is developed using the state-space model of the MG to verify the performance of the controller in different case studies. A comparison with a previously developed dynamic EMS approach is presented in the simulation. The results show that with the application of the proposed control method, constant tie-line power can be achieved despite short-term system fluctuations and on typical days of the year by maintaining battery charging/discharging within a limit.

Chapter 6

Model Predictive Power Flow Control in Networked Microgrids

Chapter Contribution Declaration

This chapter addresses the tie-line fluctuations problem in an NMG. A distributed model predictive power controller is proposed to control the tie-line power in a network of MGs connected in a common bus. Tie-line converters in a network cooperate in a distributed framework to achieve a smooth scheduled tie-line power. The proposed controller is verified in different case studies to demonstrate the performance of the controller to achieve a smooth tie-line power in an NMG despite the variations of generations and load. In addition, a performance comparison is also presented with respect to the decentralised operation of MGs to justify the necessity of the proposed control method.

This chapter includes a co-authored paper. The bibliographic details of the co-authored paper, including all authors, are:

M. Islam, F Yang, J Lu "Dynamic Power Flow Control in Networked Microgrids for Tie-line Smoothing" under preparation to submit on IEEE Transaction on Power Systems.

My contribution to this paper involved: conceptualization, system modelling, controller design, simulation experiment and analysis, the original draft writing, revising and proofreading.

Signed: _____ Date: *23.01.2021*

PhD Candidate: Mojaharul Islam (Principle Author)

Countersigned: _____ Date: *23.01.2021*

Principle Supervisor: A. Prof. Fuwen Yang (Corresponding Author)

Countersigned: _____ Date: *23.01.2021*

Associate Supervisor: Prof. Junwei Lu

6.1 Abstract

An increasing number of microgrids (MGs) in transmission and distribution networks creates an opportunity to work as a network to increase the stability, quality and reliability of power systems. Tie-line control in such a network of parallel connected residential MGs are very challenging due to fluctuating nature of renewable generations and time-varying loads. This chapter proposed a distributed model predictive power controller for tie-line inverters of a network of grid-connected residential MGs that operates in coordination with a DC-DC converter to maintain a scheduled tie-line power for the network by keeping the system constrains. MGs communicate with one another for calculating a day ahead tie-line power reference of a network and for real time adjustment of the reference power of tie-line converters based on the information of instantaneous power drawn by other MGs in the network. The proposed controller is verified in several case studies to demonstrate the performance of the controllers during dynamic changes of system disturbances and tie-line reference of MGs. Furthermore, a comparison with a decentralised operation of MGs exhibits in result to show the effectiveness of the proposed distributed operation of MGs.

6.2 Introduction

Renewable energy resources (RESs) are remarkably integrated in last decades to transmission and distribution networks for promoting green technologies in future power systems. Adaptation of RESs brings new challenges in control, operation and management of power networks. The concept of microgrids (MGs) are implemented in last decay for efficient use of RESs and to provide a reliable supply to the loads in a small power network. An MG can be defined as a small power network that consists of distributed energy resources (DERs) and energy storage systems (ESSs) to feed local loads on a low/ medium voltage power network [201, 7]. The main advantage of MGs is to operate in either grid-connected or island mode. In grid-connected mode, deficient/ surplus power in an MG is transferred to the main grid to maintain the power balance in an MG. Meanwhile, during a fault condition, an MG can operate in island mode to maintain a reliable supply to critical loads. The challenges to control and management of MGs has increased when a number of MGs are connected to a network. A networked MG (NMG) can be defined as a clusters of MGs connected through an electrical power network for efficient utilisation of RESs, to increase supply reliability, to reduce the operation cost and to reduce grid burden on grid-connected operation. The potential benefits and challenges of networked operation

of MGs were discussed in [10–12] by focusing on operation feasibility of NMGs. Fig. 6.1 shows a typical structure of an NMG connected in a distribution network.

Power flow control in an NMG is one of the challenging issue for networked operation of MGs. Power flow control in an NMG has been addressed by several studies. A pinning-based distributed secondary control was implemented in [120] for a cluster of distributed generations (DGs) in an NMG operating in P-Q and droop control mode. The steady state deviations caused by the primary level control was reduced using the proposed control method. The global reactive power sharing error in an NMG was minimised in [132] using a virtual impedance control method and a genetic algorithm was used to optimised the virtual impedance controllers. Besides that, a model predictive control method was used in [202] for scheduling the power flow amongst MGs and charging/ discharging of local ESSs under a centralised management framework. A comparison with single operation of MGs was presented to show the advantages and benefits of networked operation. A distributed control approach was employed in [203] to keep the ESS in an MG around a reference value though optimal power sharing between MGs. Meanwhile, tie-line power flow control in an NMG has recently focused in research. A distributed tie-line power flow control between two DC MGs is adopted in [204] using pinning consensus protocol to minimise the operating cost of distributed generators (DGs) in an MG. A distributed secondary control was proposed in [122] to control the tie-line power amongst MGs in an NMG operating in island mode. The main target of this studies was to avoid overloading of DGs due to variations of loads. Furthermore, a two-layers control structure is presented in [117] where the outer layer in responsible to control the power flow in an NMG using a modified droop control method. Power flow amongst MGs though tie-line converters was considered during networked operation to minimise the power drawn from the main grid. In [205], a multiagent-based distributed tie-line power flow control of an NMG is presented where several AC MGs are connected with one another in a ring structure. The study concentrated on optimisation of real time energy scheduling amongst MGs in grid-connected operation despite the variation of generations and loads. All the above studies concentrates on a tie-line power flow control where MGs are connected through a separate electrical connections amongst them. Moreover, none of the above studies consider the on grid tie-line power fluctuations in an NMG.

Tie-line power fluctuations control is an active research field of MGs to reduce dynamic natures of RESs and loads on the main grid and to maintain the stability and quality of distribution networks . Tie-line smoothing in a single MG had been studies in [39, 197, 171, 193] using demand-side management, generation control, ESS control and coordinate control method. Tie-line fluctuations in an NMG is more problematic than a single MG because of number of RESs and loads are connected in a network.

Besides that, tie-line fluctuations control in a RESs dominant MGs is very challenging because MGs in the network mainly depend on the main grid to maintain a secure power supply in such a network. Thus, this study concentrates on tie-line fluctuations in a grid-connected NMG connecting on a common bus.

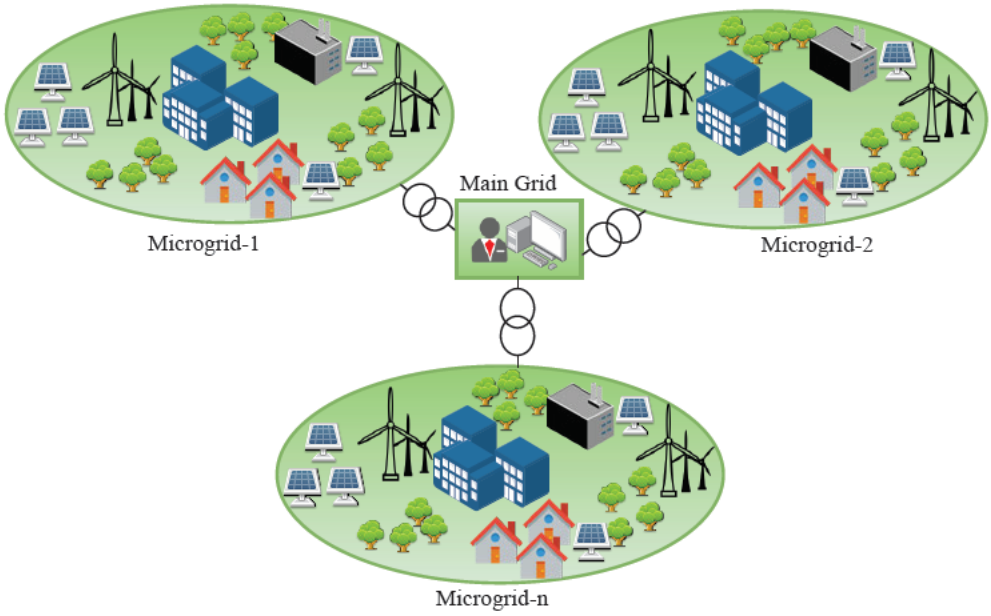

Fig. 6.1 A typical structure of a grid-connected networked microgrid in distribution networks

Recently, model predictive control (MPC) scheme is prominently used in power systems to solve the control and optimisation problems by predicting system disturbances to perform an upcoming control action and improving the transient responses of a system. As an optimal control strategy, an MPC scheme can be used in NMGs research to achieve system level energy optimisation as well as device level control. Several studies had been reported to solve the system level problems in an NMG by applying MPC to achieve economic optimisation [206–208, 202], efficient control of local storages [209–211], to minimise the energy exchange with the main grid [212] and optimal scheduling of energy [213, 146]. An MPC scheme was used in [145] for controlling frequency in an NMG by adjusting the voltage of voltage-sensitive loads and maintaining voltage constraints. This article didn't applied MPC scheme for device level control of converters in an NMG. Meanwhile, to obtain the research objectives of tie-line power flow control in an NMG, an MPC based direct tie-line power flow controller is necessary. The method of direct power flow control of inverters using finite set MPC has been addressed in [80, 214–216] for RESs dominant systems without considering multiple independent systems connecting together in a common bus for achieving a common goal. Thus, it can be concluded that the power flow control in an NMG by direct controlling the inverters power of parallel connected MGs is still unrevealed.

In this chapter, a distributed model predictive power controller (DMPPC) is proposed to control the tie-line power in an NMG connected with the main grid through interlink inverters. A number of residential MGs are connected to a common bus to form a network. A dynamic model of an NMG is obtained by combining the dynamic model of individual MGs. After that, a distributed model predictive power controller (DMMPC) was proposed to obtain a scheduled tie-line power in a grid-connected NMG despite the variations of RESs and load demand. A decentralised model predictive power controller is used to maintain a stable DC bus of individual MGs without any communication with neighbouring pairs and is responsible to control the charging/ discharging of batteries. However, interlink inverters in an NMG communicate among them through distributed communication links. A dynamic system model of interlink inverters of individual MGs is used to predict the tie-line power for next time steps. A scheduled tie-line power is determined by individual MGs based on the forecasted generation, load demand and battery State of charge (SoC). Moreover, instantaneous tie-line power information of other MGs and reference tie-line are collected from the network to determine the instantaneous tie-line power reference of individual MGs in distributed manner. Finally, a cost function is implement to achieve a smooth tie-line power of a grid-connected NMG. The performance of the proposed DMPPC is demonstrated in simulation experiment for the variations of input and output disturbances as well as a change in reference grid powers of MGs. In addition, the performance of the proposed DMPPC is validated using real weather and residential customer load data in Queensland, Australia to achieved a smooth tie-line power in a network of grid-connected residential MGs. Furthermore, a comparison with decentralised operation of MGs is presented in results to show effectiveness of the proposed control method.

The rest of the chapter is organised as follows. Section 6.3 describes the modelling of NMGs. Section 6.4 presents a DMPPC for interlink inverters in an NMG. Section 6.4 illustrates simulation results. And section 6.6 concludes the chapter.

6.3 Modelling of Networked Microgrids

A typical structure of a grid-connected NMG that consists of n number of MGs in shown in Fig. 6.2. MGs in the network are connected with the main grid using interlink inverters, LC filters and line impedances. The DC bus of each MG is connected to the interlink inverter is represented as an ideal DC source in Fig. 6.2. Interlink inverters in the network are responsible to control the power drawn/transfer to the main grid in order to provide a reliable supply to the loads. Each MG in the networked consists of a PV, a battery and an AC load. Fig. 6.3 shows the schematic diagram of the *ith* MG in the network used in

the proposed NMG system. PV i and battery i are connected to the DC bus i using a boost converter and a buck-boost converter respectively. The boost converter of the PV i operates as a maximum power point tracking controller. The buck-boost converter of the battery i is responsible to stabilise the DC bus voltage of the *ith* MG through charging/discharging of the battery. The DC bus i is connected with the AC bus i through an interlink inverter and a LC filter. The AC load of the *ith* MG is also connected to the AC bus i. The power drawn/transfer to the main grid of the *ith* MG can be represented as P_{gi} and Q_{gi}. In this study, finite set MPC algorithm is chosen to design the buck-boost controllers and interlink inverters. Thus, the model of buck-boost converters and interlink inverters are necessary to design the controllers. The next subsections will provide the model of buck-boost converter i,interlink inverter i and an NMG.

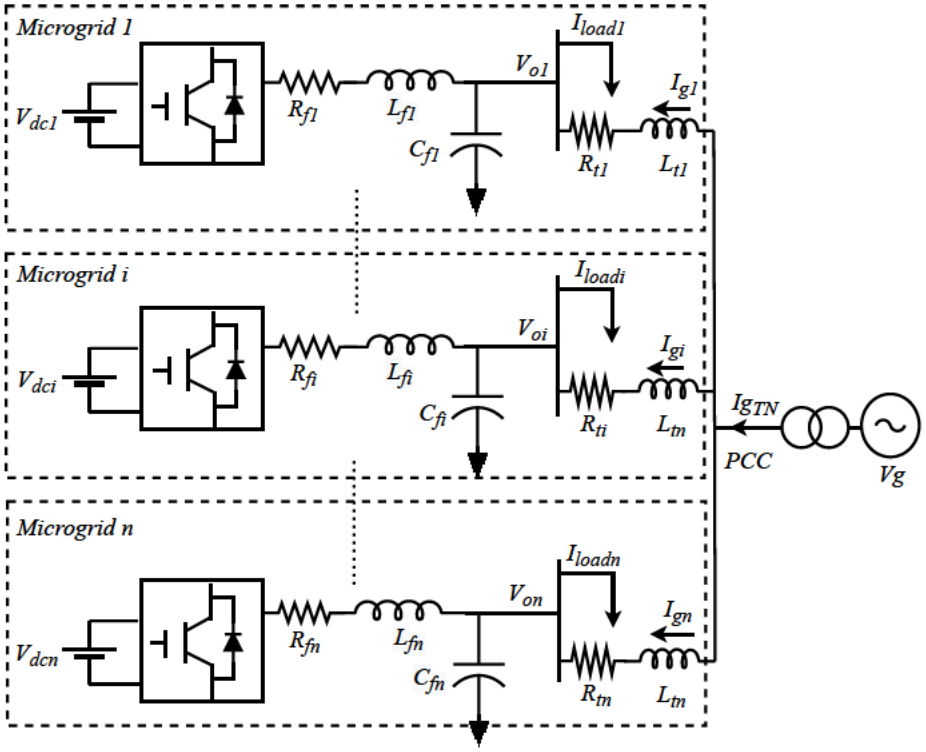

Fig. 6.2 Equivalent circuit of a networked microgrid connected in a LV distribution network

6.3.1 Modelling of Buck-boost Converters

Fig. 6.4 shows the equivalent circuit digram of the buck-boost converter i connected to the DC bus i and the battery i. The buck-boost converter consists of a filter inductance $L_{b,i}$, two switches S_{i1} and S_{i2} and a DC link capacitance $C_{dc,i}$. A buck-boost converter can only control through coordinated

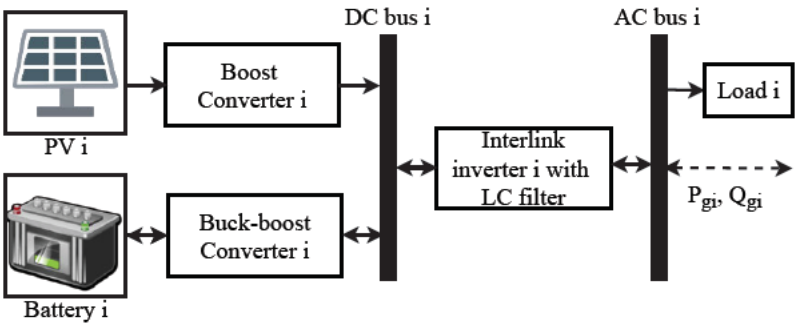

Fig. 6.3 Equivalent circuit of the MG i

switching between two switches. In buck mode, switch S_{i1} operates as main and switch S_{i2} operates as complementary. In boost mode, switch S_{i2} operates as main where as switch S_{i1} operates as complementary. The equivalent circuit of buck-boost operation of the battery module i due to different switching combinations is illustrated in Fig. 6.5. Considering the boost mode current as positive direction, the dynamic equation of the battery module i for two possible switching combinations can be written as,

$$\begin{aligned} S_{i1} = 1, S_{i2} = 0, \qquad & L_{b,i}\frac{dI_{bat,i}}{dt} = V_{bat,i} - V_{dc,i} \\ S_{i1} = 0, S_{i2} = 1, \qquad & L_{b,i}\frac{dI_{bat}}{dt} = V_{bat,i} \end{aligned} \tag{6.1}$$

The continuous time dynamic model of the battery is converted into a discrete model for a sampling period T_s can be written as,

$$\begin{aligned} S_{i1} = 1, S_{i2} = 0, I_{bat,i}(k+1) &= \frac{T_s}{L_{b,i}}(-V_{dc,i}(k) + V_{bat,i}(k)) + I_{bat,i}(k) \\ S_{i1} = 0, S_{i2} = 1, I_{bat,i}(k+1) &= \frac{T_s}{L_{b,i}}(V_{bat,i}(k)) + I_{bat,i}(k) \end{aligned} \tag{6.2}$$

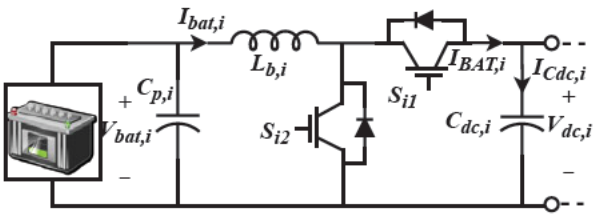

Fig. 6.4 Equivalent circuit diagram of the buck-boost converter connected in the DC bus i

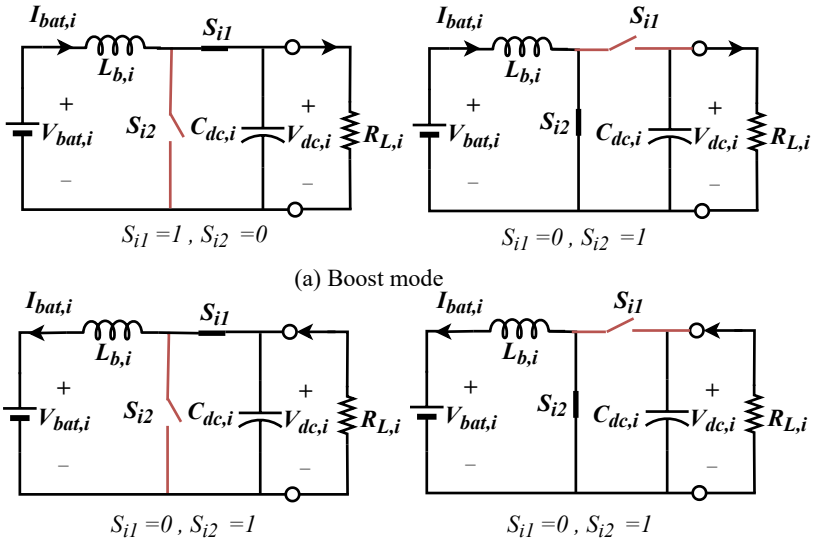

Fig. 6.5 Equivalent circuit diagram of buck-boost operation for the battery module i

6.3.2 Modelling of Interlink Inverters

Fig. 6.6 shows the equivalent circuit diagram in ac side of the MG i. It is assumed that a single phase two-legs inverter is connected between DC bus i and AC bus i through an LC filter. Each leg of the inverter consists of two switches. There are four possible switching combinations to obtain three possible voltage vectors of a single phase inverter and can be written as,

$$\begin{aligned} v_{in} = &+ V_{dc}, (S_1, S_4 = 1; S_2 = S_3 = 0) \\ &- V_{dc}, (S_1, S_4 = 0; S_2 = S_3 = 1) \\ &0, (S_1 to S_4 = 1/0) \end{aligned} \tag{6.3}$$

Now, by applying KVL and KCL to the inverter model i, the following differential equations can be obtained.

$$L_{fi}\frac{di_{fi}}{dt} = -R_{fi}i_{fi} + v_{ini} - v_{0i} \tag{6.4}$$

$$C_{fi}\frac{dv_{0i}}{dt} = i_{fi} + i_{gi} - i_{loadi} \tag{6.5}$$

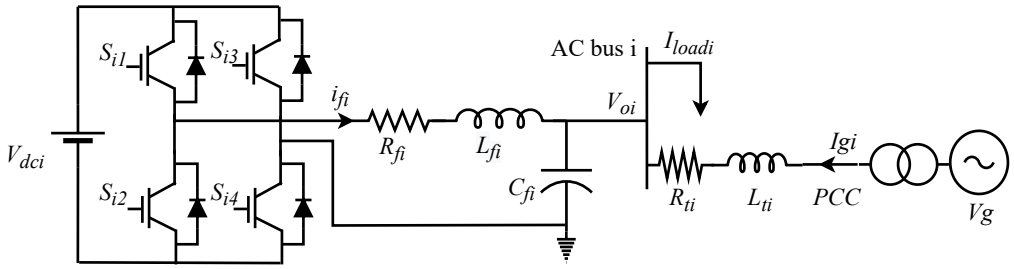

Fig. 6.6 Equivalent circuit of ac side of the MG i

Where R_{fi}, L_{fi} and C_{fi} are the filter resistance, inductance and capacitance of the inverter i respectively. i_{fi} is filter current, i_{gi} is grid current , i_{loadi} is load current and v_{0i} is voltage in AC bus of the ith MG.

The dynamic model of the inverter i can be represent as state-space equation,

$$\dot{x_i} = A_i x_i + B_i u_i + F_i w_i \tag{6.6}$$

Where, x_i is the system states, u_i is the system input and w_i is the system disturbance. To fulfil the requirement of the model, grid current and load current are represented as a disturbance of the system. In practice, they are assumed as an external input of the system.

$$x_i = \begin{bmatrix} i_{fi} \\ v_{0i} \end{bmatrix}, u_i = [v_{ini}], w_i = \begin{bmatrix} i_{loadi} \\ i_{gi} \end{bmatrix}$$

The system coefficients are expressed as,

$$A_i = \begin{bmatrix} -\frac{R_{fi}}{L_{fi}} & -\frac{1}{L_{fi}} \\ \frac{1}{C_{fi}} & 0 \end{bmatrix}, B_i = \begin{bmatrix} \frac{1}{L_{fi}} \end{bmatrix}, F_i = \begin{bmatrix} 0 & 0 \\ \frac{1}{C_{fi}} & -\frac{1}{C_{fi}} \end{bmatrix}$$

The state space model in Equation (6.6) can be transformed intro discrete form for a sampling time T_s by using Euler difference method,

$$x_i(k+1) = C_i x_i(k) + D_i u_i(k) + E_i w_i(k) \tag{6.7}$$

Where

$$C_i = e^{T_s A_i}, D_i = A_i^{-1}(e^{T_s A_i} - 1)B_i, E_i = A_i^{-1}(e^{T_s A_i} - I_{2\times 2})F_i$$

6.3.3 Modelling of an NMG

The dynamic model of an NMG can be obtained by aggregating ac side dynamic equations of each individual MG in the network,

$$\begin{bmatrix} x_1(k+1) \\ x_2(k+1) \\ \vdots \\ x_i(k+1) \\ \vdots \\ x_n(k+1) \end{bmatrix} = C \begin{bmatrix} x_1(k) \\ x_2(k) \\ \vdots \\ x_i(k) \\ \vdots \\ x_n(k) \end{bmatrix} + D \begin{bmatrix} u_1(k) \\ u_2(k) \\ \vdots \\ u_i(k) \\ \vdots \\ u_n(k) \end{bmatrix} + E \begin{bmatrix} w_1(k) \\ w_2(k) \\ \vdots \\ w_i(k) \\ \vdots \\ w_n(k) \end{bmatrix} \tag{6.8}$$

Where C, D and E are the NMG coefficient. All elements of the coefficient matrices are zero except the diagonal element.

$$C = \begin{pmatrix} C_{11} & \cdots & C_{1n} \\ \vdots & \ddots & \vdots \\ C_{i1} & \cdots & C_{in} \\ \vdots & \ddots & \vdots \\ C_{1n} & \cdots & C_{nn} \end{pmatrix}, D = \begin{pmatrix} D_{11} & \cdots & D_{1n} \\ \vdots & \ddots & \vdots \\ D_{i1} & \cdots & D_{in} \\ \vdots & \ddots & \vdots \\ D_{1n} & \cdots & D_{nn} \end{pmatrix}, E = \begin{pmatrix} E_{11} & \cdots & E_{1n} \\ \vdots & \ddots & \vdots \\ E_{i1} & \cdots & E_{in} \\ \vdots & \ddots & \vdots \\ E_{1n} & \cdots & E_{nn} \end{pmatrix}$$

The integrated model of an NMG can be represented as,

$$x(k+1) = Cx(k) + Du(k) + Ew(k) \tag{6.9}$$

6.4 Distributed Model Predictive Power Control for Tie-line Inverters in a Networked Microgrid

The flexible power flow control in a MG can be obtained by controlling the filter current of the interlink inverter. An interlink inverter of an MG usually connect with rest of the system using an L/LC/LCL

filter. The inverter current can be controlled by regulating the switching behavior based on the dynamic equation of the filter loop. A regulated inverter power can be achieved through controlling the inverter current. Meanwhile, the grid power control in an MG is more challenging than the inverter power control because of the absence of direct relation with the inverter input voltage. Besides that, due to high penetration of RESs in low/medium distribution networks, the grid power control is essential for efficient use of RESs and obtaining a smooth/flat tie-line power in grid-connected operation of an MG. The consequence of grid power control in an NMG is more complex than a single MG operating in grid-connected mode. Communication in the network is important for efficient control and operation of such networks. A centralised controller can be dedicated to aggregate information from the network and to predict the future value of grid power in the network . A complete model of the whole network should be used by the central controller to predict the future value of the grid power. At the same time, aggregated information from the network is used to determine the optimal power reference for each MG. To implement a central control approach, a dedicated, reliable and high band communication network is necessary. In addition, a central control approach requires more installation, operation and maintenance cost compare with decentralised and distributed control approach. To overcome the necessity of a central controller, a distributed model predictive power control has been proposed in this chapter to control the tie-line power in an NMG. Interlink inverter of individual MG will communicate with each other is distributed fashion to maintain the tie-line power of an NMG near to the reference. Each inverter will predict the grid power for (k+1) time step. Moreover, reference grid power of each MG for (k+1) time step will be determined based on the grid power information from all MGs in a network operating is distributed control mode, gird power reference of individual MGs and grid power reference of the network.

Now, the prediction of grid current for (k+1) time step can be obtained by applying KCL in AC bus of ith MG and can be expressed as,

$$i_{gi}(k+1) = i_{loadi}(k+1) - i_{fi}(k+1) + \frac{T_s}{C_{fi}}(v_0 i(k+1) - v_0 i(k)) \tag{6.10}$$

For a small time step, load current for two consecutive time step is assumed as $i_{loadi}(k+1) \simeq i_{loadi}(k)$. The filter current $i_{fi}(k+1)$ and capacitor voltage $v_0(k+1)$ can be predicted using the discrete time state space model in equation (7) and can be written as,

$$i_{fi}(k+1) = \frac{T_s}{L_{fi}}(v_{in}(k) - v_0(k) - R_{fi} i_{fi}(k)) + i_{fi}(k) \tag{6.11}$$

$$v_{0i}(k+1) = \frac{T_s}{C_{fi}}(i_{fi}(k) + i_{gi}(k) - i_{loadi}(k)) + v_{0i}(k) \tag{6.12}$$

Now, by applying instantaneous power theory [217, 218], the instantaneous active and reactive power equation for a single phase system in $\alpha - \beta$ coordinate can be written as,

$$\begin{aligned} P &= \frac{1}{2}Re(VI^*) = \frac{1}{2}(v_\alpha i_\alpha + v_\beta i_\beta), \\ Q &= \frac{1}{2}Im(VI^*) = \frac{1}{2}(v_\beta i_\alpha - v_\alpha i_\beta) \end{aligned} \tag{6.13}$$

Where * is represented as complex conjugate. Re and Im are represented as real and imaginary components.

Using Equation (6.13), the instantaneous active and reactive grid power of the *ith* MG for (k+1) time step can be predicted as,

$$\begin{aligned} P_{g,i}(k+1) &= \frac{1}{2}(v_{g\alpha}(k+1)i_{g\alpha,i}(k+1) + v_{g\beta}(k+1)i_{g\beta,i}(k+1)), \\ Q_{g,i}(k+1) &= \frac{1}{2}(v_{g\beta}(k+1)i_{g\alpha,i}(k+1) - v_{g\alpha}(k+1)i_{g\beta,i}(k+1)) \end{aligned} \tag{6.14}$$

As the sampling frequency is very small compare with the grid fundamental frequency, the grid voltage is assumed to be constant for two consecutive sampling period. Thus, $v_{g\alpha}(k+1) = v_{g\alpha}(k)$ and $v_{g\beta}(k+1) = v_{g\beta}(k)$.

Now, if the MGs in a network will operate in decentralised manner, then each interlink inverter will control the grid power of the corresponding MG without any communication with other MGs. The cost function to regulate the grid power of *ith* MG in decentralised manner can be written as,

$$\begin{aligned} J_{Pgi} = (P_{gi}^{ref}(k+1) - P_{gi}(k+1))^2 + (Q_{gi}^{ref}(k+1) - Q_{gi}(k+1))^2, \\ s.t. \quad I_{f,i} \leq I_{inv(rated),i} \end{aligned} \tag{6.15}$$

In the cost function, the reference active and reactive power needs to design carefully to obtain a regulated grid power considering the system constrains. For residential applications, the reactive

power supplied by the grid is usually set to Q_{gi}^{ref}=0 to maintain an unity power factor. The active power reference P_{gi}^{ref} is usually determined by the energy management system (EMS) of individual MG. In this study, a day ahead tie-line power scheduling is done based on forecasted generation and load from the distributed network operator (DNO) and the battery SoC at the end of each day. Due to development of technologies, it is assumed that forecasting of generations and loads can be done accurately. The application of day ahead forecasting is discussed in several studies [219]. Thus, the forecasting of generations and loads is out of scope of this chapter. Fig. 6.7 shows the flow chart to determine the tie-line power power scheduling of MG i. Finally, the scheduled active power reference has sent to the corresponding interlink inverters based on the battery SoC to avoid over charging/discharging of batteries.

Meanwhile, to implement the DMPPC, the reference grid power of interlink inverter of the *ith* MG in the network should be revised based on the networked tie-line reference power and information of grid power drawn from other MGs in the network. The reference active grid power P_{gT} and reactive grid power Q_{gT} for (k+1) time step from the day ahead energy scheduling of the network. Meanwhile, the instantaneous grid power of the other MGs in the networked can be obtained through a communication between MGs. Then, the grid power oscillation in the network can be obtained which will share by the MGs in a network to achieve a smooth tie-line power in an NMG. Finally, the grid power reference of each individual MG can be adjusted by adding the oscillating grid power in a network with the reference grid power of individual MG in decentralised operation. Equation (6.16) shows the active and reactive grid power reference of the *ith* MG for distributed operation of interlink inverters in an NMG. Fig. 6.8 shows the block diagram of a DMPPC to control the interlink inverter of MG i.

$$\begin{aligned}\tilde{P}_{gi}^{ref}(k+1) &= P_{gi}^{ref}(k+1) + g_p(P_{gT}^{ref}(k+1) - \sum_{j=1}^{n}\zeta_i P_{gj}(k)) \\ \tilde{Q}_{gi}^{ref}(k+1) &= Q_{gi}^{ref}(k+1) + g_q(Q_{gT}^{ref}(k+1) - \sum_{j=1}^{n}\zeta_i Q_{gj}(k))\end{aligned} \tag{6.16}$$

Where ζ_i is a binary value that represents the concern of the individual MG to continue distributed coordinated operation. g_p, g_q are the active and reactive power sharing ratio during distributed coordinated operation of MGs. In this proposed network, it is assumed that each MG will equally share the oscillatory tie-line power. Thus, the value of the g_p and g_q can be written as $\frac{1}{n}$.

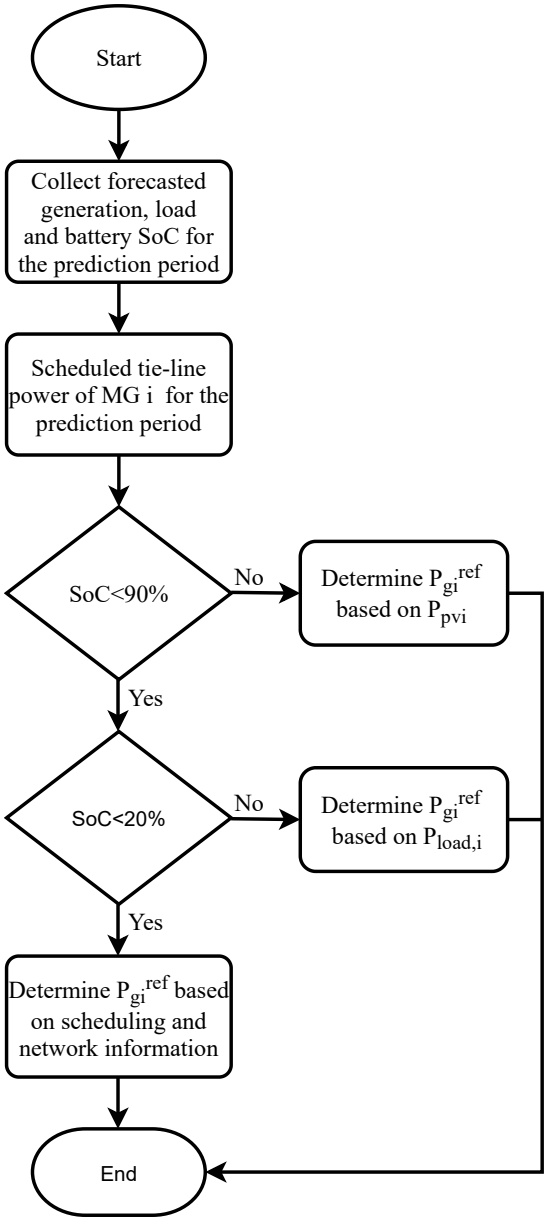

Fig. 6.7 Flow chart to determine the reference tie-line power of MG i

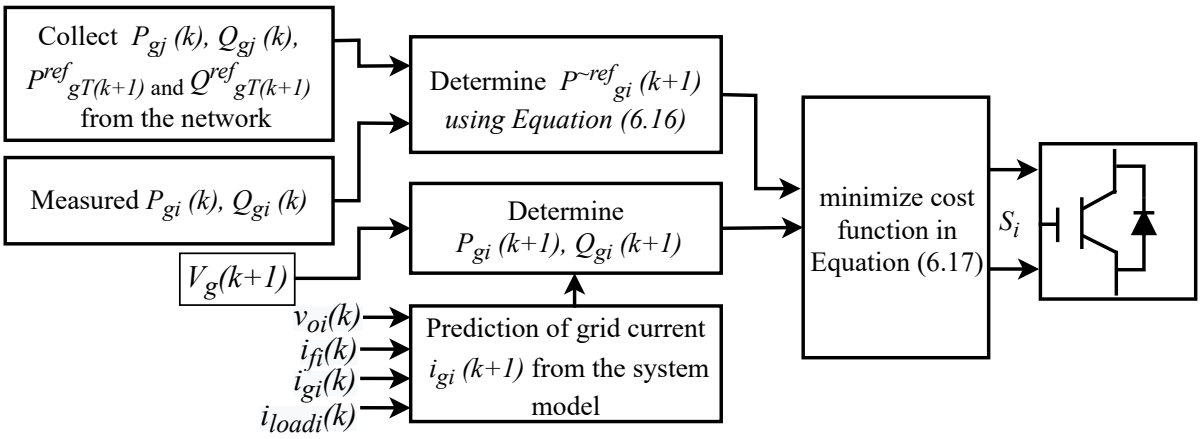

Fig. 6.8 Block diagram for DMPPC of the MG i

Table 6.1 System Configuration of MGs

Parameter	Value
PV	3 kWp
Battery module	10 kWh
Load demand/day of MG 1	22.5 kWh
Load demand/day of MG 2	17 kWh
DC voltage	400 V
Grid voltage	240 V(rms)
Grid frequency	50 Hz
DC-link capacitance	50 mF
Battery filter inductance	5.5 mH
Filter inductance	15 mH
Filter capacitance	2.5 μF
Line resistance	0.75 Ω
Line inductance	8 μH

Finally, the revised cost function for gird power control of the *ith* MG to obtain a smooth tie-line power in an NMG can be written as,

$$J_{Pgi,smooth} = (\tilde{P}^*_{gi}(k+1) - P_{gi}(k+1))^2 + (\tilde{Q}^*_{gi}(k+1) - Q_{gi}(k+1))^2$$
$$s.t. \qquad P_{pv,i} + P_{bat,i} + P_{g,i} = P_{load,i}; I_{f,i} \leq I_{inv(rated),i}. \tag{6.17}$$

To implement the cost function, three different predicted grid powers will be calculated using the Equations (6.10),(6.11) and (6.14) for three different values of the inverter voltage. The set of the inverter voltage for possible switching sequences in a single phase inverter has presented in Equation (6.3). The switching sequence that will minimise the cost function in Equation (6.17) will be applied as an input of the interlink inverter of the *ith* MG to achieve a smooth tie-line power in a grid-connected NMG.

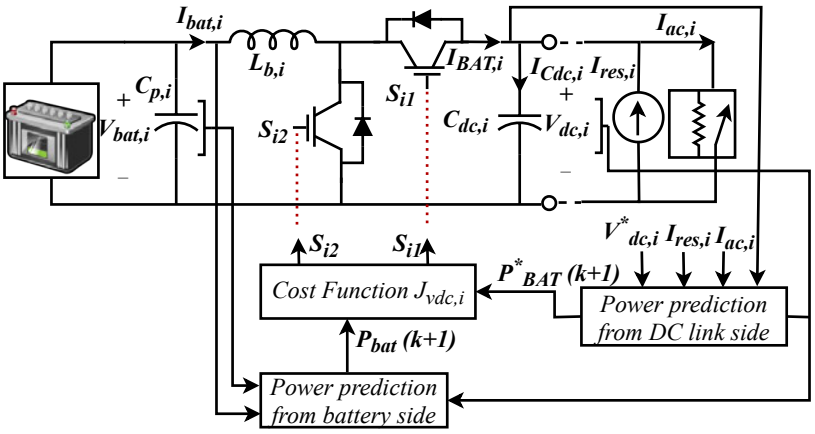

Fig. 6.9 Block diagram to control DC-DC buck-boost converter using model predictive power control

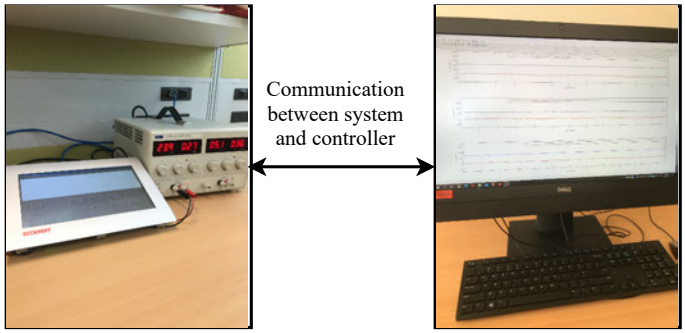

Fig. 6.10 Experimental set up for NMG

6.5 Experimental Results

To evaluate the performance of the proposed DMPPC, a experiment has been conducted for an NMG using MATLAB simulink. The study NMG consists of two MGs connected to the main grid through a line impedance. A 3 KWp PV and a 10 KWh battery has been installed in each MG to supply two different load demand. The average 24 hours load of MG 1 and MG 2 is considered as 22.5 KWh and 17 KWh respectively. The system parameters in Table 5.1 are used to develop the NMG model. The battery

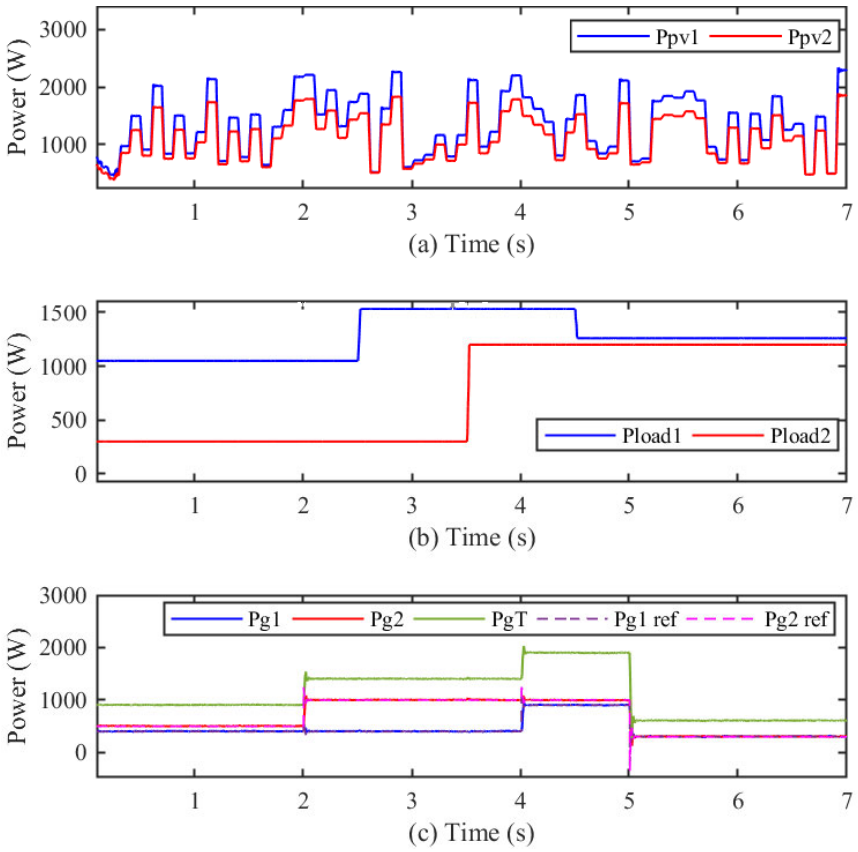

Fig. 6.11 PV power, load power and grid power of MG 1 and MG 2, and tie-line power

module in a hybrid MG is usually responsible to control the charging/ discharging power of the battery in grid-connected mode by keeping battery constrains. The reference of charging/ discharging power is determined by the e EMS of an MG to achieve predefined objectives. However, to take the opportunity of grid power control by controlling the interlink inverter of a hybrid MG, the responsibility of controlling the DC bus voltage is shifted to the battery. A decentralised DC bus voltage control is adopted in this chapter from [214] to control the buck-boost converter of the individual MGs in a network. All the battery modules in a network will operate in decentralised manner without any communication amongst

them. A battery module in an MG is only responsible to maintain the DC bus voltage of that MG near to reference value through charging/ discharging of battery power. Fig. 6.9 shows the schematic diagram of the buck-boost converter to implement model predictive voltage control for the MG i. Meanwhile,

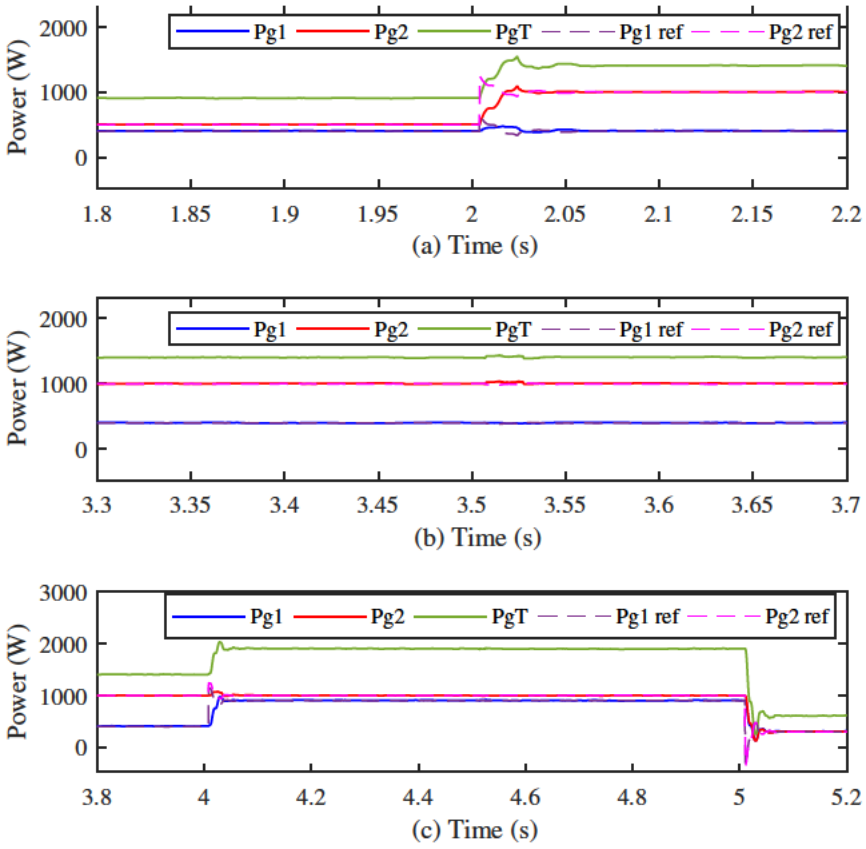

Fig. 6.12 Extended view of grid power of MG 1 and MG 2 and tie-line power during reference and load changes

three different case studies are conducted to show the performance of the proposed control method is different operation scenarios. In first case, the performance of the proposed DMPPC is demonstrated during a dramatic weather and load variations in a network. Moreover, the performance of the controller is presented for changing the reference grid power of MGs in a network. In second case, the performance of a controller is demonstrated for 24 hours duration using real radiation and load data in Queensland, Australia. In third case, a comparison of the proposed controller is demonstrated with decentralised operation of the controllers in the network. Fig. 6.10 shows the experiential set up that will use to implement a PC based controller using Beckhoff industrial panel PC and an NMG system model will develop in designer PC using MATLAB SIMULINK.

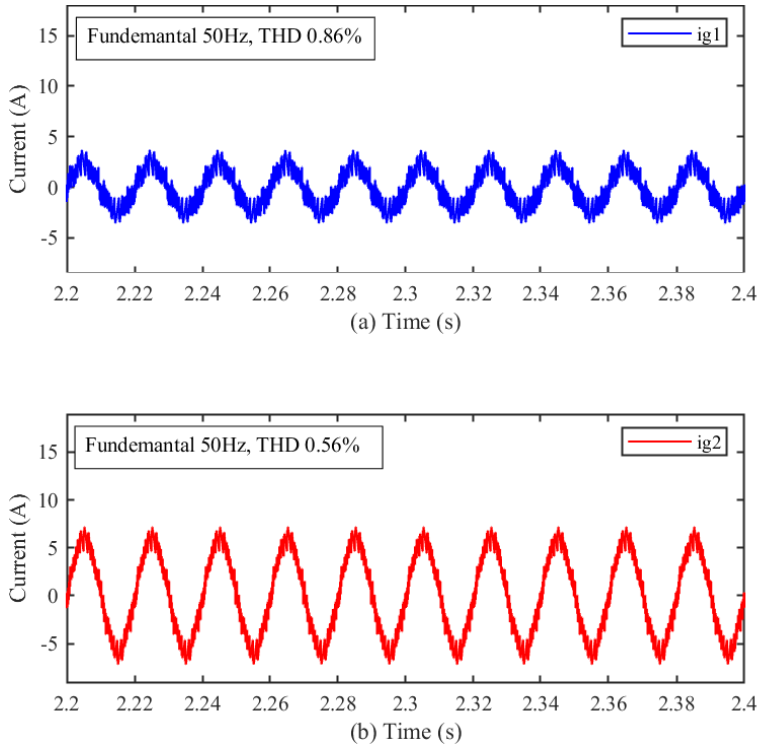

Fig. 6.13 Grid current of MG 1 and MG 2

6.5.1 Case-I: Dynamic Performance of DMPPCs during System Disturbances

In case I, dynamic performance of the proposed control method is demonstrated by considering the dramatic change of PV power, load power and reference grid power of MGs in the network. The PV outputs and load demands are the uncontrollable units in the proposed NMG structure. So, the PV powers and load powers are considered as input and output system disturbance respectively and the target of a controller is to mitigate the fluctuating nature of PV and Load demand through charging/ discharging of the battery. Moreover, the grid power reference of MGs needs to adjust to maintain the reliability of supply and to keep the battery SoC within limits. Thus, response of controllers during the change in reference power is included in the performance evaluation of the proposed DMPPCs. The Fig. 6.11 presents a simulation scenario for 7 sec. that demonstrates controllers performance during system disturbances and changes to reference powers. Random values of the PV power is generated in Fig. 6.11(a) to illustrates the dynamic nature of the PV modules for the simulation time. The Fig. 6.11(b) shows the changes of load powers in the network. At 2.5 sec., load power of the MG 1 is increased from 1.5 KW to 2.2 KW and is decreased to 1.8 KW at 3.5s. The load power of the MG2 is increased

at 3.5 sec. from 0.3 KW to 1.2 KW. The Fig. 6.11(c) shows that the grid powers of MG1 and MG2 are following the given references despite the variations of loads and PV generations in the network. Moreover, the reference grid power of the MG 1 and MG 2 have changed at 2 sec., 4 sec. and 6 sec. The reference grid power of MG 2 has increased at 2 sec. from 0.5 KW to 1 KW and is decreased to 0.3 KW at 6 sec. The Fig. 6.11 (c) shows that the grid power of MG 2 has moved to the new reference point within a very short time. Similarly, the reference grid power of the MG 1 is increased at 4s from 0.4 KW to 0.9 KW and is decreased to 0.3 KW at 6 sec. The result shows that the grid of MG1 is following the reference without a large fluctuation. To demonstrate the response of the power controllers an extended view of Fig. 6.11 (c) is presented in Fig. 6.12. Fig. 6.12 (a) shows the extended view of Fig. 6.11 (c) from 1.8 sec. to 2.2 sec. The result shows that the reference tie-line power is achieved within 0.02 sec. after changing the reference power. The Fig. 6.12(b) shows the extended view of Fig. 6.11 (c) from 3.3

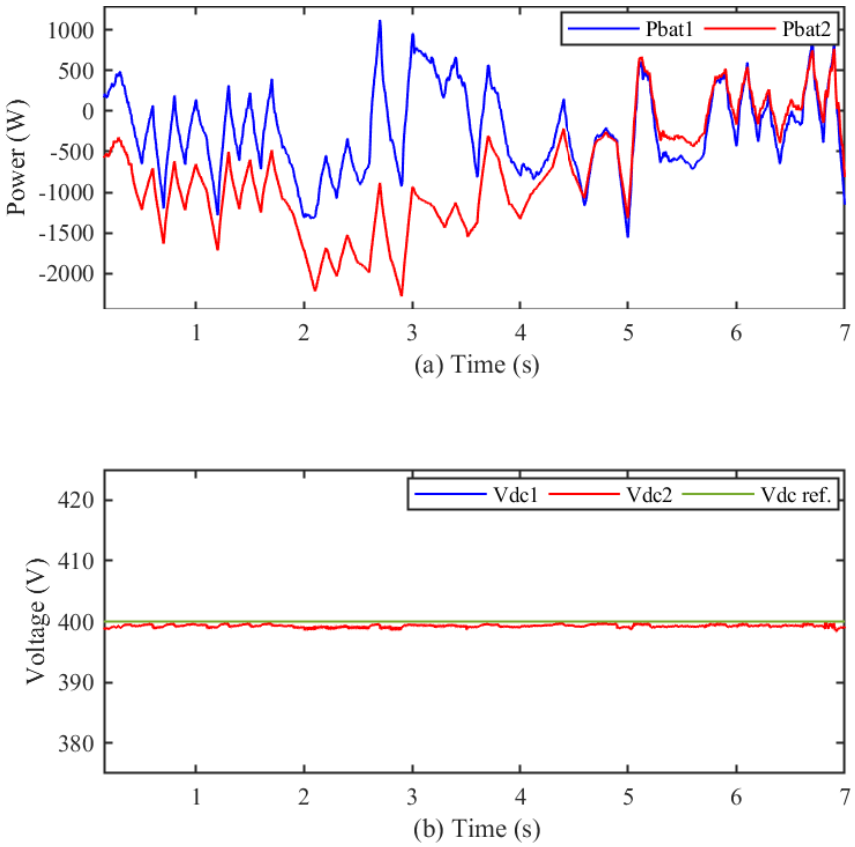

Fig. 6.14 Battery power and DC link voltage of MG1 and MG2 with respect to reference

sec. to 3.5 sec. The results show that tie-line powers are following the reference powers with a very little fluctuations despite a large change in load power of MG 2. Fig. 6.12(c) shows the response of the controller during changing the reference power of MG 1 and MG 2 at 5sec. The results show that

distributed controllers are achieved the new reference within 0.02 sec. for a sudden change in reference powers. The result also shows a smooth tie-line power of the network within a very little fluctuations. To maintain the grid powers to the references, required charging/ discharging of batteries are necessary. The battery powers of MG 1 and MG 2 are shown in Fig. 6.14(a) for the simulation period. The results show that batteries are charging/ discharging for maintaining a constant tie-line power by the interlink inverters as well as to maintain the DC bus voltages of MGs. The Fig. 6.14(b) shows the DC bus voltages of MG 1 and MG 2 that are following the reference voltage through charging/ discharging of the battery. Fig. 6.13 (a) and Fig. 6.13(b) show the grid current of MG 1 and MG 2 for the simulation period. The results show that grid currents drawn by the proposed MPPPCs have a THD of 0.86% and 0.56% which is less than the maximum limit of 5% .

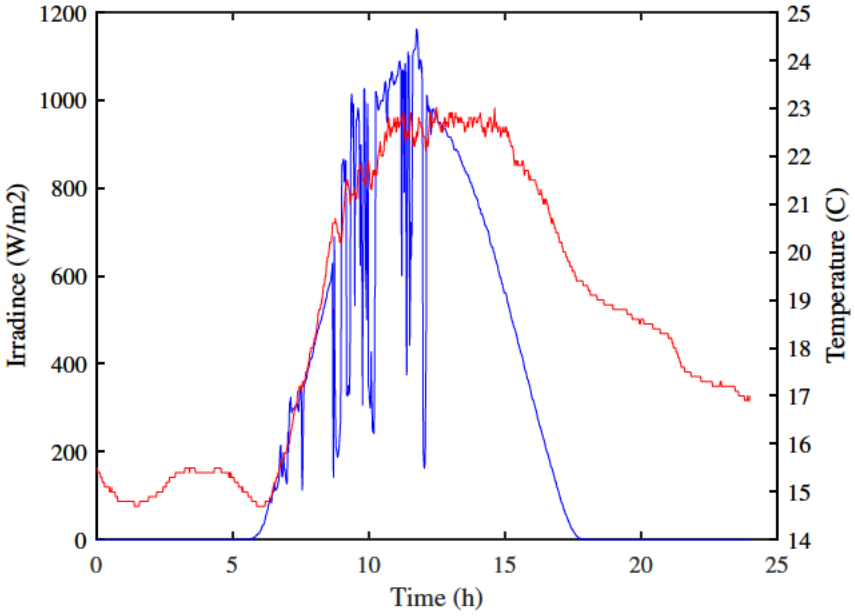

Fig. 6.15 Weather information on typical days of the year

6.5.2 Case-II: Dynamic Performance of the DMPPC using Real Weather and Load Variations

In case II, the performance of the proposed DMPPC is demonstrated for 24 h duration using real weather and load data in Queensland, Australia. In this case, the statistical weather and load data for a typical day in September 2017 is selected on random basis to evaluate the performance of the proposed method. The sun radiation and temperature data of Brisbane, Australia in September 2017 are obtained from

the statistical weather information database of building N44, Griffith University. The radiation and temperature data are collected from 5 am to 7 pm at 1 min intervals. Fig. 6.15 shows the statistical

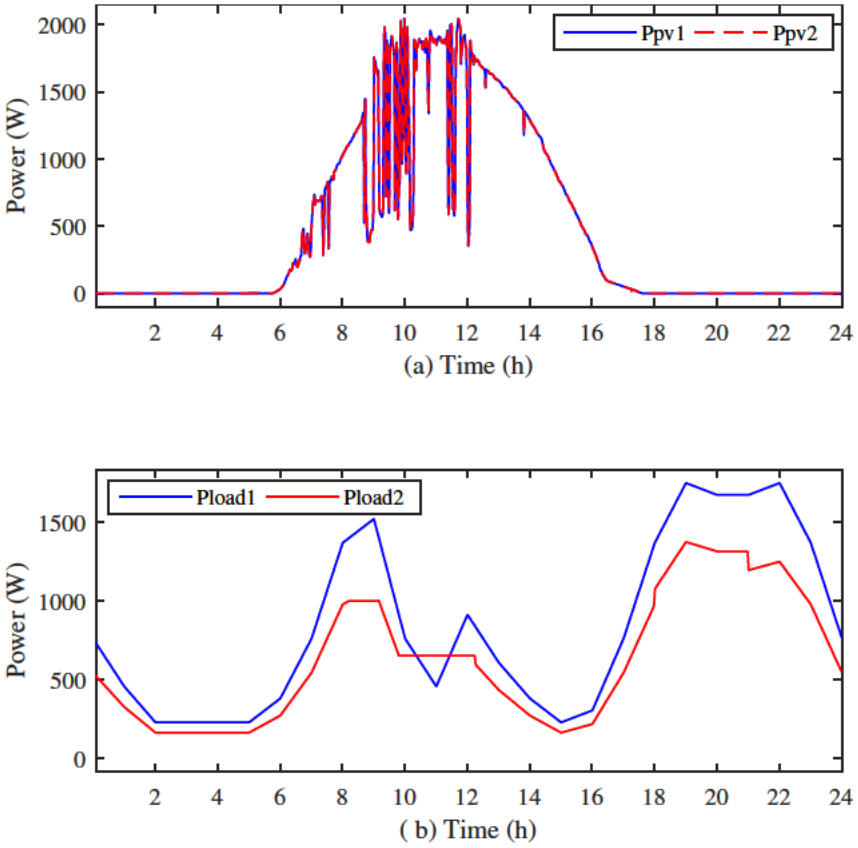

Fig. 6.16 PV and load power of MG 1 and MG 2

weather information on a typical day in September 2017. The statistical weather information is used to generate the PV profiles of MG 1 and MG 2 in Fig. 6.16(a). Moreover, residential load data for two typical houses in Queensland are collected at 1 min intervals to generate the load profiles of MG 1 and MG 2. The load profile of MG 1 and MG 2 are shown in Fig. 6.16(b). Meanwhile, the target of the proposed distributed power controllers is to maintain a smooth tie-line power in an NMG for a typical day of the year. It is assumed that each MG EMS calculates its grid power reference for a day using a day ahead forecasted generation, load demand and battery SoC. The shortage/surplus power will import/export from/to the main grid to maintain the power balance in a MG. Based on the statistical data, the shortage amount of power in MG 1 and MG 2 are approximately 49% and 33% of the total load demand on that day. So, the reference grid power in an MG is calculated by the MG EMS to draw the required amount power from the main grid. The calculated reference grid power is sent to the interlink inverter as a reference and to DNO to calculate the total reference power of the network.

Besides that, grid power information from the other MGs in a network is also collected to determine the reference grid power of a DMPPC. The Fig. 6.17(a) and Fig. 6.17(b) show the real and reactive power

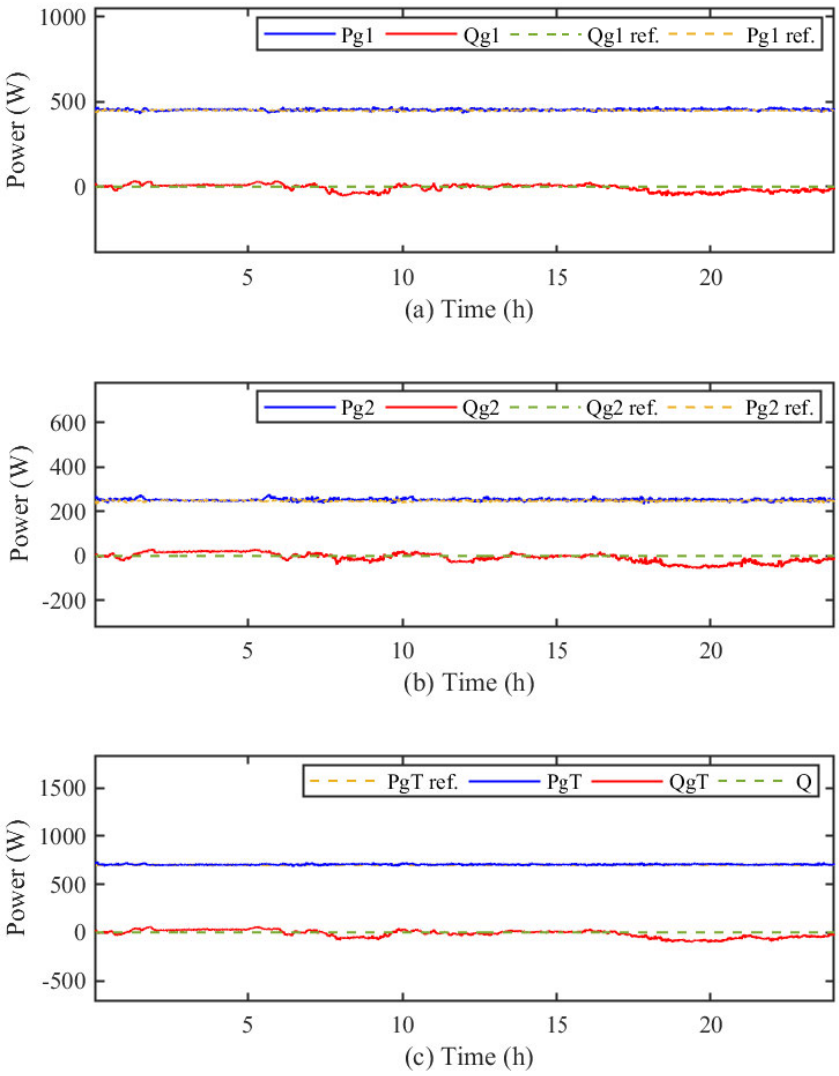

Fig. 6.17 Comparison of active and reactive grid power of MG 1, MG 2 and the network

drawn by the MG 1 and MG 2 respectively. The results shows that the real and reactive power of MGs are following the reference with a little fluctuations. The Fig. 6.17(c) shows the tie-line power in an NMG. The result demonstrates a smooth lie line power in an NMG for a typical day of the year. The Fig. 6.18(a) and Fig. 6.18(b) show the battery power and battery SoC of MG 1 and MG 2. The results show that batteries are charging and discharging in a limit to maintain a healthy life of the batteries. Fig. 6.18(c) shows that decentralised operation of batteries are also maintained DC bus voltages of MGs near to the reference.

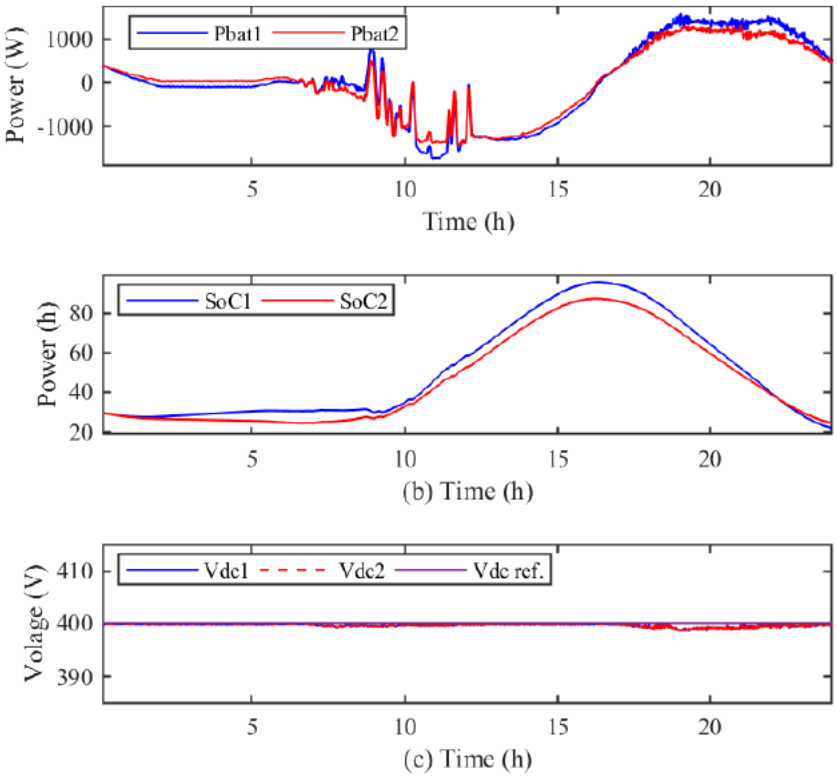

Fig. 6.18 Battery power, battery SoC and DC bus voltage of MG 1 and MG 2

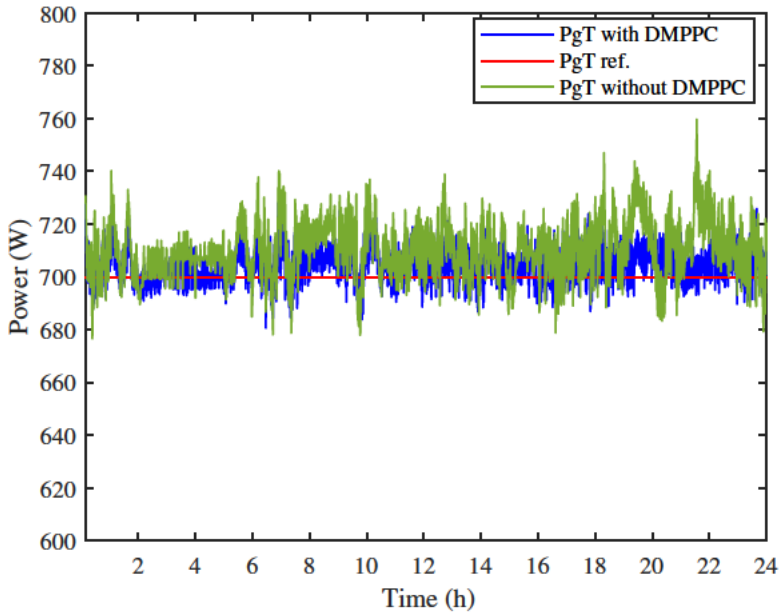

Fig. 6.19 Comparison of DMPPC method with respect to decentralised MPC based method

6.5.3 Case-III: Performance Comparison of the DMPPC with Decentralised Operation

In case III, the performance of the proposed DMPPC is compared with the decentralised operation mode of MG. In decentralised operation, there is no information sharing in the network nd each MG is only responsible to maintain the tie-line power of individual MGs. The Fig. 6.19 shows the comparison of real powers of an NMG during distributed and decentralised operation. The result shows that proposed DMMPC is reduced the tie-line fluctuation in an NMG in compared with decentralised operation of MGs.

6.6 Conclusions

In this chapter, a DMPPC is deigned for controlling the tie-line power in a networked of grid-connected residential MGs using a finite set MPC. A decentralised MPC is utilised for DC-DC converters of batteries that works in coordination with a DMPPC of tie-line inverters to overcome the tie-line fluctuations in an NMG. The main responsibility of DMMPCs is to achieve a scheduled tie-line power for an NMG through dynamic control of tie-line inverters despite the variations of PV and load powers in the network. Communication between MGs is established to determine the reference power for DMPPCs in distributed manner. Furthermore, a simulation model of an NMG consists of two grid-connected residential MGs are developed to perform simulation experiments in different case studies. A comparative study with a decentralised operation of MGs is presented in simulation. The results show that the proposed control method provides a smooth tie-line power for a network of residential MGs despite a dramatic system disturbances in the network.

Chapter 7

Conclusions and Future Works

This chapter presents a summary of outcomes of this thesis and provides some future research directions in the relevant field.

7.1 Concluding Remarks

This thesis focused on tie-line fluctuation problem of grid-connected MGs and presented several control and optimisation methods to achieve a smooth tie-line power in grid-connected MGs. The four research outcomes are summarised as follows:

1. A fuzzy logic-based power flow control method has been proposed in Chapter 3 to reduce the tie-line fluctuations in a grid-connected residential MG. The output of the fuzzy logic is the control reference of the battery power. Membership functions and rules of the fuzzy logic were optimised using an offline optimisation method based on the system constraints. The proposed fuzzy logic controller was implemented in MATLAB SIMULINK fuzzy interface system by following the designed constraints. A simulation experiment was used for four different radiation days to show the performance of the proposed controller for predefined performance parameters. Two other rule-based methods have been compared with the fuzzy control method to demonstrate the effectiveness of the proposed controller. The present results reduced tie-line fluctuations in a grid-connected residential MG despite the variations in generations and load demand.

2. A non-linear programming-based battery power control strategy has been presented in Chapter 4 to

minimise the tie-line fluctuations in a grid-connected residential MG. A golden section search method was applied in the EMS of the MG by maintaining the system constraints. A residential MG model was developed in MATLAB SIMULINK Simscape Electrical™tool, and the proposed power flow control method was implemented in a dynamic EMS to control the MG battery. The simulation experiment was conducted for several days based on the statistical weather and load information in Queensland, Australia to show the performance of the proposed power flow control method. A comparison with other two rule-based methods have been presented in the results to validate the efficacy of the proposed power flow control method.

3. A grid power control method for the interlink inverter of an MG has been proposed in Chapter 5 to achieve a constant tie-line power for typical days of the year. Firstly, a dynamic model of the entire MG was developed. Next, a grid power controller was designed to control the tie-line power of the MG. Finally, a reference grid power was calculated by using the MG controller based on the battery capacity, statistical weather and load data in Queensland, Australia. Moreover, a small signal model of the MG was obtained by linearising the dynamic model near a steady-state point, and an eigenvalue-based stability analysis was conducted for the variations in system parameters. The performance of the proposed tie-line control method was presented through different case studies for short term system disturbances, such as a sudden cloud appearance or a dramatic change in load demand. A simulation experiment was also conducted for real weather and load data in Queensland, Australia to show the performance of the controller on typical days of the year. Moreover, a comparison with the fuzzy logic-based dynamic EMS was presented in the results. The results have shown that the proposed grid power control method achieved a smooth tie-line power in a grid-connected residential MG by keeping the battery states within a predefined limit.

4. A distributed model predictive tie-line power control method was proposed in Chapter 6 to achieve a smooth tie-line power in NMGs. A decentralised model predictive power controller was employed to control the DC bus of individual MGs that have been working in cooperation with a DMPPC using to control the interlink inverter of an MG. The interlink inverters of the NMG were operated in a distributed manner to control the tie-line power of the grid-connected NMG. The amount of gird power drawn by the MGs were shared with each other through a communication link to calculate the grid power reference of individual MGs to achieve a scheduled tie-line power by maintaining system constraints of individual MGs. The proposed DMPPC method was verified in simulation experiment though several

case studies to show the performance of the distributed grid power controller for the variation in system disturbances and the reference power. A comparative analysis of the proposed method was conducted with respect to decentralised operation of MGs presented in the results to show the effectiveness of the proposed control method. The results showed that a smooth tie-line power can be obtained in an NMG for typical days of the year despite the variations in generations and load demand.

7.2 Future Work

1. Real-time experimental validation is an important consideration for any method. The proposed methods can be verified in hardware experiments to validate the practical implementation of the proposed methods. In Chapter 6, the NMG system was modelled in MATLAB SIMULINK in a designer PC. Meanwhile, implementing a controller in an embedded system will provide a faster response than PC-based implementation. The proposed DMMPC method should be verified in an actual hardware set up to compare the performance of the controller with the simulation experimental results. The real MG set up in Griffith University, Nathan campus, Brisbane, Australia can be used as a test system to perform the real-time hardware experiment. In the future, the industrial panel PC can be connected to real hardware to implement the proposed control method.

2. An efficient EMS is prerequisite for determining the reference power in any control method. Weather and load forecasting are one of the popular ways to schedule power in an EMS. Forecasting- based power flow control was excluded in this thesis. Thus, additional studies can be anticipated for an efficient tie-line power flow in an MG based on forecasted generations and load demand by securing the system constraints.

3. Tie-line power flow control in an NMG during mutual power sharing amongst MGs is another challenge. Power sharing between MGs during surplus/shortage generations was excluded in this study. Thus, adaptive control methods should be developed to control the tie-line power in an NMG to attain the benefits of mutual power sharing amongst MGs.

4. A reliable communication network is assumed for power flow control in NMGs. Meanwhile, the effect of communication link failure on the NMG operation should be addressed in the future. Moreover, cyber security is a major concern in NMGs given that different types of communication networks can be used

by MGs in a network. Thus, adaptive control methods that deal with possible cyber security issues for NMGs should be developed to achieve their secure power transfer.

Appendix A

Permissions from Publisher for Thesis / Dissertation Reuse

Journal papers included in Chapter 2, Chapter 3 and Chapter 5 have published by JOHN WiLEY AND SONS. The author of this thesis has taken permission from the publisher added as follows.

WILEY

Control and optimisation of networked microgrids: A review

Author: Mojaharul Islam, Fuwen Yang, Mohammad Amin

Publication: IET Renewable Power Generation

Publisher: John Wiley and Sons

Date: Feb 23, 2021

JOHN WILEY AND SONS LICENSE TERMS AND CONDITIONS

Dec 15, 2020

This Agreement between Griffith University -- Mojaharul Islam ("You") and John Wiley and Sons ("John Wiley and Sons") consists of your license details and the terms and conditions provided by John Wiley and Sons and Copyright Clearance Center.

License Number	4963390038952
License date	Dec 06, 2020
Licensed Content Publisher	John Wiley and Sons
Licensed Content Publication	INTERNATIONAL TRANSACTIONS ON ELECTRICAL ENERGY SYSTEMS
Licensed Content Title	Grid power fluctuation reduction by fuzzy control based energy management system in residential microgrids
Licensed Content Author	Mohammad Amin, Chandima Ekanayek, Fuwen Yang, et al
Licensed Content Date	Oct 28, 2018
Licensed Content Volume	29
Licensed Content Issue	3
Licensed Content Pages	14
Type of Use	Dissertation/Thesis
Requestor type	Author of this Wiley article
Format	Electronic
Portion	Full article
Will you be translating?	No
Title	Dynamic control of grid-connected microgrids for tie-line smoothing
Institution name	Griffith University
Expected presentation date	Jan 2021
Requestor Location	Griffith University 2/3 central street,labrador Gold Coast, QLD 4215 Australia Attn: Griffith University
Publisher Tax ID	EU826007151
Total	**0.00 AUD**
Terms and Conditions	

TERMS AND CONDITIONS

This copyrighted material is owned by or exclusively licensed to John Wiley & Sons, Inc. or one of its group companies (each a"Wiley Company") or handled on behalf of a society with which a Wiley Company has exclusive publishing rights in relation to a particular work (collectively "WILEY"). By clicking "accept" in connection with completing this licensing transaction, you agree that the following terms and conditions apply to this transaction (along with the billing and payment terms and conditions established by the Copyright Clearance Center Inc., ("CCC's Billing and Payment terms and conditions"), at the time that you opened your RightsLink account (these are available at any time at http://myaccount.copyright.com).

Terms and Conditions

- The materials you have requested permission to reproduce or reuse (the "Wiley Materials") are protected by copyright.
- You are hereby granted a personal, non-exclusive, non-sub licensable (on a stand-alone basis), non-transferable, worldwide, limited license to reproduce the Wiley Materials for the purpose specified in the licensing process. This license, **and any CONTENT (PDF or image file) purchased as part of your order,** is for a one-time use only and limited to any maximum distribution number specified in the license. The first instance of republication or reuse granted

by this license must be completed within two years of the date of the grant of this license (although copies prepared before the end date may be distributed thereafter). The Wiley Materials shall not be used in any other manner or for any other purpose, beyond what is granted in the license. Permission is granted subject to an appropriate acknowledgement given to the author, title of the material/book/journal and the publisher. You shall also duplicate the copyright notice that appears in the Wiley publication in your use of the Wiley Material. Permission is also granted on the understanding that nowhere in the text is a previously published source acknowledged for all or part of this Wiley Material. Any third party content is expressly excluded from this permission.

- With respect to the Wiley Materials, all rights are reserved. Except as expressly granted by the terms of the license, no part of the Wiley Materials may be copied, modified, adapted (except for minor reformatting required by the new Publication), translated, reproduced, transferred or distributed, in any form or by any means, and no derivative works may be made based on the Wiley Materials without the prior permission of the respective copyright owner.**For STM Signatory Publishers clearing permission under the terms of the STM Permissions Guidelines only, the terms of the license are extended to include subsequent editions and for editions in other languages, provided such editions are for the work as a whole in situ and does not involve the separate exploitation of the permitted figures or extracts,** You may not alter, remove or suppress in any manner any copyright, trademark or other notices displayed by the Wiley Materials. You may not license, rent, sell, loan, lease, pledge, offer as security, transfer or assign the Wiley Materials on a stand-alone basis, or any of the rights granted to you hereunder to any other person.

- The Wiley Materials and all of the intellectual property rights therein shall at all times remain the exclusive property of John Wiley & Sons Inc, the Wiley Companies, or their respective licensors, and your interest therein is only that of having possession of and the right to reproduce the Wiley Materials pursuant to Section 2 herein during the continuance of this Agreement. You agree that you own no right, title or interest in or to the Wiley Materials or any of the intellectual property rights therein. You shall have no rights hereunder other than the license as provided for above in Section 2. No right, license or interest to any trademark, trade name, service mark or other branding ("Marks") of WILEY or its licensors is granted hereunder, and you agree that you shall not assert any such right, license or interest with respect thereto

- NEITHER WILEY NOR ITS LICENSORS MAKES ANY WARRANTY OR REPRESENTATION OF ANY KIND TO YOU OR ANY THIRD PARTY, EXPRESS, IMPLIED OR STATUTORY, WITH RESPECT TO THE MATERIALS OR THE ACCURACY OF ANY INFORMATION CONTAINED IN THE MATERIALS, INCLUDING, WITHOUT LIMITATION, ANY IMPLIED WARRANTY OF MERCHANTABILITY, ACCURACY, SATISFACTORY QUALITY, FITNESS FOR A PARTICULAR PURPOSE, USABILITY, INTEGRATION OR NON-INFRINGEMENT AND ALL SUCH WARRANTIES ARE HEREBY EXCLUDED BY WILEY AND ITS LICENSORS AND WAIVED BY YOU.

- WILEY shall have the right to terminate this Agreement immediately upon breach of this Agreement by you.

- You shall indemnify, defend and hold harmless WILEY, its Licensors and their respective directors, officers, agents and employees, from and against any actual or threatened claims, demands, causes of action or proceedings arising from any breach of this Agreement by you.

- IN NO EVENT SHALL WILEY OR ITS LICENSORS BE LIABLE TO YOU OR ANY OTHER PARTY OR ANY OTHER PERSON OR ENTITY FOR ANY SPECIAL, CONSEQUENTIAL, INCIDENTAL, INDIRECT, EXEMPLARY OR PUNITIVE DAMAGES, HOWEVER CAUSED, ARISING OUT OF OR IN CONNECTION WITH THE DOWNLOADING, PROVISIONING, VIEWING OR USE OF THE MATERIALS REGARDLESS OF THE FORM OF ACTION, WHETHER FOR BREACH OF CONTRACT, BREACH OF WARRANTY, TORT, NEGLIGENCE, INFRINGEMENT OR OTHERWISE (INCLUDING, WITHOUT LIMITATION, DAMAGES BASED ON LOSS OF PROFITS, DATA, FILES, USE, BUSINESS OPPORTUNITY OR CLAIMS OF THIRD PARTIES), AND WHETHER OR NOT THE PARTY HAS BEEN ADVISED OF THE POSSIBILITY OF SUCH DAMAGES. THIS LIMITATION SHALL APPLY NOTWITHSTANDING ANY FAILURE OF ESSENTIAL PURPOSE OF ANY LIMITED REMEDY PROVIDED HEREIN.

- Should any provision of this Agreement be held by a court of competent jurisdiction to be illegal, invalid, or unenforceable, that provision shall be deemed amended to achieve as nearly as poss ble the same economic effect as the original provision, and the legality, validity and enforceability of the remaining provisions of this Agreement shall not be affected or impaired thereby.

- The failure of either party to enforce any term or condition of this Agreement shall not constitute a waiver of either party's right to enforce each and every term and condition of this Agreement. No breach under this agreement shall be deemed waived or excused by either party unless such waiver or consent is in writing signed by the party granting such waiver or consent. The waiver by or consent of a party to a breach of any provision of this Agreement shall not operate or be construed as a waiver of or consent to any other or subsequent breach by such other party.

- This Agreement may not be assigned (including by operation of law or otherwise) by you without WILEY's prior written consent.

- Any fee required for this permission shall be non-refundable after thirty (30) days from receipt by the CCC.
- These terms and conditions together with CCC's Billing and Payment terms and conditions (which are incorporated herein) form the entire agreement between you and WILEY concerning this licensing transaction and (in the absence of fraud) supersedes all prior agreements and representations of the parties, oral or written. This Agreement may not be amended except in writing signed by both parties. This Agreement shall be binding upon and inure to the benefit of the parties' successors, legal representatives, and authorized assigns.
- In the event of any conflict between your obligations established by these terms and conditions and those established by CCC's Billing and Payment terms and conditions, these terms and conditions shall prevail.
- WILEY expressly reserves all rights not specifically granted in the combination of (i) the license details provided by you and accepted in the course of this licensing transaction, (ii) these terms and conditions and (iii) CCC's Billing and Payment terms and conditions.
- This Agreement will be void if the Type of Use, Format, Circulation, or Requestor Type was misrepresented during the licensing process.
- This Agreement shall be governed by and construed in accordance with the laws of the State of New York, USA, without regards to such state's conflict of law rules. Any legal action, suit or proceeding arising out of or relating to these Terms and Conditions or the breach thereof shall be instituted in a court of competent jurisdiction in New York County in the State of New York in the United States of America and each party hereby consents and submits to the personal jurisdiction of such court, waives any objection to venue in such court and consents to service of process by registered or certified mail, return receipt requested, at the last known address of such party.

WILEY OPEN ACCESS TERMS AND CONDITIONS

Wiley Publishes Open Access Articles in fully Open Access Journals and in Subscription journals offering Online Open. Although most of the fully Open Access journals publish open access articles under the terms of the Creative Commons Attr bution (CC BY) License only, the subscription journals and a few of the Open Access Journals offer a choice of Creative Commons Licenses. The license type is clearly identified on the article.

The Creative Commons Attribution License

The Creative Commons Attr bution License (CC-BY) allows users to copy, distribute and transmit an article, adapt the article and make commercial use of the article. The CC-BY license permits commercial and non-

Creative Commons Attribution Non-Commercial License

The Creative Commons Attr bution Non-Commercial (CC-BY-NC)License permits use, distribution and reproduction in any medium, provided the original work is properly cited and is not used for commercial purposes.(see below)

Creative Commons Attribution-Non-Commercial-NoDerivs License

The Creative Commons Attr bution Non-Commercial-NoDerivs License (CC-BY-NC-ND) permits use, distr bution and reproduction in any medium, provided the original work is properly cited, is not used for commercial purposes and no modifications or adaptations are made. (see below)

Use by commercial "for-profit" organizations

Use of Wiley Open Access articles for commercial, promotional, or marketing purposes requires further explicit permission from Wiley and will be subject to a fee.

Further details can be found on Wiley Online Library http://olabout.wiley.com/WileyCDA/Section/id-410895.html

Other Terms and Conditions:

v1.10 Last updated September 2015

Questions? customercare@copyright.com or +1-855-239-3415 (toll free in the US) or +1-978-646-2777.

JOHN WILEY AND SONS LICENSE TERMS AND CONDITIONS

Jan 03, 2021

This Agreement between Griffith University -- Mojaharul Islam ("You") and John Wiley and Sons ("John Wiley and Sons") consists of your license details and the terms and conditions provided by John Wiley and Sons and Copyright Clearance Center.

License Number	4981330553913
License date	Jan 03, 2021
Licensed Content Publisher	John Wiley and Sons
Licensed Content Publication	INTERNATIONAL TRANSACTIONS ON ELECTRICAL ENERGY SYSTEMS
Licensed Content Title	Dynamic control of grid-connected microgrids for tie-line smoothing
Licensed Content Author	Mohammad Amin, Fuwen Yang, Mojaharul Islam
Licensed Content Date	Sep 21, 2020
Licensed Content Volume	30
Licensed Content Issue	11
Licensed Content Pages	17
Type of Use	Dissertation/Thesis
Requestor type	Author of this Wiley article
Format	Electronic
Portion	Full article
Will you be translating?	No
Title	Dynamic control of grid-connected microgrids for tie-line smoothing
Institution name	Griffith University
Expected presentation date	Jan 2021
Requestor Location	Griffith University 2/3 central street,labrador Gold Coast, QLD 4215 Australia Attn: Griffith University
Publisher Tax ID	EU826007151
Total	**0.00 AUD**
Terms and Conditions	

TERMS AND CONDITIONS

This copyrighted material is owned by or exclusively licensed to John Wiley & Sons, Inc. or one of its group companies (each a"Wiley Company") or handled on behalf of a society with which a Wiley Company has exclusive publishing rights in relation to a particular work (collectively "WILEY"). By clicking "accept" in connection with completing this licensing transaction, you agree that the following terms and conditions apply to this transaction (along with the billing and payment terms and conditions established by the Copyright Clearance Center Inc., ("CCC's Billing and Payment terms and conditions"), at the time that you opened your RightsLink account (these are available at any time at http://myaccount.copyright.com).

Terms and Conditions

- The materials you have requested permission to reproduce or reuse (the "Wiley Materials") are protected by copyright.
- You are hereby granted a personal, non-exclusive, non-sub licensable (on a stand-alone basis), non-transferable, worldwide, limited license to reproduce the Wiley Materials for the purpose specified in the licensing process. This license, **and any CONTENT (PDF or image file) purchased as part of your order,** is for a one-time use only and limited to any maximum

distribution number specified in the license. The first instance of republication or reuse granted by this license must be completed within two years of the date of the grant of this license (although copies prepared before the end date may be distributed thereafter). The Wiley Materials shall not be used in any other manner or for any other purpose, beyond what is granted in the license. Permission is granted subject to an appropriate acknowledgement given to the author, title of the material/book/journal and the publisher. You shall also duplicate the copyright notice that appears in the Wiley publication in your use of the Wiley Material. Permission is also granted on the understanding that nowhere in the text is a previously published source acknowledged for all or part of this Wiley Material. Any third party content is expressly excluded from this permission.

- With respect to the Wiley Materials, all rights are reserved. Except as expressly granted by the terms of the license, no part of the Wiley Materials may be copied, modified, adapted (except for minor reformatting required by the new Publication), translated, reproduced, transferred or distr buted, in any form or by any means, and no derivative works may be made based on the Wiley Materials without the prior permission of the respective copyright owner.**For STM Signatory Publishers clearing permission under the terms of the STM Permissions Guidelines only, the terms of the license are extended to include subsequent editions and for editions in other languages, provided such editions are for the work as a whole in situ and does not involve the separate exploitation of the permitted figures or extracts,** You may not alter, remove or suppress in any manner any copyright, trademark or other notices displayed by the Wiley Materials. You may not license, rent, sell, loan, lease, pledge, offer as security, transfer or assign the Wiley Materials on a stand-alone basis, or any of the rights granted to you hereunder to any other person.

- The Wiley Materials and all of the intellectual property rights therein shall at all times remain the exclusive property of John Wiley & Sons Inc, the Wiley Companies, or their respective licensors, and your interest therein is only that of having possession of and the right to reproduce the Wiley Materials pursuant to Section 2 herein during the continuance of this Agreement. You agree that you own no right, title or interest in or to the Wiley Materials or any of the intellectual property rights therein. You shall have no rights hereunder other than the license as provided for above in Section 2. No right, license or interest to any trademark, trade name, service mark or other branding ("Marks") of WILEY or its licensors is granted hereunder, and you agree that you shall not assert any such right, license or interest with respect thereto

- NEITHER WILEY NOR ITS LICENSORS MAKES ANY WARRANTY OR REPRESENTATION OF ANY KIND TO YOU OR ANY THIRD PARTY, EXPRESS, IMPLIED OR STATUTORY, WITH RESPECT TO THE MATERIALS OR THE ACCURACY OF ANY INFORMATION CONTAINED IN THE MATERIALS, INCLUDING, WITHOUT LIMITATION, ANY IMPLIED WARRANTY OF MERCHANTABILITY, ACCURACY, SATISFACTORY QUALITY, FITNESS FOR A PARTICULAR PURPOSE, USABILITY, INTEGRATION OR NON-INFRINGEMENT AND ALL SUCH WARRANTIES ARE HEREBY EXCLUDED BY WILEY AND ITS LICENSORS AND WAIVED BY YOU.

- WILEY shall have the right to terminate this Agreement immediately upon breach of this Agreement by you.

- You shall indemnify, defend and hold harmless WILEY, its Licensors and their respective directors, officers, agents and employees, from and against any actual or threatened claims, demands, causes of action or proceedings arising from any breach of this Agreement by you.

- IN NO EVENT SHALL WILEY OR ITS LICENSORS BE LIABLE TO YOU OR ANY OTHER PARTY OR ANY OTHER PERSON OR ENTITY FOR ANY SPECIAL, CONSEQUENTIAL, INCIDENTAL, INDIRECT, EXEMPLARY OR PUNITIVE DAMAGES, HOWEVER CAUSED, ARISING OUT OF OR IN CONNECTION WITH THE DOWNLOADING, PROVISIONING, VIEWING OR USE OF THE MATERIALS REGARDLESS OF THE FORM OF ACTION, WHETHER FOR BREACH OF CONTRACT, BREACH OF WARRANTY, TORT, NEGLIGENCE, INFRINGEMENT OR OTHERWISE (INCLUDING, WITHOUT LIMITATION, DAMAGES BASED ON LOSS OF PROFITS, DATA, FILES, USE, BUSINESS OPPORTUNITY OR CLAIMS OF THIRD PARTIES), AND WHETHER OR NOT THE PARTY HAS BEEN ADVISED OF THE POSSIBILITY OF SUCH DAMAGES. THIS LIMITATION SHALL APPLY NOTWITHSTANDING ANY FAILURE OF ESSENTIAL PURPOSE OF ANY LIMITED REMEDY PROVIDED HEREIN.

- Should any provision of this Agreement be held by a court of competent jurisdiction to be illegal, invalid, or unenforceable, that provision shall be deemed amended to achieve as nearly as poss ble the same economic effect as the original provision, and the legality, validity and enforceability of the remaining provisions of this Agreement shall not be affected or impaired thereby.

- The failure of either party to enforce any term or condition of this Agreement shall not constitute a waiver of either party's right to enforce each and every term and condition of this Agreement. No breach under this agreement shall be deemed waived or excused by either party unless such waiver or consent is in writing signed by the party granting such waiver or consent. The waiver by or consent of a party to a breach of any provision of this Agreement shall not operate or be construed as a waiver

of or consent to any other or subsequent breach by such other party.

- This Agreement may not be assigned (including by operation of law or otherwise) by you without WILEY's prior written consent.
- Any fee required for this permission shall be non-refundable after thirty (30) days from receipt by the CCC.
- These terms and conditions together with CCC's Billing and Payment terms and conditions (which are incorporated herein) form the entire agreement between you and WILEY concerning this licensing transaction and (in the absence of fraud) supersedes all prior agreements and representations of the parties, oral or written. This Agreement may not be amended except in writing signed by both parties. This Agreement shall be binding upon and inure to the benefit of the parties' successors, legal representatives, and authorized assigns.
- In the event of any conflict between your obligations established by these terms and conditions and those established by CCC's Billing and Payment terms and conditions, these terms and conditions shall prevail.
- WILEY expressly reserves all rights not specifically granted in the combination of (i) the license details provided by you and accepted in the course of this licensing transaction, (ii) these terms and conditions and (iii) CCC's Billing and Payment terms and conditions.
- This Agreement will be void if the Type of Use, Format, Circulation, or Requestor Type was misrepresented during the licensing process.
- This Agreement shall be governed by and construed in accordance with the laws of the State of New York, USA, without regards to such state's conflict of law rules. Any legal action, suit or proceeding arising out of or relating to these Terms and Conditions or the breach thereof shall be instituted in a court of competent jurisdiction in New York County in the State of New York in the United States of America and each party hereby consents and submits to the personal jurisdiction of such court, waives any objection to venue in such court and consents to service of process by registered or certified mail, return receipt requested, at the last known address of such party.

WILEY OPEN ACCESS TERMS AND CONDITIONS

Wiley Publishes Open Access Articles in fully Open Access Journals and in Subscription journals offering Online Open. Although most of the fully Open Access journals publish open access articles under the terms of the Creative Commons Attribution (CC BY) License only, the subscription journals and a few of the Open Access Journals offer a choice of Creative Commons Licenses. The license type is clearly identified on the article.

The Creative Commons Attribution License

The Creative Commons Attribution License (CC-BY) allows users to copy, distribute and transmit an article, adapt the article and make commercial use of the article. The CC-BY license permits commercial and non-

Creative Commons Attribution Non-Commercial License

The Creative Commons Attribution Non-Commercial (CC-BY-NC)License permits use, distr bution and reproduction in any medium, provided the original work is properly cited and is not used for commercial purposes.(see below)

Creative Commons Attribution-Non-Commercial-NoDerivs License

The Creative Commons Attribution Non-Commercial-NoDerivs License (CC-BY-NC-ND) permits use, distribution and reproduction in any medium, provided the original work is properly cited, is not used for commercial purposes and no modifications or adaptations are made. (see below)

Use by commercial "for-profit" organizations

Use of Wiley Open Access articles for commercial, promotional, or marketing purposes requires further explicit permission from Wiley and will be subject to a fee.

Further details can be found on Wiley Online Library http://olabout.wiley.com/WileyCDA/Section/id-410895.html

Other Terms and Conditions:

v1.10 Last updated September 2015

Questions? customercare@copyright.com or +1-855-239-3415 (toll free in the US) or +1-978-646-2777.

The conference paper included in Chapter 4 has published by IEEE. IEEE policy for thesis / dissertation reuse added as follows.

IEEE Policy for Thesis / Dissertation Reuse

The IEEE does not require individuals working on a thesis to obtain a formal reuse license, however, you may print out this statement to be used as a permission grant:

Requirements to be followed when using any portion (e.g., figure, graph, table, or textual material) of an IEEE copyrighted paper in a thesis:

1) In the case of textual material (e.g., using short quotes or referring to the work within these papers) users must give full credit to the original source (author, paper, publication) followed by the IEEE copyright line © 2011 IEEE. 2) In the case of illustrations or tabular material, we require that the copyright line © [Year of original publication] IEEE appear prominently with each reprinted figure and/or table. 3) If a substantial portion of the original paper is to be used, and if you are not the senior author, also obtain the senior author's approval.

Requirements to be followed when using an entire IEEE copyrighted paper in a thesis:

1) The following IEEE copyright/ credit notice should be placed prominently in the references: © [year of original publication] IEEE. Reprinted, with permission, from [author names, paper title, IEEE publication title, and month/year of publication] 2) Only the accepted version of an IEEE copyrighted paper can be used when posting the paper or your thesis on-line. 3) In placing the thesis on the author's university website, please display the following message in a prominent place on the website: In reference to IEEE copyrighted material which is used with permission in this thesis, the IEEE does not endorse any of [university/educational entity's name goes here]'s products or services. Internal or personal use of this material is permitted. If interested in reprinting/republishing IEEE copyrighted material for advertising or promotional purposes or for creating new collective works for resale or redistribution, please go to http://www.ieee.org/publications_standards/publications/rights/rights_link.html to learn how to obtain a License from RightsLink.

If applicable, University Microfilms and/or ProQuest Library, or the Archives of Canada may supply single copies of the dissertation.

References

[1] R. H. Lasseter, "Microgrids," in *Power Engineering Society Winter Meeting, 2002. IEEE*, vol. 1, pp. 305–308, IEEE.

[2] R. H. Lasseter and P. Paigi, "Microgrid: A conceptual solution," in *Power Electronics Specialists Conference, 2004. PESC 04. 2004 IEEE 35th Annual*, vol. 6, pp. 4285–4290, IEEE.

[3] N. Lidula and A. Rajapakse, "Microgrids research: A review of experimental microgrids and test systems," *Renewable and Sustainable Energy Reviews*, vol. 15, no. 1, pp. 186–202, 2011.

[4] J. J. Justo, F. Mwasilu, J. Lee, and J.-W. Jung, "Ac-microgrids versus dc-microgrids with distributed energy resources: A review," *Renewable and Sustainable Energy Reviews*, vol. 24, pp. 387–405, 2013.

[5] Y. Yoldaş, A. Önen, S. Muyeen, A. V. Vasilakos, and r. Alan, "Enhancing smart grid with microgrids: Challenges and opportunities," *Renewable and Sustainable Energy Reviews*, vol. 72, pp. 205–214, 2017.

[6] M. Farrelly and S. Tawfik, "Engaging in disruption: A review of emerging microgrids in victoria, australia," *Renewable and Sustainable Energy Reviews*, vol. 117, p. 109491, 2020.

[7] M. Islam, F. W. Yang, C. Ekanayek, and M. Amin, "Grid power fluctuation reduction by fuzzy control based energy management system in residential microgrids," *International Transactions on Electrical Energy Systems*, vol. 29, no. 3, p. e2758, 2019.

[8] S. A. Arefifar, Y. A.-R. I. Mohamed, and T. El-Fouly, "Optimized multiple microgrid-based clustering of active distribution systems considering communication and control requirements," *IEEE Transactions on Industrial Electronics*, vol. 62, no. 2, pp. 711–723, 2014.

[9] D. Rua, L. M. Pereira, N. Gil, and J. P. Lopes, "Impact of multi-microgrid communication systems in islanded operation," in *2011 2nd IEEE PES International Conference and Exhibition on Innovative Smart Grid Technologies*, pp. 1–6, IEEE.

[10] C. Yuen and A. Oudalov, "The feasibility and profitability of ancillary services provision from multi-microgrids," in *Power Tech, 2007 IEEE Lausanne*, pp. 598–603, IEEE.

[11] Z. Li, M. Shahidehpour, F. Aminifar, A. Alabdulwahab, and Y. Al-Turki, "Networked microgrids for enhancing the power system resilience," *Proceedings of the IEEE*, vol. 105, no. 7, pp. 1289–1310, 2017.

[12] S. Marzal, R. Salas, R. González-Medina, G. Garcerá, and E. Figueres, "Current challenges and future trends in the field of communication architectures for microgrids," *Renewable and Sustainable Energy Reviews*, vol. 82, pp. 3610–3622, 2018.

[13] Z. Xu, P. Yang, C. Zheng, Y. Zhang, J. Peng, and Z. Zeng, "Analysis on the organization and development of multi-microgrids," *Renewable and Sustainable Energy Reviews*, vol. 81, pp. 2204–2216, 2017.

[14] L. Meng, Q. Shafiee, G. F. Trecate, H. Karimi, D. Fulwani, X. Lu, and J. M. Guerrero, "Review on control of dc microgrids and multiple microgrid clusters," *IEEE Journal of Emerging and Selected Topics in Power Electronics*, vol. 5, no. 3, pp. 928–948, 2017.

[15] M. N. Alam, S. Chakrabarti, and A. Ghosh, "Networked microgrids: State-of-the-art and future perspectives," *IEEE Transactions on Industrial Informatics*, vol. 15, no. 3, pp. 1238–1250, 2018.

[16] B. Chen, J. Wang, X. Lu, C. Chen, and S. Zhao, "Networked microgrids for grid resilience, robustness, and efficiency: A review," *IEEE Transactions on Smart Grid*, vol. 12, no. 1, pp. 18–32, 2021.

[17] Q. Zhou, M. Shahidehpour, A. Paaso, S. Bahramirad, A. Alabdulwahab, and A. Abusorrah, "Distributed control and communication strategies in networked microgrids," *IEEE Communications Surveys Tutorials*, vol. 22, no. 4, pp. 2586–2633, 2020.

[18] H. Zou, S. Mao, Y. Wang, F. Zhang, X. Chen, and L. Cheng, "A survey of energy management in interconnected multi-microgrids," *IEEE Access*, vol. 7, pp. 72158–72169, 2019.

[19] F. Katiraei, R. Iravani, N. Hatziargyriou, and A. Dimeas, "Microgrids management," *IEEE power and energy magazine*, vol. 6, no. 3, 2008.

[20] R. Palma-Behnke, C. Benavides, F. Lanas, B. Severino, L. Reyes, J. Llanos, and D. Sáez, "A microgrid energy management system based on the rolling horizon strategy," *IEEE Transactions on Smart Grid*, vol. 4, no. 2, pp. 996–1006, 2013.

[21] R. Palma-Behnke, C. Benavides, E. Aranda, J. Llanos, and D. Sáez, "Energy management system for a renewable based microgrid with a demand side management mechanism," in *Computational intelligence applications in smart grid (CIASG), 2011 IEEE symposium on*, pp. 1–8, IEEE.

[22] A. Bagherian and S. M. Tafreshi, "A developed energy management system for a microgrid in the competitive electricity market," in *PowerTech, 2009 IEEE Bucharest*, pp. 1–6, IEEE.

[23] I. Prodan and E. Zio, "A model predictive control framework for reliable microgrid energy management," *International Journal of Electrical Power Energy Systems*, vol. 61, pp. 399–409, 2014.

[24] S. Mohammadi, S. Soleymani, and B. Mozafari, "Scenario-based stochastic operation management of microgrid including wind, photovoltaic, micro-turbine, fuel cell and energy storage devices," *International Journal of Electrical Power Energy Systems*, vol. 54, pp. 525–535, 2014.

[25] H. Zhou, T. Bhattacharya, D. Tran, T. S. T. Siew, and A. M. Khambadkone, "Composite energy storage system involving battery and ultracapacitor with dynamic energy management in microgrid applications," *IEEE transactions on power electronics*, vol. 26, no. 3, pp. 923–930, 2011.

[26] Y.-K. Chen, Y.-C. Wu, C.-C. Song, and Y.-S. Chen, "Design and implementation of energy management system with fuzzy control for dc microgrid systems," *IEEE Transactions on Power Electronics*, vol. 28, no. 4, pp. 1563–1570, 2013.

[27] Y. Meng, "A rule-based energy management system for smart micro-grid," in *2019 29th Australasian Universities Power Engineering Conference (AUPEC)*, pp. 1–6, IEEE.

[28] T. Pippia, J. Sijs, and B. De Schutter, "A single-level rule-based model predictive control approach for energy management of grid-connected microgrids," *IEEE Transactions on Control Systems Technology*, vol. 28, no. 6, pp. 2364–2376, 2019.

[29] A. L. Bukar, C. W. Tan, L. K. Yiew, R. Ayop, and W.-S. Tan, "A rule-based energy management scheme for long-term optimal capacity planning of grid-independent microgrid optimized by multi-objective grasshopper optimization algorithm," *Energy Conversion and Management*, vol. 221, p. 113161, 2020.

[30] M. Moghimi, D. Leskarac, C. Bennett, J. Lu, and S. Stegen, "Rule-based energy management system in an experimental microgrid with the presence of time of use tariffs," in *MATEC Web of Conferences*, vol. 70, p. 10011, EDP Sciences.

[31] C. Sun, G. Joos, S. Q. Ali, J. N. Paquin, C. M. Rangel, F. Al Jajeh, I. Novickij, and F. Bouffard, "Design and real-time implementation of a centralized microgrid control system with rule-based dispatch and seamless transition function," *IEEE Transactions on Industry Applications*, vol. 56, no. 3, pp. 3168–3177, 2020.

[32] S. H. C. Cherukuri, B. Saravanan, and G. Arunkumar, "A rule-based approach for improvement of autonomous operation of hybrid microgrids," *Electrical Engineering*, pp. 1–16, 2020.

[33] M. Jafari and Z. Malekjamshidi, "Optimal energy management of a residential-based hybrid renewable energy system using rule-based real-time control and 2d dynamic programming optimization method," *Renewable Energy*, vol. 146, pp. 254–266, 2020.

[34] M. Seydenschwanz, C. Gottschalk, B. D. Lee, and D. Ablakovic, "Rule-based dispatching of microgrids with coupled electricity and heat power systems," in *2020 IEEE PES Innovative Smart Grid Technologies Europe (ISGT-Europe)*, pp. 519–523, IEEE.

[35] A. Kanwar, D. I. H. Rodríguez, J. von Appen, and M. Braun, *A comparative study of optimization- and rule-based control for microgrid operation.* Universitätsbibliothek Dortmund, 2015.

[36] Z. Haoran, W. Qiuwei, W. Chengshan, L. Cheng, and C. N. Rasmussen, "Fuzzy logic based coordinated control of battery energy storage system and dispatchable distributed generation for microgrid," *Journal of Modern Power Systems and Clean Energy*, vol. 3, no. 3, pp. 422–428, 2015.

[37] G. Kyriakarakos, A. I. Dounis, K. G. Arvanitis, and G. Papadakis, "A fuzzy logic energy management system for polygeneration microgrids," *Renewable Energy*, vol. 41, pp. 315–327, 2012.

[38] D. Arcos-Aviles, N. Espinosa, F. Guinjoan, L. Marroyo, and P. Sanchis, "Improved fuzzy controller design for battery energy management in a grid connected microgrid," in *Industrial Electronics Society, IECON 2014-40th Annual Conference of the IEEE*, pp. 2128–2133, IEEE.

[39] D. Arcos-Aviles, J. Pascual, L. Marroyo, P. Sanchis, and F. Guinjoan, "Fuzzy logic-based energy management system design for residential grid-connected microgrids," *IEEE Transactions on Smart Grid*, vol. 9, no. 2, pp. 530–543, 2016.

[40] Y. S. Manjili, A. Rajaee, M. Jamshidi, and B. T. Kelley, "Fuzzy control of electricity storage unit for energy management of micro-grids," in *World Automation Congress 2012*, pp. 1–6, IEEE.

[41] T. T. Teo, T. Logenthiran, W. L. Woo, and K. Abidi, "Fuzzy logic control of energy storage system in microgrid operation," in *2016 IEEE Innovative Smart Grid Technologies-Asia (ISGT-Asia)*, pp. 65–70, IEEE.

[42] E. De Santis, A. Rizzi, A. Sadeghiany, and F. M. F. Mascioli, "Genetic optimization of a fuzzy control system for energy flow management in micro-grids," in *2013 Joint IFSA World Congress and NAFIPS Annual Meeting (IFSA/NAFIPS)*, pp. 418–423, IEEE.

[43] A. Chaouachi, R. M. Kamel, R. Andoulsi, and K. Nagasaka, "Multiobjective intelligent energy management for a microgrid," *IEEE transactions on Industrial Electronics*, vol. 60, no. 4, pp. 1688–1699, 2012.

[44] M. Hosseinzadeh and F. R. Salmasi, "Power management of an isolated hybrid ac/dc micro-grid with fuzzy control of battery banks," *IET Renewable Power Generation*, vol. 9, no. 5, pp. 484–493, 2015.

[45] J. P. Fossati, A. Galarza, A. Martin-Villate, J. M. Echeverria, and L. Fontan, "Optimal scheduling of a microgrid with a fuzzy logic controlled storage system," *International Journal of Electrical Power Energy Systems*, vol. 68, pp. 61–70, 2015.

[46] S. Al-Sakkaf, M. Kassas, M. Khalid, and M. A. Abido, "An energy management system for residential autonomous dc microgrid using optimized fuzzy logic controller considering economic dispatch," *Energies*, vol. 12, no. 8, p. 1457, 2019.

[47] F. J. Vivas, F. Segura, J. M. Andújar, A. Palacio, J. L. Saenz, F. Isorna, and E. López, "Multi-objective fuzzy logic-based energy management system for microgrids with battery and hydrogen energy storage system," *Electronics*, vol. 9, no. 7, p. 1074, 2020.

[48] D. Oliveira, A. Z. de Souza, M. Santos, A. Almeida, B. Lopes, and O. Saavedra, "A fuzzy-based approach for microgrids islanded operation," *Electric Power Systems Research*, vol. 149, pp. 178–189, 2017.

[49] M. Yousif, Q. Ai, Y. Gao, W. A. Wattoo, Z. Jiang, and R. Hao, "An optimal dispatch strategy for distributed microgrids using pso," *CSEE Journal of Power and Energy Systems*, vol. 6, no. 3, pp. 724–734, 2019.

[50] J. Radosavljević, M. Jevtić, and D. Klimenta, "Energy and operation management of a microgrid using particle swarm optimization," *Engineering Optimization*, vol. 48, no. 5, pp. 811–830, 2016.

[51] C. G. Marcelino, M. Baumann, P. E. M. de Almeida, E. F. Wanner, and M. Weil, "A new model for optimization of hybrid microgrids using evolutionary algorithms," *IEEE Latin America Transactions*, vol. 16, no. 3, pp. 799–805, 2018.

[52] M. Manbachi and M. Ordonez, "Ami-based energy management for islanded ac/dc microgrids utilizing energy conservation and optimization," *IEEE Transactions on Smart Grid*, vol. 10, no. 1, pp. 293–304, 2017.

[53] V. Mohan, J. G. Singh, and W. Ongsakul, "An efficient two stage stochastic optimal energy and reserve management in a microgrid," *Applied energy*, vol. 160, pp. 28–38, 2015.

[54] A. A. Moghaddam, A. Seifi, T. Niknam, and M. R. A. Pahlavani, "Multi-objective operation management of a renewable mg (micro-grid) with back-up micro-turbine/fuel cell/battery hybrid power source," *Energy*, vol. 36, no. 11, pp. 6490–6507, 2011.

[55] M. Yang, L. Sun, and J. Wang, "Multi-objective optimization scheduling considering the operation performance of islanded microgrid," *IEEE Access*, vol. 8, pp. 83405–83413, 2020.

[56] C.-Y. Lee and M. Tuegeh, "Optimal optimisation-based microgrid scheduling considering impacts of unexpected forecast errors due to the uncertainty of renewable generation and loads fluctuation," *IET Renewable Power Generation*, vol. 14, no. 2, pp. 321–331, 2019.

[57] S. Shafiq, N. Javaid, and S. Aslam, "Optimal power flow control in a smart micro-grid using bird swarm algorithm," in *2018 5th International Multi-Topic ICT Conference (IMTIC)*, pp. 1–7, IEEE.

[58] W. Al-Saedi, S. W. Lachowicz, D. Habibi, and O. Bass, "Power flow control in grid-connected microgrid operation using particle swarm optimization under variable load conditions," *International Journal of Electrical Power Energy Systems*, vol. 49, pp. 76–85, 2013.

[59] P. Li, D. Xu, Z. Zhou, W.-J. Lee, and B. Zhao, "Stochastic optimal operation of microgrid based on chaotic binary particle swarm optimization," *IEEE Transactions on Smart Grid*, vol. 7, no. 1, pp. 66–73, 2015.

[60] A. Litchy and M. Nehrir, "Real-time energy management of an islanded microgrid using multi-objective particle swarm optimization," in *2014 IEEE PES General Meeting| Conference Exposition*, pp. 1–5, IEEE.

[61] A. Raghavan, P. Maan, and A. K. Shenoy, "Optimization of day-ahead energy storage system scheduling in microgrid using genetic algorithm and particle swarm optimization," *IEEE Access*, vol. 8, pp. 173068–173078, 2020.

[62] S. Golshannavaz, S. Afsharnia, and P. Siano, "A comprehensive stochastic energy management system in reconfigurable microgrids," *International Journal of Energy Research*, vol. 40, no. 11, pp. 1518–1531, 2016.

[63] A. Askarzadeh, "A memory-based genetic algorithm for optimization of power generation in a microgrid," *IEEE transactions on sustainable energy*, vol. 9, no. 3, pp. 1081–1089, 2017.

[64] M. Elsied, A. Oukaour, H. Gualous, R. Hassan, and A. Amin, "An advanced energy management of microgrid system based on genetic algorithm," in *2014 IEEE 23rd International Symposium on Industrial Electronics (ISIE)*, pp. 2541–2547, IEEE.

[65] C. Changsong, D. Shanxu, C. Tao, L. Bangyin, and Y. Jinjun, "Energy trading model for optimal microgrid scheduling based on genetic algorithm," in *2009 IEEE 6th International Power Electronics and Motion Control Conference*, pp. 2136–2139, IEEE.

[66] V. Suresh and P. Janik, "Optimal power flow in microgrids using genetic algorithm," in *2019 2nd International Conference on Power and Embedded Drive Control (ICPEDC)*, pp. 483–487, IEEE.

[67] C. Chen, S. Duan, T. Cai, B. Liu, and G. Hu, "Smart energy management system for optimal microgrid economic operation," *IET renewable power generation*, vol. 5, no. 3, pp. 258–267, 2011.

[68] J. Zhang, Y. Wu, Y. Guo, B. Wang, H. Wang, and H. Liu, "A hybrid harmony search algorithm with differential evolution for day-ahead scheduling problem of a microgrid with consideration of power flow constraints," *Applied energy*, vol. 183, pp. 791–804, 2016.

[69] M. Marzband, S. S. Ghazimirsaeid, H. Uppal, and T. Fernando, "A real-time evaluation of energy management systems for smart hybrid home microgrids," *Electric Power Systems Research*, vol. 143, pp. 624–633, 2017.

[70] M. Marzband, F. Azarinejadian, M. Savaghebi, and J. M. Guerrero, "An optimal energy management system for islanded microgrids based on multiperiod artificial bee colony combined with markov chain," *IEEE Systems Journal*, vol. 11, no. 3, pp. 1712–1722, 2015.

[71] G. K. Venayagamoorthy, R. K. Sharma, P. K. Gautam, and A. Ahmadi, "Dynamic energy management system for a smart microgrid," *IEEE transactions on neural networks and learning systems*, vol. 27, no. 8, pp. 1643–1656, 2016.

[72] M. E. G. Urias, E. N. Sanchez, and L. J. Ricalde, "Electrical microgrid optimization via a new recurrent neural network," *IEEE Systems Journal*, vol. 9, no. 3, pp. 945–953, 2014.

[73] M. Marzband, M. Ghadimi, A. Sumper, and J. L. Domínguez-García, "Experimental validation of a real-time energy management system using multi-period gravitational search algorithm for microgrids in islanded mode," *Applied energy*, vol. 128, pp. 164–174, 2014.

[74] M. Motevasel, A. R. Seifi, and T. Niknam, "Multi-objective energy management of chp (combined heat and power)-based micro-grid," *Energy*, vol. 51, pp. 123–136, 2013.

[75] M. Marzband, E. Yousefnejad, A. Sumper, and J. L. Domínguez-García, "Real time experimental implementation of optimum energy management system in standalone microgrid by using multi-layer ant colony optimization," *International Journal of Electrical Power Energy Systems*, vol. 75, pp. 265–274, 2016.

[76] E. Kuznetsova, Y.-F. Li, C. Ruiz, E. Zio, G. Ault, and K. Bell, "Reinforcement learning for microgrid energy management," *Energy*, vol. 59, pp. 133–146, 2013.

[77] S. G. M. Rokni, M. Radmehr, and A. Zakariazadeh, "Optimum energy resource scheduling in a microgrid using a distributed algorithm framework," *Sustainable cities and society*, vol. 37, pp. 222–231, 2018.

[78] U. R. Nair and R. Costa-Castelló, "A model predictive control based energy management scheme for hybrid storage system in islanded microgrids," *IEEE Access*, vol. 8, pp. 97809 – 97822, 2020.

[79] J. Sachs and O. Sawodny, "A two-stage model predictive control strategy for economic diesel-pv-battery island microgrid operation in rural areas," *IEEE Transactions on Sustainable Energy*, vol. 7, no. 3, pp. 903–913, 2016.

[80] K. Tan, P. So, Y. Chu, and M. Chen, "Coordinated control and energy management of distributed generation inverters in a microgrid," *IEEE transactions on power delivery*, vol. 28, no. 2, pp. 704–713, 2013.

[81] Y. Zheng, S. Li, and R. Tan, "Distributed model predictive control for on-connected microgrid power management," *IEEE Transactions on Control Systems Technology*, vol. 26, no. 3, pp. 1028–1039, 2017.

[82] M. J. Rana and M. A. Abido, "Energy management in dc microgrid with energy storage and model predictive controlled ac–dc converter," *IET Generation, Transmission Distribution*, vol. 11, no. 15, pp. 3694–3702, 2017.

[83] A. Olama, P. R. Mendes, and E. F. Camacho, "Lyapunov-based hybrid model predictive control for energy management of microgrids," *IET Generation, Transmission Distribution*, vol. 12, no. 21, pp. 5770–5780, 2018.

[84] X. Guo, Z. Bao, H. Lai, and W. Yan, "Model predictive control considering scenario optimisation for microgrid dispatching with wind power and electric vehicle," *The Journal of Engineering*, vol. 2017, no. 13, pp. 2539–2543, 2017.

[85] Y. Zhang, R. Wang, T. Zhang, Y. Liu, and B. Guo, "Model predictive control-based operation management for a residential microgrid with considering forecast uncertainties and demand response strategies," *IET Generation, Transmission Distribution*, vol. 10, no. 10, pp. 2367–2378, 2016.

[86] Y. Li, X. Fan, Z. Cai, and B. Yu, "Optimal active power dispatching of microgrid and distribution network based on model predictive control," *Tsinghua Science and Technology*, vol. 23, no. 3, pp. 266–276, 2018.

[87] F. Garcia-Torres and C. Bordons, "Optimal economical schedule of hydrogen-based microgrids with hybrid storage using model predictive control," *IEEE Transactions on Industrial Electronics*, vol. 62, no. 8, pp. 5195–5207, 2015.

[88] J. Lee, P. Zhang, L. K. Gan, D. A. Howey, M. A. Osborne, A. Tosi, and S. Duncan, "Optimal operation of an energy management system using model predictive control and gaussian process time-series modeling," *IEEE Journal of Emerging and Selected Topics in Power Electronics*, vol. 6, no. 4, pp. 1783–1795, 2018.

[89] D. E. Olivares, C. A. Cañizares, and M. Kazerani, "A centralized energy management system for isolated microgrids," *IEEE Transactions on smart grid*, vol. 5, no. 4, pp. 1864–1875, 2014.

[90] J. Shen, C. Jiang, Y. Liu, and J. Qian, "A microgrid energy management system with demand response for providing grid peak shaving," *Electric Power Components and Systems*, vol. 44, no. 8, pp. 843–852, 2016.

[91] D. Tenfen and E. C. Finardi, "A mixed integer linear programming model for the energy management problem of microgrids," *Electric Power Systems Research*, vol. 122, pp. 19–28, 2015.

[92] S. Helal, R. Najee, M. Hanna, M. F. Shaaban, A. Osman, and M. Hassan, "An energy management system for hybrid microgrids in remote communities," in *2017 IEEE 30th Canadian Conference on Electrical and Computer Engineering (CCECE)*, pp. 1–4, IEEE.

[93] S. Sukumar, H. Mokhlis, S. Mekhilef, K. Naidu, and M. Karimi, "Mix-mode energy management strategy and battery sizing for economic operation of grid-tied microgrid," *Energy*, vol. 118, pp. 1322–1333, 2017.

[94] G. Comodi, A. Giantomassi, M. Severini, S. Squartini, F. Ferracuti, A. Fonti, D. N. Cesarini, M. Morodo, and F. Polonara, "Multi-apartment residential microgrid with electrical and thermal storage devices: Experimental analysis and simulation of energy management strategies," *Applied Energy*, vol. 137, pp. 854–866, 2015.

[95] L. K. Panwar, S. R. Konda, A. Verma, B. K. Panigrahi, and R. Kumar, "Operation window constrained strategic energy management of microgrid with electric vehicle and distributed resources," *IET Generation, Transmission Distribution*, vol. 11, no. 3, pp. 615–626, 2017.

[96] C. Corchero, M. Cruz-Zambrano, and F.-J. Heredia, "Optimal energy management for a residential microgrid including a vehicle-to-grid system," *IEEE transactions on smart grid*, vol. 5, no. 4, pp. 2163–2172, 2014.

[97] N. Anglani, G. Oriti, and M. Colombini, "Optimized energy management system to reduce fuel consumption in remote military microgrids," *IEEE Transactions on Industry Applications*, vol. 53, no. 6, pp. 5777–5785, 2017.

[98] P. P. Vergara, J. C. López, L. C. da Silva, and M. J. Rider, "Security-constrained optimal energy management system for three-phase residential microgrids," *Electric Power Systems Research*, vol. 146, pp. 371–382, 2017.

[99] M. H. Amrollahi and S. M. T. Bathaee, "Techno-economic optimization of hybrid photovoltaic/wind generation together with energy storage system in a stand-alone micro-grid subjected to demand response," *Applied energy*, vol. 202, pp. 66–77, 2017.

[100] K. Yu, Q. Ai, S. Wang, J. Ni, and T. Lv, "Analysis and optimization of droop controller for microgrid system based on small-signal dynamic model," *IEEE Transactions on Smart Grid*, vol. 7, no. 2, pp. 695–705, 2015.

[101] B. Babaiahgari, M. H. Ullah, and J.-D. Park, "Coordinated control and dynamic optimization in dc microgrid systems," *International Journal of Electrical Power Energy Systems*, vol. 113, pp. 832–841, 2019.

[102] S. Adhikari and F. Li, "Coordinated vf and pq control of solar photovoltaic generators with mppt and battery storage in microgrids," *IEEE Transactions on Smart grid*, vol. 5, no. 3, pp. 1270–1281, 2014.

[103] B. Liang, L. Kang, J. He, F. Zheng, Y. Xia, Z. Zhang, Z. Zhang, G. Liu, and Y. Zhao, "Coordination control of hybrid ac/dc microgrid," *The Journal of Engineering*, vol. 2019, no. 16, pp. 3264–3269, 2019.

[104] J. Li, R. Xiong, Q. Yang, F. Liang, M. Zhang, and W. Yuan, "Design/test of a hybrid energy storage system for primary frequency control using a dynamic droop method in an isolated microgrid power system," *Applied Energy*, vol. 201, pp. 257–269, 2017.

[105] S. Bae and A. Kwasinski, "Dynamic modeling and operation strategy for a microgrid with wind and photovoltaic resources," *IEEE Transactions on smart grid*, vol. 3, no. 4, pp. 1867–1876, 2012.

[106] S. Teimourzadeh, F. Aminifar, M. Davarpanah, and M. Shahidehpour, "Adaptive control of microgrid security," *IEEE Transactions on Smart Grid*, vol. 9, no. 4, pp. 3909–3910, 2018.

[107] M. Falahi, K. Butler-Purry, and M. Ehsani, "Dynamic reactive power control of islanded microgrids," *IEEE Transactions on Power Systems*, vol. 28, no. 4, pp. 3649–3657, 2013.

[108] X. Tang, W. Deng, and Z. Qi, "Investigation of the dynamic stability of microgrid," *IEEE Transactions on Power Systems*, vol. 29, no. 2, pp. 698–706, 2013.

[109] M. G. Molina and P. E. Mercado, "Power flow stabilization and control of microgrid with wind generation by superconducting magnetic energy storage," *IEEE Transactions on Power Electronics*, vol. 26, no. 3, pp. 910–922, 2010.

[110] K. Rajesh, S. Dash, R. Rajagopal, and R. Sridhar, "A review on control of ac microgrid," *Renewable and sustainable energy reviews*, vol. 71, pp. 814–819, 2017.

[111] P. Borazjani, N. I. A. Wahab, H. B. Hizam, and A. B. C. Soh, "A review on microgrid control techniques," in *Innovative Smart Grid Technologies-Asia (ISGT Asia), 2014 IEEE*, pp. 749–753, IEEE.

[112] M. Yazdanian and A. Mehrizi-Sani, "Distributed control techniques in microgrids," *IEEE Transactions on Smart Grid*, vol. 5, no. 6, pp. 2901–2909, 2014.

[113] M. R. Miveh, M. F. Rahmat, A. A. Ghadimi, and M. W. Mustafa, "Control techniques for three-phase four-leg voltage source inverters in autonomous microgrids: A review," *Renewable and Sustainable Energy Reviews*, vol. 54, pp. 1592–1610, 2016.

[114] M. Raeispour, H. Atrianfar, H. R. Baghaee, and G. B. Gharehpetian, "Robust sliding mode and mixed h_2/h_∞ output feedback primary control of ac microgrids," *IEEE Systems Journal*, pp. 1–12, 2020.

[115] S. Gholami, S. Saha, and M. Aldeen, "Robust multiobjective control method for power sharing among distributed energy resources in islanded microgrids with unbalanced and nonlinear loads," *International Journal of Electrical Power Energy Systems*, vol. 94, pp. 321–338, 2018.

[116] F. Zhang, H. Zhao, and M. Hong, "Operation of networked microgrids in a distribution system," *CSEE Journal of Power and Energy Systems*, vol. 1, no. 4, pp. 12–21, 2015.

[117] R. Zamora and A. K. Srivastava, "Multi-layer architecture for voltage and frequency control in networked microgrids," *IEEE Transactions on Smart Grid*, vol. 9, no. 3, pp. 2076–2085, 2018.

[118] D. O. Amoateng, M. Al Hosani, M. S. El Moursi, K. Turitsyn, and J. L. Kirtley, "Adaptive voltage and frequency control of islanded multi-microgrids," *IEEE Transactions on Power Systems*, vol. 33, no. 4, 2018.

[119] W. Liu, W. Gu, J. Wang, W. Yu, and X. Xi, "Game theoretic non-cooperative distributed coordination control for multi-microgrids," *IEEE Transactions on Smart Grid*, vol. 9, no. 6, pp. 6986–6997, 2018.

[120] W. Liu, W. Gu, Y. Xu, Y. Wang, and K. Zhang, "General distributed secondary control for multi-microgrids with both pq-controlled and droop-controlled distributed generators," *IET Generation, Transmission Distribution*, vol. 11, no. 3, pp. 707–718, 2017.

[121] T. John and S. P. Lam, "Voltage and frequency control during microgrid islanding in a multi-area multi-microgrid system," *IET Generation, Transmission Distribution*, vol. 11, no. 6, pp. 1502–1512, 2017.

[122] M. S. Golsorkhi, D. J. Hill, and H. R. Karshenas, "Distributed voltage control and power management of networked microgrids," *IEEE Journal of Emerging and Selected Topics in Power Electronics*, vol. 6, no. 4, pp. 1892–1902, 2017.

[123] X. Lu, J. Lai, X. Yu, Y. Wang, and J. M. Guerrero, "Distributed coordination of islanded microgrid clusters using a two-layer intermittent communication network," *IEEE Transactions on Industrial Informatics*, vol. 14, no. 9, pp. 3956–3969, 2017.

[124] J. Lai, X. Lu, X. Yu, and A. Monti, "Cluster-oriented distributed cooperative control for multiple ac microgrids," *IEEE Transactions on Industrial Informatics*, vol. 15, no. 11, pp. 5906–5918, 2019.

[125] N. Radhakrishnan, I. Chakraborty, J. Xie, P. T. Mana, F. K. Tuffner, B. P. Bhattarai, and K. P. Schneider, "Improving primary frequency response in networked microgrid operations using multilayer perceptron-driven reinforcement learning," *IET Smart Grid*, vol. 3, no. 4, pp. 500–507, 2020.

[126] Y. Li, P. Dong, M. Liu, and G. Yang, "A distributed coordination control based on finite-time consensus algorithm for a cluster of dc microgrids," *IEEE Transactions on Power Systems*, vol. 34, no. 3, pp. 2205–2215, 2018.

[127] Y. Fu, Z. Zhang, Y. Mi, Z. Li, and F. Li, "Droop control for dc multi-microgrids based on local adaptive fuzzy approach and global power allocation correction," *IEEE Transactions on Smart Grid*, vol. 10, no. 5, pp. 5468–5478, 2018.

[128] Y. Li, P. Zhang, and P. B. Luh, "Formal analysis of networked microgrids dynamics," *IEEE Transactions on Power Systems*, vol. 33, no. 3, pp. 3418–3427, 2018.

[129] A. K. Verma, B. Singh, and D. Shahani, "Grid to vehicle and vehicle to grid energy transfer using single-phase bidirectional ac-dc converter and bidirectional dc-dc converter," in *Energy, Automation, and Signal (ICEAS), 2011 International Conference on*, pp. 1–5, IEEE.

[130] S. A. Arefifar, M. Ordonez, and Y. A.-R. I. Mohamed, "Voltage and current controllability in multi-microgrid smart distribution systems," *IEEE Transactions on Smart Grid*, vol. 9, no. 2, pp. 817–826, 2018.

[131] C. Wang, P. Yang, C. Ye, Y. Wang, and Z. Xu, "Voltage control strategy for three/single phase hybrid multimicrogrid," *IEEE Transactions on Energy Conversion*, vol. 31, no. 4, pp. 1498–1509, 2016.

[132] Y. Zhu, F. Zhuo, F. Wang, B. Liu, R. Gou, and Y. Zhao, "A virtual impedance optimization method for reactive power sharing in networked microgrid," *IEEE Transactions on Power Electronics*, vol. 31, no. 4, pp. 2890–2904, 2016.

[133] S. Moayedi and A. Davoudi, "Distributed tertiary control of dc microgrid clusters," *IEEE Transactions on Power Electronics*, vol. 31, no. 2, pp. 1717–1733, 2015.

[134] Y. Wang, Y. Tang, Y. Xu, and Y. Xu, "A distributed control scheme of thermostatically controlled loads for the building-microgrid community," *IEEE Transactions on Sustainable Energy*, vol. 11, no. 1, pp. 350–360, 2019.

[135] Q. Li, C. Peng, M. Chen, F. Chen, W. Kang, J. M. Guerrero, and D. Abbott, "Networked and distributed control method with optimal power dispatch for islanded microgrids," *IEEE Transactions on Industrial Electronics*, vol. 64, no. 1, pp. 493–504, 2016.

[136] U. B. Tayab, M. A. B. Roslan, L. J. Hwai, and M. Kashif, "A review of droop control techniques for microgrid," *Renewable and Sustainable Energy Reviews*, vol. 76, pp. 717–727, 2017.

[137] E. Planas, A. Gil-de Muro, J. Andreu, I. Kortabarria, and I. M. de Alegría, "General aspects, hierarchical controls and droop methods in microgrids: A review," *Renewable and Sustainable Energy Reviews*, vol. 17, pp. 147–159, 2013.

[138] X. Wu, X. Wu, Y. Xu, and J. He, "A hierarchical control framework for islanded multi-microgrid systems," in *2018 IEEE Power Energy Society General Meeting (PESGM)*, pp. 1–5, IEEE.

[139] S. K. Sahoo and N. Kishore, "Coordinated control and operation of a multi-microgrid system," in *2017 7th International Conference on Power Systems (ICPS)*, pp. 283–288, IEEE.

[140] W. Qingzhu and X. Chan, "Coordination control for multi-microgrid system with parallel structure based on improved droop control strategy," in *2018 International Conference on Smart Grid and Electrical Automation (ICSGEA)*, pp. 299–302, IEEE.

[141] Y. Zhu, B. Liu, F. Wang, F. Zhuo, and Y. Zhao, "A virtual resistance based reactive power sharing strategy for networked microgrid," in *Power Electronics and ECCE Asia (ICPE-ECCE Asia), 2015 9th International Conference on*, pp. 1564–1572, IEEE.

[142] Q. Qiu, F. Yang, and Y. Zhu, "Distributed model predictive control with switching topology network," in *Control Conference (ASCC), 2017 11th Asian*, pp. 2364–2369, IEEE.

[143] F. Yang, Q. Sun, Q.-L. Han, and Z. Wu, "Cooperative model predictive control for distributed photovoltaic power generation systems," *IEEE Journal of Emerging and Selected Topics in Power Electronics*, vol. 4, no. 2, pp. 414–420, 2016.

[144] G. Lou, W. Gu, W. Sheng, X. Song, and F. Gao, "Distributed model predictive secondary voltage control of islanded microgrids with feedback linearization," *IEEE Access*, vol. 6, pp. 50169–50178, 2018.

[145] K. Liu, T. Liu, Z. Tang, and D. J. Hill, "Distributed mpc-based frequency control in networked microgrids with voltage constraints," *IEEE Transactions on Smart Grid*, vol. 10, no. 6, pp. 6343–6354, 2019.

[146] P. Kou, D. Liang, and L. Gao, "Distributed empc of multiple microgrids for coordinated stochastic energy management," *Applied Energy*, vol. 185, pp. 939–952, 2017.

[147] M. S. Mahmoud, N. M. Alyazidi, and M. I. Abouheaf, "Adaptive intelligent techniques for microgrid control systems: A survey," *International Journal of Electrical Power Energy Systems*, vol. 90, pp. 292–305, 2017.

[148] N. Chettibi, A. Mellit, G. Sulligoi, and A. M. Pavan, "Adaptive neural network-based control of a hybrid ac/dc microgrid," *IEEE Transactions on Smart Grid*, vol. 9, no. 3, pp. 1667–1679, 2016.

[149] L. Yin, T. Yu, B. Yang, and X. Zhang, "Adaptive deep dynamic programming for integrated frequency control of multi-area multi-microgrid systems," *Neurocomputing*, vol. 344, pp. 49–60, 2019.

[150] Z. Zhao, P. Yang, Y. Wang, Z. Xu, and J. M. Guerrero, "Dynamic characteristics analysis and stabilization of pv-based multiple microgrid clusters," *Ieee Transactions on Smart Grid*, vol. 10, no. 1, pp. 805–818, 2017.

[151] W. Liu, Z. Wen, Y. Shen, and Z. Zhang, "Reinforcement learning-based distributed secondary optimal control for multi-microgrids," in *2017 IEEE Conference on Energy Internet and Energy System Integration (EI2)*, pp. 1–4, IEEE.

[152] Y. Wang, T.-L. Nguyen, Y. Xu, Q.-T. Tran, and R. Caire, "Peer-to-peer control for networked microgrids: Multi-layer and multi-agent architecture design," *IEEE Transactions on Smart Grid*, vol. 11, no. 6, pp. 4688–4699, 2020.

[153] J. Ni and Q. Ai, "Economic power transaction using coalitional game strategy in micro-grids," *IET Generation, Transmission Distribution*, vol. 10, no. 1, pp. 10–18, 2016.

[154] P. Tian, X. Xiao, K. Wang, and R. Ding, "A hierarchical energy management system based on hierarchical optimization for microgrid community economic operation," *IEEE Transactions on Smart Grid*, vol. 7, no. 5, pp. 2230–2241, 2016.

[155] Z. Zhou, F. Xiong, B. Huang, C. Xu, R. Jiao, B. Liao, Z. Yin, and J. Li, "Game-theoretical energy management for energy internet with big data-based renewable power forecasting," *IEEE Access*, vol. 5, pp. 5731–5746, 2017.

[156] X. Xing, L. Xie, H. Meng, X. Guo, L. Yue, and J. M. Guerrero, "Energy management strategy considering multi-time-scale operational modes of batteries for the grid-connected microgrids community," *CSEE Journal of Power and Energy Systems*, vol. 6, no. 1, pp. 111–121, 2019.

[157] V.-H. Bui, A. Hussain, and H.-M. Kim, "A multiagent-based hierarchical energy management strategy for multi-microgrids considering adjustable power and demand response," *IEEE Transactions on Smart Grid*, vol. 9, no. 2, pp. 1323–1333, 2016.

[158] A. R. Malekpour and A. Pahwa, "Stochastic networked microgrid energy management with correlated wind generators," *IEEE TRANSACTIONS ON POWER SYSTEMS*, vol. 32, no. 5, pp. 3681–3693, 2017.

[159] T. Lv and Q. Ai, "Interactive energy management of networked microgrids-based active distribution system considering large-scale integration of renewable energy resources," *Applied Energy*, vol. 163, pp. 408–422, 2016.

[160] C. A. Cortes, S. F. Contreras, and M. Shahidehpour, "Microgrid topology planning for enhancing the reliability of active distribution networks," *IEEE Transactions on Smart Grid*, vol. 9, no. 6, pp. 6369–6377, 2017.

[161] N. Nikmehr and S. Najafi-Ravadanegh, "Reliability evaluation in multi-microgrids under probabilistic optimum operation using heuristic algorithm," in *Smart Grid Conference (SGC), 2015*, pp. 92–98, IEEE.

[162] N. Nikmehr and S. N. Ravadanegh, "Reliability evaluation of multi-microgrids considering optimal operation of small scale energy zones under load-generation uncertainties," *International Journal of Electrical Power Energy Systems*, vol. 78, pp. 80–87, 2016.

[163] X. Fang, Q. Yang, J. Wang, and W. Yan, "Coordinated dispatch in multiple cooperative autonomous islanded microgrids," *Applied Energy*, vol. 162, pp. 40–48, 2016.

[164] R. S. de Carvalho and S. Mohagheghi, "Analyzing impact of communication network topologies on reconfiguration of networked microgrids, impact of communication system on smart grid reliability, security and operation," in *2016 North American Power Symposium (NAPS)*, pp. 1–6, IEEE.

[165] V. Venkataramanan, Y. Zhou, and A. Srivastava, "Analyzing impact of communication network topologies on reconfiguration of networked microgrids," in *North American Power Symposium (NAPS), 2016*, pp. 1–6, IEEE.

[166] S. Abhinav, H. Modares, F. L. Lewis, F. Ferrese, and A. Davoudi, "Synchrony in networked microgrids under attacks," *IEEE Transactions on Smart Grid*, vol. 9, no. 6, pp. 6731–6741, 2017.

[167] Q. Zhou, M. Shahidehpour, A. Alabdulwahab, and A. Abusorrah, "A cyber-attack resilient distributed control strategy in islanded microgrids," *IEEE Transactions on Smart Grid*, vol. 11, no. 5, pp. 3690–3701, 2020.

[168] S. A. Gopalan, V. Sreeram, and H. H. Iu, "A review of coordination strategies and protection schemes for microgrids," *Renewable and Sustainable Energy Reviews*, vol. 32, pp. 222–228, 2014.

[169] A. Alabdulwahab and M. Shahidehpour, "Microgrid networking for the monitoring, control and protection of modern power systems," *The Electricity Journal*, vol. 29, no. 10, pp. 1–7, 2016.

[170] B. J. Brearley and R. R. Prabu, "A review on issues and approaches for microgrid protection," *Renewable and Sustainable Energy Reviews*, vol. 67, pp. 988–997, 2017.

[171] P. Malysz, S. Sirouspour, and A. Emadi, "An optimal energy storage control strategy for grid-connected microgrids," *IEEE Transactions on Smart Grid*, vol. 5, no. 4, pp. 1785–1796, 2014.

[172] J. Pascual, J. Barricarte, P. Sanchis, and L. Marroyo, "Energy management strategy for a renewable-based residential microgrid with generation and demand forecasting," *Applied Energy*, vol. 158, pp. 12–25, 2015.

[173] D. Arcos-Aviles, J. Pascual, F. Guinjoan, L. Marroyo, P. Sanchis, and M. P. Marietta, "Low complexity energy management strategy for grid profile smoothing of a residential grid-connected microgrid using generation and demand forecasting," *Applied Energy*, vol. 205, pp. 69–84, 2017.

[174] D. Wang, S. Ge, H. Jia, C. Wang, Y. Zhou, N. Lu, and X. Kong, "A demand response and battery storage coordination algorithm for providing microgrid tie-line smoothing services," *IEEE Transactions on Sustainable Energy*, vol. 5, no. 2, pp. 476–486, 2014.

[175] S. Koohi-Kamali, N. Rahim, and H. Mokhlis, "Smart power management algorithm in microgrid consisting of photovoltaic, diesel, and battery storage plants considering variations in sunlight, temperature, and load," *Energy Conversion and Management*, vol. 84, pp. 562–582, 2014.

[176] 2017, December 31.

[177] R. Garmabdari, M. Moghimi, F. Yang, J. Lu, H. Li, and Z. Yang, "Optimisation of battery energy storage capacity for a grid-tied renewable microgrid," in *Innovative Smart Grid Technologies-Asia (ISGT-Asia), 2017 IEEE*, pp. 1–6, IEEE.

[178] S. S. Zhang, "The effect of the charging protocol on the cycle life of a li-ion battery," *Journal of power sources*, vol. 161, no. 2, pp. 1385–1391, 2006.

[179] S. Anuphappharadorn, S. Sukchai, C. Sirisamphanwong, and N. Ketjoy, "Comparison the economic analysis of the battery between lithium-ion and lead-acid in pv stand-alone application," *Energy Procedia*, vol. 56, pp. 352–358, 2014.

[180] S. Tong, M. P. Klein, and J. W. Park, "On-line optimization of battery open circuit voltage for improved state-of-charge and state-of-health estimation," *Journal of Power Sources*, vol. 293, pp. 416–428, 2015.

[181] S. S. Zhang, "The effect of the charging protocol on the cycle life of a li-ion battery," *Journal of power sources*, vol. 161, no. 2, pp. 1385–1391, 2006.

[182] E. K. Chong and S. H. Zak, *An introduction to optimization*, vol. 76. John Wiley Sons, 2013.

[183] E. Unamuno and J. A. Barrena, "Hybrid ac/dc microgrids—part i: Review and classification of topologies," *Renewable and Sustainable Energy Reviews*, vol. 52, pp. 1251–1259, 2015.

[184] J. P. Lopes, C. Moreira, and A. Madureira, "Defining control strategies for microgrids islanded operation," *IEEE Transactions on power systems*, vol. 21, no. 2, pp. 916–924, 2006.

[185] H. Bevrani and S. Shokoohi, "An intelligent droop control for simultaneous voltage and frequency regulation in islanded microgrids," *IEEE transactions on smart grid*, vol. 4, no. 3, pp. 1505–1513, 2013.

[186] C. Dou, X. An, D. Yue, and F. Li, "Two-level decentralized optimization power dispatch control strategies for an islanded microgrid without communication network," *International Transactions on Electrical Energy Systems*, vol. 27, no. 1, p. e2244, 2017.

[187] M. Hosseinzadeh and F. R. Salmasi, "Robust optimal power management system for a hybrid ac/dc micro-grid," *IEEE Transactions on Sustainable Energy*, vol. 6, no. 3, pp. 675–687, 2015.

[188] Y. Karimi, H. Oraee, M. S. Golsorkhi, and J. M. Guerrero, "Decentralized method for load sharing and power management in a pv/battery hybrid source islanded microgrid," *IEEE Transactions on Power Electronics*, vol. 32, no. 5, pp. 3525–3535, 2016.

[189] C. Zhang, W. Lin, D. Ke, and Y. Sun, "Smoothing tie-line power fluctuations for industrial microgrids by demand side control: An output regulation approach," *IEEE Transactions on Power Systems*, vol. 34, no. 5, pp. 3716–3728, 2019.

[190] Y. Sun, X. Tang, X. Sun, D. Jia, and G. Zhang, "Microgrid tie-line power fluctuation mitigation with virtual energy storage," *The Journal of Engineering*, vol. 2019, no. 16, pp. 1001–1004, 2019.

[191] J. Pascual, P. Sanchis, and L. Marroyo, "Implementation and control of a residential electrothermal microgrid based on renewable energies, a hybrid storage system and demand side management," *Energies*, vol. 7, no. 1, pp. 210–237, 2014.

[192] Y. Zhang, T. Zhang, R. Wang, Y. Liu, and B. Guo, "Optimal operation of a smart residential microgrid based on model predictive control by considering uncertainties and storage impacts," *Solar Energy*, vol. 122, pp. 1052–1065, 2015.

[193] J. Shen, C. Jiang, Y. Liu, X. Wang, and J. Qian, "Microgrid operation optimization with regulation of grid tie-line power fluctuations and risk management," *International Transactions on Electrical Energy Systems*, vol. 26, no. 11, pp. 2308–2321, 2016.

[194] M. BiazarGhadikolaei, M. Shahabi, and T. Barforoushi, "Expansion planning of energy storages in microgrid under uncertainties and demand response," *International Transactions on Electrical Energy Systems*, vol. 29, no. 11, p. e12110, 2019.

[195] J. Kathiresan, S. K. Natarajan, and G. Jothimani, "Energy management of distributed renewable energy sources for residential dc microgrid applications," *International Transactions on Electrical Energy Systems*, vol. 30, no. 3, p. e12258, 2019.

[196] A. C. Luna, N. L. Diaz, M. Graells, J. C. Vasquez, and J. M. Guerrero, "Mixed-integer-linear-programming-based energy management system for hybrid pv-wind-battery microgrids: Modeling, design, and experimental verification," *IEEE Transactions on Power Electronics*, vol. 32, no. 4, pp. 2769–2783, 2016.

[197] Z.-x. Xiao, J. M. Guerrero, J. Shuang, D. Sera, E. Schaltz, and J. C. Vásquez, "Flat tie-line power scheduling control of grid-connected hybrid microgrids," *Applied energy*, vol. 210, pp. 786–799, 2018.

[198] M. Rasheduzzaman, "Small signal modeling and analysis of microgrid systems," 2015.

[199] M. A. Eltawil and Z. Zhao, "Mppt techniques for photovoltaic applications," *Renewable and sustainable energy reviews*, vol. 25, pp. 793–813, 2013.

[200] J. Schonbergerschonberger, R. Duke, and S. D. Round, "Dc-bus signaling: A distributed control strategy for a hybrid renewable nanogrid," *IEEE Transactions on Industrial Electronics*, vol. 53, no. 5, pp. 1453–1460, 2006.

[201] M. Islam, F. Yang, and M. Amin, "Dynamic control of grid-connected microgrids for tie-line smoothing," *International Transactions on Electrical Energy Systems*, vol. 30, no. 11, p. e12557, 2020.

[202] A. Ouammi, H. Dagdougui, L. Dessaint, and R. Sacile, "Coordinated model predictive-based power flows control in a cooperative network of smart microgrids," *IEEE Transactions on Smart grid*, vol. 6, no. 5, pp. 2233–2244, 2015.

[203] H. Dagdougui and R. Sacile, "Decentralized control of the power flows in a network of smart microgrids modeled as a team of cooperative agents," *IEEE Transactions on Control Systems Technology*, vol. 22, no. 2, pp. 510–519, 2014.

[204] S. Mudaliyar, B. Duggal, and S. Mishra, "Distributed tie-line power flow control of autonomous dc microgrid clusters," *IEEE Transactions on Power Electronics*, vol. 35, no. 10, pp. 11250–11266, 2020.

[205] Y. Liu, Y. Li, H. Xin, H. B. Gooi, and J. Pan, "Distributed optimal tie-line power flow control for multiple interconnected ac microgrids," *IEEE Transactions on Power Systems*, vol. 34, no. 3, pp. 1869–1880, 2018.

[206] F. Garcia-Torres, C. Bordons, and M. A. Ridao, "Optimal economic schedule for a network of microgrids with hybrid energy storage system using distributed model predictive control," *IEEE transactions on industrial electronics*, vol. 66, no. 3, pp. 1919–1929, 2018.

[207] Z. Zhao, J. Guo, C. S. Lai, H. Xiao, K. Zhou, and L. L. Lai, "Distributed model predictive control strategy for islands multi-microgrids based on non-cooperative game," *IEEE Transactions on Industrial Informatics*, vol. 17, no. 6, pp. 3803–3814, 2020.

[208] W. Ananduta, J. M. Maestre, C. Ocampo-Martinez, and H. Ishii, "Resilient distributed model predictive control for energy management of interconnected microgrids," *Optimal Control Applications and Methods*, vol. 41, no. 1, pp. 146–169, 2020.

[209] N. Bazmohammadi, A. Tahsiri, A. Anvari-Moghaddam, and J. M. Guerrero, "Optimal operation management of a regional network of microgrids based on chance-constrained model predictive control," *IET Generation, Transmission Distribution*, vol. 12, no. 15, pp. 3772–3779, 2018.

[210] Y. Zhang, T. Zhang, R. Wang, Y. Liu, and B. Guo, "Dynamic dispatch of isolated neighboring multi-microgrids based on model predictive control," in *Smart Grid and Clean Energy Technologies (ICSGCE), 2016 International Conference on*, pp. 50–55, IEEE.

[211] F. Tedesco, L. Mariam, M. Basu, A. Casavola, and M. F. Conlon, "Economic model predictive control-based strategies for cost-effective supervision of community microgrids considering battery lifetime," *IEEE Journal of emerging and selected topics in power electronics*, vol. 3, no. 4, pp. 1067–1077, 2015.

[212] A. Parisio, C. Wiezorek, T. Kyntäjä, J. Elo, K. Strunz, and K. H. Johansson, "Cooperative mpc-based energy management for networked microgrids," *IEEE Transactions on Smart Grid*, vol. 8, no. 6, pp. 3066–3074, 2017.

[213] B. Li and R. Roche, "Optimal scheduling of multiple multi-energy supply microgrids considering future prediction impacts based on model predictive control," *Energy*, vol. 197, p. 117180, 2020.

[214] J. Hu, J. Zhu, and D. G. Dorrell, "Model predictive control of inverters for both islanded and grid-connected operations in renewable power generations," *IET Renewable Power Generation*, vol. 8, no. 3, pp. 240–248, 2013.

[215] X. Li, H. Zhang, M. B. Shadmand, and R. S. Balog, "Model predictive control of a voltage-source inverter with seamless transition between islanded and grid-connected operations," *IEEE Transactions on Industrial Electronics*, vol. 64, no. 10, pp. 7906–7918, 2017.

[216] D.-K. Choi and K.-B. Lee, "Dynamic performance improvement of ac/dc converter using model predictive direct power control with finite control set," *IEEE Transactions on Industrial Electronics*, vol. 62, no. 2, pp. 757–767, 2014.

[217] A. d. J. Chica Leal, C. L. Trujillo Rodríguez, and F. Santamaria, "Comparative of power calculation methods for single-phase systems under sinusoidal and non-sinusoidal operation," *Energies*, vol. 13, no. 17, p. 4322, 2020.

[218] X. Li and R. S. Balog, "Pll-less robust active and reactive power controller for single phase grid-connected inverter with lcl filter," in *2015 IEEE Applied Power Electronics Conference and Exposition (APEC)*, pp. 2154–2159, IEEE.

[219] M. Q. Raza, M. Nadarajah, and C. Ekanayake, "On recent advances in pv output power forecast," *Solar Energy*, vol. 136, pp. 125–144, 2016.